EVALUATION OF ALTERNATIVE TRUCK LANE MANAGEMENT STRATEGIES ALONG A SECTION OF I-81

Hesham Rakha, Sangjun Park, Mazen Arafeh, and Ihab El-Shawarby

Virginia Tech Transportation Institute
3500 Transportation Research Plaza (0536)
Blacksburg, VA 24061
Phone: (540) 231-1505
Fax: (540) 231-1555
E-mail: hrakha@vt.edu

19 May 2008

TABLE OF CONTENTS

1. INTRODUCTION

I-81 is one of the top eight truck routes in the U.S. In the state of Virginia, I-81 traverses 325.51 miles from Tennessee in the south to the West Virginia border in the north and passes through 12 counties. The highway was designed for a 15 percent truck volume, however trucks now account for somewhere between 20 to 40 percent of the total traffic volume. In 2001, the Virginia Department of Transportation (VDOT) developed a list of key improvements for I-81. The improvements include: developing the corridor as a multi-modal facility, incorporating a high degree of efficiency and safety for all users, which may include the physical separation of commercial and passenger vehicles; considering transit or other higher occupancy travel in and around growing urban areas, and using Intelligent Transportation Systems (ITSs) as short-, mid-, and long-term solutions to improving transportation flow and management (VDOT 2004). In 2003, a U.S. house transportation bill included $1.5 billion in federal funding for dedicated truck lanes. According to Representative Don Young (Alaska), author of the bill and a strong proponent of truck-only lanes, "Separate lanes for trucks will move freight more efficiently and make our highways significantly safer." Mr. Young expressed interest in making I-81 a national pilot project (2005). In 2005, FHWA approved the Tier 1 Draft EIS (VDOT 2005). Some of the key findings of the study were: (a) 2004 traffic volumes will nearly double by 2035; (b) Nearly the entire corridor needs additional capacity by 2035; (c) Estimates of future traffic volume do not support building two additional lanes in each direction for use only by trucks. Such a design would provide too much roadway capacity for trucks and not enough capacity for cars; and (d) Up to 37% of I-81 requires one additional lane in each direction, while much of the remainder may need up to two additional lanes in each direction to handle future traffic.

In 2006, a cross-functional group of VDOT engineers recommended a number of measures, including: (a) building dedicated truck climbing lanes at selected locations; (b) increasing the number of on- and off-ramps; (c) installing guardrails along narrow medians to help prevent crossover crashes; and (d) correcting horizontal curvature problems, among others.

Based on these recommendations and the Tier 1 EIS, FHWA concluded that there is an immediate need for smaller, independent safety and operational improvements along I-81. These short-term improvements include truck climbing lanes from approximately Milepost 195 to Milepost 202 northbound and Milepost 128 to 119 southbound with funding identified in SAFETEA-LU (FHWA 2007b).

This report compares alternative truck and lane management strategies along a significant grade section of I-81 in the state of Virginia. These strategies are compared in terms of the transportation system efficiency, energy consumption, environmental, and safety impacts using microscopic traffic simulation. The study then conducts a benefit-cost analysis to compare all alternatives in an objective manner. Network-level impacts are determined from an analysis of microscopic simulation results using the INTEGRATION traffic simulation software (Van Aerde and Rakha 2007a; Van Aerde and Rakha 2007b). Four scenarios are analyzed. The first scenario is the base case with no addition of lanes. The second scenario involves adding an additional lane from milepost 125 to 120.7 and restricting the median lane to cars only from milepost 128 to 118. The third scenario is identical to scenario 1, with one additional lane from milepost 128 to 118. The two leftmost lanes within the 4-lane sections are dedicated as car-only lanes while a single lane is dedicated to cars only for the section from milepost 125 to 120.7. The final scenario is identical to Scenario 3 with the addition of a forth lane from milepost 125 to 120.7 and restricting the two leftmost lanes to light-duty vehicles only.

The first section provides a brief background of the spatial and temporal scope of the Study Area, the concepts used to define the different management strategies and the measures of effectiveness (MOEs) considered as part of this study. Subsequently, a description of the calibration procedures that were utilized to calibrate the traffic simulation software, including the data collection efforts that were conducted and the input parameters is presented together with the procedures used to extrapolate future demands. The next section presents a summary of how the network was constructed and the results of the simulation runs. Subsequently, a benefit-cost analysis is described. Finally, the conclusions of the study are presented together with recommendations for further research.

2. BACKGROUND

This section first describes the spatial extent of the Study Area and describes the various concepts that were considered in the study. In addition, the section describes the unique features of the INTEGRATION software for the modeling of trucks and their impacts on traffic stream behavior. Finally, the section describes the various measures of effectiveness (MOEs) that were considered in the study. These measures include efficiency;

energy consumption; emissions of carbon monoxide (CO), carbon dioxide (CO_2), hydrocarbons (HC), oxides of nitrogen (NO_x), and particulate matter (PM); and safety.

2.1 Study Area

The study section is the southbound section of I-81 between milepost 132 and 118. This section is traveled by vehicles commuting to the Roanoke/Salem area, a metropolitan area of 200,000 people. The terrain along the I-81 Study Section varies from gently rolling to mountainous.

The Study Area is part of the corridor that connects the town of Blacksburg, City of Salem, and City of Roanoke. In addition to being used as a corridor for traffic to and from the Eastern and Western States, the corridor is heavily used by local traffic.

2.2 Managed-Lane Facilities

A managed-lane facility "is a lane that increases freeway efficiency by packaging various operational and design actions" (TXDOT 2004). Lane management operations may be adjusted at any time to better match regional goals. The restrictions that can be applied to this type of lane include: vehicle-type restrictions, allowing access for a specific type of vehicle; and time-of-day-restrictions, allowing access at certain periods or value pricing. The benefits of this type of lane are: maximizing existing capacity, improving safety, managing demand, reducing environmental impacts, and generating revenue (TXDOT 2004).

A 1999 report by the Virginia Department of Transportation (VDOT) used simulation to represent restricted truck lanes on specific sections of I-81 in Virginia (Hoel and Peek 1999). The conclusions of the report included: (1) restricting trucks from the use of the left lane along steep grade sections may decrease the traffic density and the number of lane changes, (2) restricting trucks from the right lane may increase the number of lane changes for sites without entry and exit ramps, (3) site characteristics have an impact on the effects of truck lane restrictions, and (4) trucks should be restricted from the left lanes on sections with grades of 4 percent or higher. Another traffic simulation study using VISSIM concluded that the practice of prohibiting trucks from the leftmost lane where there are three or more lanes of travel in a single direction has no negative effect on traffic safety or efficiency; furthermore, as the intensity of the uphill grade is increased, the operational benefits to lighter vehicles become sizable (Cate and Urbanik 2004).

2.3 Truck Climbing Lanes

A climbing lane is defined by AASHTO as an extra lane for a vehicle moving slowly uphill so that other vehicles using the normal lanes are not restricted and are able to pass the slower moving vehicle (AASHTO 1994). AASHTO recommends that a 16-km/h reduction criterion be used as the general guide for determining critical lengths of grades and locating truck-climbing lanes. Any one of the following criteria are used to justify climbing lanes: (1) upgrade traffic flow rate is in excess of 200 veh/h, (2) upgrade truck flow rate is in excess of 20 veh/h, or (3) either a 16 km/h or greater reduction in speed is expected for a typical truck, or Level-of-service E or F exists on the grade or a reduction of two or more levels of service is experienced when moving from the approach segment to the grade segment. The TruckSIM software (Rakha and Yu 2004), developed by Virginia Tech, provides a flexible tool for locating truck-climbing lanes that mimics the AASHTO procedures. Specifically, the software identifies the start and end points of climbing lanes considering the AASHTO criteria previously specified. The application of the model to the Study Area is discussed later in this report.

2.4 INTEGRATION Model Overview

This section provides a brief overview of the INTEGRATION software given that it was utilized to conduct the study. The INTEGRATION software is a microscopic traffic assignment and simulation software that was developed over the past decade (Van Aerde and Rakha 2007a; Van Aerde and Rakha 2007b; Van Aerde and Yagar 1988a; Van Aerde and Yagar 1988b). It was conceived as an integrated simulation and traffic assignment model and performs traffic simulations by tracking the movement of individual vehicles every 1/10th of a second. This allows detailed analyses of lane-changing movements and shock wave propagations. It also permits considerable flexibility in representing spatial and temporal variations in traffic conditions. In addition to estimating stops and delays (Dion et al. 2004; Rakha et al. 2001a; Rakha et al. 2000a), the model can also estimate the fuel consumed by individual vehicles, as well as the emissions (Ahn et al. 2004; Ahn et al. 2001; Rakha et al. 2004; Rakha et al. 2000b). Finally, the model also estimates the expected number of vehicle crashes using a time-based crash prediction model (Avgoustis et al. 2004). A more detailed description of the INTEGRATION modeling approach is provided in Appendix C.

The INTEGRATION model updates vehicle speeds every deci-second based on a user-specified steady-state spacing and the speed differential between the subject vehicle and the vehicle immediately ahead of it. In order to ensure realistic vehicle accelerations, the model uses a vehicle dynamics model that estimates the maximum vehicle acceleration level. Specifically, the model utilizes a variable power vehicle dynamics model to estimate the vehicle's tractive force that implicitly accounts for gear-shifting on vehicle acceleration. This model is described in more detail later in the literature (Rakha and Lucic 2002; Rakha et al. 2001b).

The car-following model is formulated as

$$u_n(t+\Delta t) = \min\left\{\begin{array}{l} u_n(t) + a_n(t)\Delta t, \\ \dfrac{-c_1' + c_3 u_f + \tilde{s}_n(t) - \sqrt{\left[c_1' - c_3 u_f - \tilde{s}_n(t)\right]^2 - 4c_3\left[\tilde{s}_n(t)u_f - c_1' u_f - c_2\right]}}{2c_3} \end{array}\right\} \quad [1]$$

The model constants are computed as

$c_1' = \dfrac{u_f}{k_j u_c^2}\left(2u_c - u_f\right) + \max\left(\dfrac{u_n^2(t) - u_{n-1}^2(t)}{2d}, 0\right); \quad c_2 = \dfrac{u_f}{k_j u_c^2}\left(u_f - u_c\right)^2; \quad c_3 = \dfrac{1}{q_c} - \dfrac{u_f}{k_j u_c^2}$; and the vehicle spacing is computed as

$$\tilde{s}_n(t) = x_{n-1}(t) - x_n(t) + \left[u_{n-1}(t+\Delta t) - u_n(t)\right]\Delta t + 0.5 a_{n-1}(t+\Delta t)\Delta t^2 .$$

Here $u_n(t+\Delta t)$ is the speed of the following vehicle (vehicle n) at time $t+\Delta t$; $a_n(t)$ is the acceleration of the subject vehicle (vehicle n); u_f is the roadway mean free-flow speed; u_c is the roadway mean speed-at-capacity; q_c is the roadway mean capacity; k_j is the roadway mean jam density; $x_n(t)$ is the position of the subject vehicle at time t; and $x_{n-1}(t)$ is the position of the lead vehicle at time t. This model ensures that the vehicle acceleration does not exceed the vehicle dynamics maximum acceleration level.

The INTEGRATION model computes a number of MOEs, including the network efficiency. Efficiency evaluation of highway alternatives involves computing the average speed and vehicle delay. The average vehicle speed is computed as the average of all vehicle speeds, where the vehicle speed is computed as the trip distance divided by the trip duration. Conversely, the instantaneous delay incurred by a vehicle over a given interval can be estimated as the difference between the time it would take the vehicle to complete its trip while traveling at the free-flow speed of the facility and the time the vehicle actually took. As expressed by Equation 1, the total delay would then be obtained by summing the delays incurred in all intervals comprised within the recorded trip. Subsequently, the delay is computed for all vehicles within the network.

$$D = \sum_{i=1}^{N} d_i = \sum_{i=1}^{N}\left(1 - \frac{u(t+i\Delta t)}{u_f}\right)\cdot \Delta t \quad [2]$$

Where D is the total delay incurred over entire trip; d_i is the delay incurred during interval i; Δt is the duration of interval; $u(t+i\Delta t)$ is the vehicle instantaneous speed in interval i; u_f is the expected free-flow speed of the facility on which the vehicle is traveling; and N is the number of time intervals in a speed profile. This model has been validated against state-of-the-art delay estimation procedures using queuing theory and shockwave analysis (Dion et al. 2004).

Second-by-second speed and acceleration data in conjunction with microscopic fuel consumption and emission models are used to estimate a vehicle's instantaneous fuel consumption and emission rate. From a general point of view, the use of instantaneous speed and acceleration data for the estimation of energy and emission impacts of traffic improvement projects provide a major advantage over state-of-practice methods that estimate vehicle fuel consumption and emissions based exclusively on the average speed and number of vehicle miles traveled by vehicles on a given transportation link. These methods assume that differences in driver behavior can be neglected and implicitly assume that all vehicles traveling on a link pollute similarly for an identical average speed and vehicle-miles traveled. In reality, different speed and acceleration profiles with the same average speed and vehicle-miles traveled could result in different levels of fuel consumption and emissions. As with fuel consumption models, the emission models are sensitive to the instantaneous-vehicle speed and acceleration levels. Applications of these models have shown that the emission of compounds, hot-stabilized tail-pipe hydrocarbon (HC), carbon monoxide (CO), carbon dioxide (CO_2), oxides of nitrogen (NO_x), and particulate matter (PM) are related to vehicle travel time, distance, speed, and fuel consumption in an often highly nonlinear fashion. Consequently, traffic management strategies that may have a significant positive impact on one measure are not always guaranteed to have an impact of the same magnitude or even sign on any of the other measures. A more detailed description of INTEGRATION's energy and emission modeling approach is provided in Appendix C.

The INTEGRATION model computes the speed of vehicles each deci-second. This permits the steady-state fuel consumption rate for each vehicle to be computed each second on the basis of its current instantaneous speed and acceleration level (Ahn et al. 2004; Ahn et al. 2001; Rakha and Ahn 2004; Rakha et al. 2003; Rakha et al. 2004; Rakha et al. 2000b). These models were developed using data that were collected on a chassis dynamometer at the Oak Ridge National Labs (ORNL), data gathered by the Environmental Protection Agency (EPA), and data gathered using an on-board emission measurement device (OBD). The models use instantaneous speed and acceleration levels as independent variables. Vehicle accelerations have significant impacts of vehicle fuel consumption rates especially at high speeds with the resulting high engine loads. The fuel consumption analysis features are built into the model and are executed every second for every vehicle in the network. They are applied in a fashion that is consistent across all facility types, operating regimes, and control strategies. This consistent internal use permits a very objective assessment of the fuel consumption implications across a wide range of potential traffic or demand management strategies.

As was mentioned earlier the INTEGRATION software incorporates a variable power vehicle dynamics model that computes the vehicle's tractive effort, aerodynamic, rolling, and grade-resistance forces, as described in detail in the literature (Rakha and Lucic 2002; Rakha et al. 2001b). The INTEGRATION model has not only been validated against standard traffic flow theory (Dion et al. 2004; Rakha and Crowther 2002; Rakha and Crowther 2003; Rakha et al. 2001a), but also has been utilized for the evaluation of real-life applications (Rakha 1990; Rakha et al. 2005a; Rakha et al. 1998). The types of analyses that can be performed with these built-in models extend far beyond the capabilities of EPA's MOBILE5 model (Park and Rakha 2006; Rakha et al. 2003).

The INTEGRATION software uses a safety model that was developed using the US national crash statistics. The model computes the crash risk for 14 different crash types as a function of the facility speed limit and a time-dependent measure of exposure (Avgoustis et al. 2004). The use of a time-dependent measure of exposure allows the model to capture differences in the crash risk that result from differences in the network efficiency. The model also computes the vehicle damage and level of injury to the passengers involved in the crash based on the vehicle's instantaneous speed. The use of the instantaneous speed means that the crash damage and injury level is responsive to the level of congestion. Consequently, the model can capture the safety impacts of operational-level alternatives including Intelligent Transportation Systems (ITS's). A field and simulation application of the model indicated that it produces results that are consistent with the General Estimates System national database. Furthermore, the results indicate that the model can be applied to evaluate the safety impacts of alternative traffic-flow improvement projects, like for example lane management strategies. A more detailed description of the INTEGRATION safety modeling framework is provided in Appendix D.

3. TRAFFIC ANALYSIS

This section describes how the link flows were forecast and how the traffic demands were calibrated using the link flows. The traffic demands were then input to the traffic simulation software to model different scenarios for various horizon years.

The 2004 existing peak hour traffic volumes and the 2035 design hour traffic volumes were provided in the I-81 Corridor Improvement Study Technical Report, as illustrated in Figure 1 (heavy vehicle counts are in parethesis). Using the two sets of volume counts link specific growth rates were computed, as summarized in Table 1. These growth rates varied between 0.0% and 3.6% in the case of light duty vehicles and 2.3% and 3.0% in the case of the heavy duty trucks depending on the link under consideration.

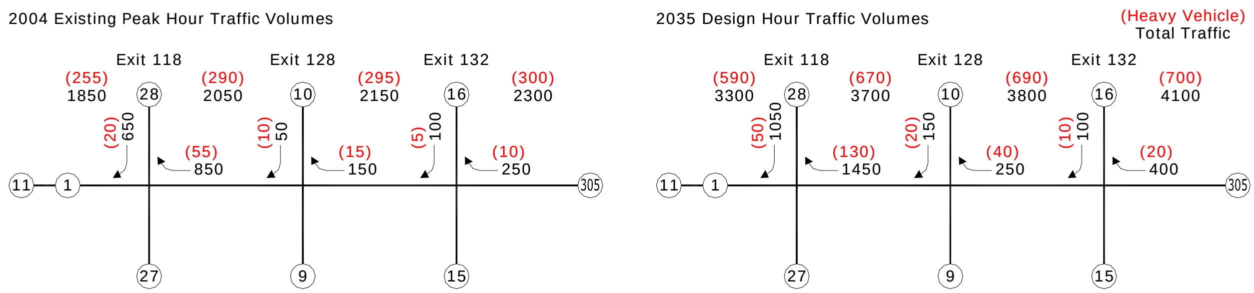

Figure 1: 2004 Peak Hour Volumes & 2035 Design Hour Volumes

Table 1: Annual Growth Rates

Classification	Link		2004		2035		Annual Growth Rates	
	From	To	PHTV[1]	PHHVV[2]	DHTV[3]	DHHVV[4]	DHTV	DHHVV
Through Traffic	Exit 137	Exit 132	2300	300	4100	700	1.9%	2.8%
	Exit 132	Exit 128	2150	295	3800	690	1.9%	2.8%
	Exit 128	Exit 118	2050	290	3700	670	1.9%	2.7%
	Exit 118	Exit 114	1850	255	3300	590	1.9%	2.7%
Local Traffic	Exit 137	Exit 132 Out	250	10	400	20	1.5%	2.3%
	Exit 132 In	Exit 128	100	5	100	10	0.0%	2.3%
	Exit 132	Exit 128 Out	150	15	250	40	1.7%	3.2%
	Exit 128 In	Exit 118	50	10	150	20	3.6%	2.3%
	Exit 128	Exit 118 Out	850	55	1450	130	1.7%	2.8%
	Exit 118 In	Exit 114	650	20	1050	50	1.6%	3.0%

1. PHTV: Peak Hour Traffic Volume
2. PHHVV: Peak Hour Heavy Vehicle Volume
3. DHTV: Design Hour Traffic Volume
4. DHHVV: Design Hour Heavy Vehicle Volume

Using the average annual growth rates, the traffic volumes for 2010, 2015, 2020, 2025, and 2030 were computed and, as summarized in Table 2.

Table 2: Link Volume Projections

	Link		2010		2015		2020		2025		2030		2035	
	From	To	Car	Truck	Car	Truck	Car	Truck	Car	Truck	Car	Truck	Car	Truck
Through Traffic	Exit 137	Exit 132	2219	353	2419	405	2635	465	2869	533	3124	611	3400	700
	Exit 132	Exit 128	2053	348	2233	399	2428	457	2637	525	2864	602	3110	690
	Exit 128	Exit 118	1957	341	2138	390	2333	447	2547	511	2779	585	3030	670
	Exit 118	Exit 114	1769	300	1929	343	2101	393	2288	450	2491	515	2710	590
Local Traffic	Exit 137	Exit 132 Out	263	11	282	13	305	14	328	16	353	18	380	20
	Exit 132 In	Exit 128	94	6	94	6	93	7	92	8	91	9	90	10
	Exit 132	Exit 128 Out	148	18	159	21	170	25	183	29	196	34	210	40
	Exit 128 In	Exit 118	51	11	61	13	74	14	89	16	108	18	130	20
	Exit 128	Exit 118 Out	878	65	952	75	1034	86	1123	98	1217	113	1320	130
	Exit 118 In	Exit 114	689	24	743	28	801	32	863	37	929	43	1000	50

3.1 Traffic Data collection and Demand Calibration

Given the projected traffic volumes, the next step in the analysis was to compute the O-D matrix for use as input to the simulation software. This section describes the calibration of O-D demands.

The calibration of O-D demands to field observed link flows is a problem that has been the focus of extensive research. The most renowned of the approaches is the maximum likelihood approach that was first formulated by Van Zuylen and Willumsen (Van Zuylen and Willumsen 1980) and Willumsen (Willumsen 1978) and by Van Aerde *et al*. . The traffic demands for the individual model years were estimated using a maximum likelihood synthetic O-D estimation software entitled QUEENSOD (Hellinga and Van Aerde 1998; Rakha et al. 2005b; Van Aerde et al. 1993; Van Aerde et al. 2003). The QUEENSOD software estimates the maximum likelihood O-D table that replicates the observed link flows (projected link flows here) solving Equation [3]. The numerical solution begins by building a minimum path tree and performing an all-or-nothing traffic assignment of the seed matrix. A relative or absolute link flow error is computed depending on user input. Using the link-flow errors, O-D adjustment factors are computed and utilized to modify the seed O-D matrix. The adjustment of the O-D matrix continues until one of two criteria are met, namely the change in O-D error reaches a user-specified minimum or the number of iterations criterion is met.

$$\text{Max.} \quad T\ln\left(\frac{T}{t}\right)-\sum_{ij}T_{ij}\ln\left(\frac{T_{ij}}{t_{ij}}\right)-\sum_{ij}\left(\lambda_{ij}\cdot 2\left(\sum_{a}\left(V_a\cdot p_{ij}^{a}\right)-\left(\sum_{a}p_{ij}^{a}\left(\sum_{xy}T_{xy}p_{xy}^{a}\right)\right)\right)\right) \qquad [3]$$

Where T_{ij} is the estimated number of trips between zones *i* and *j* for the analysis period for all trip purposes; t_{ij} = is the seed trips between zones *i* and *j;* T is the total number of trips ($\Sigma\Sigma T_{ij} = T$); t is the total number of trips based on seed O-D matrix ($\Sigma\Sigma t_{ij} = t$); p^{a}_{ij} is the probability of O-D pair *ij* to utilize link *a;* λ_{ij} is the Lagrange multiplier for O-D pair *ij*; and V_a is the actual observed link volume on link *a*.

The traffic link flow data were input to the QueensOD software to estimate a synthetic O-D table. The projected flows together with the flows predicted by QueensOD by assigning the traffic demand to the network are shown in Figure 2. Figure 2 clearly demonstrates a high level of consistency between the model output and projected link flows with R^2 ranging from 0.9854 to 0.9857 for cars and 0.9825 to 0.9830 for trucks, respectively.

(a) 2010

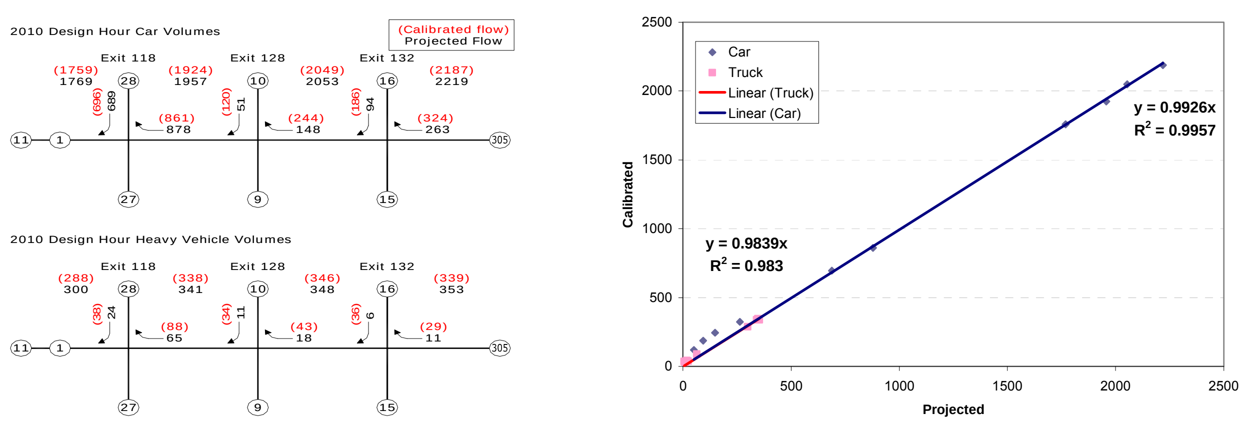

(b) 2015

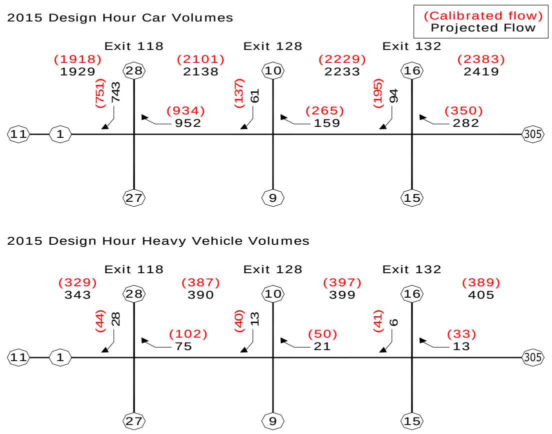

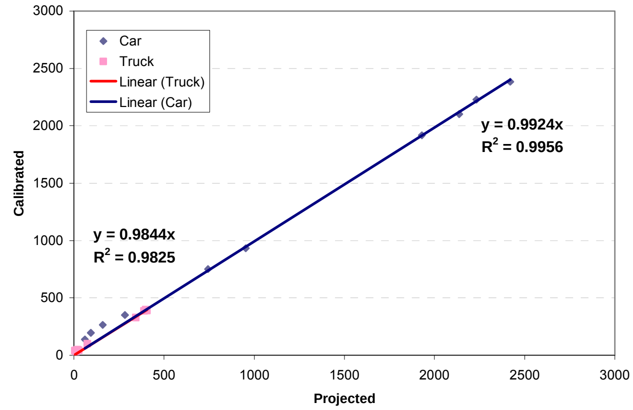

(c) 2020

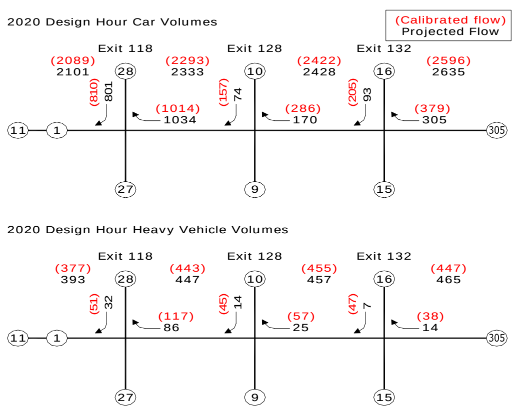

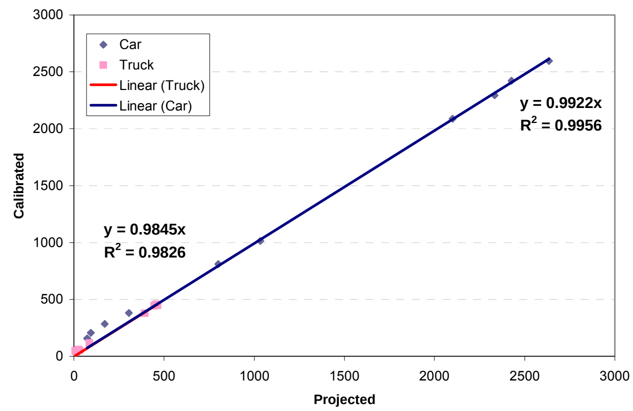

(d) 2025

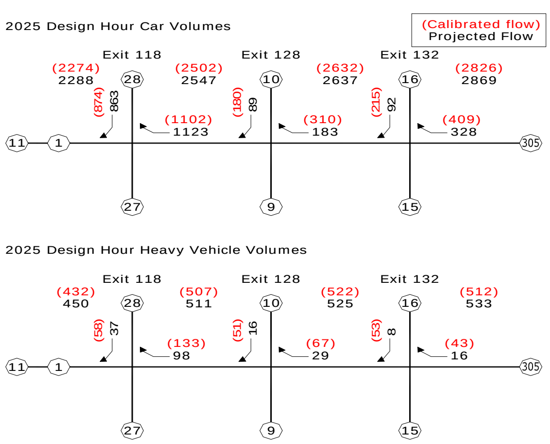

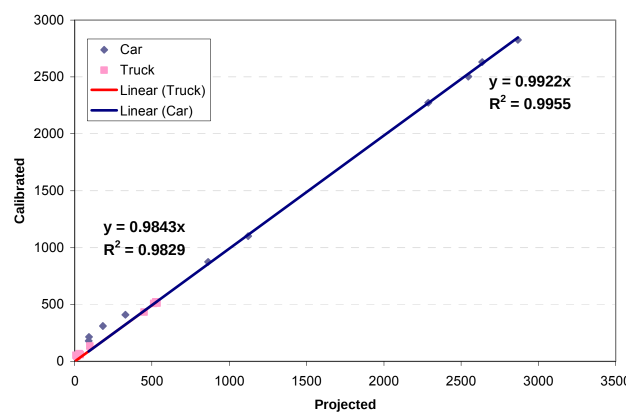

(e) 2030

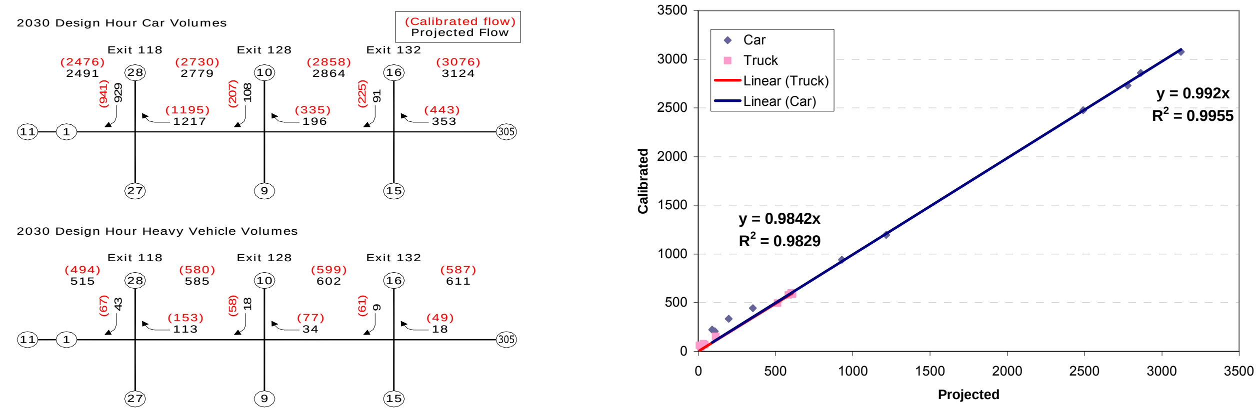

(f) 2035

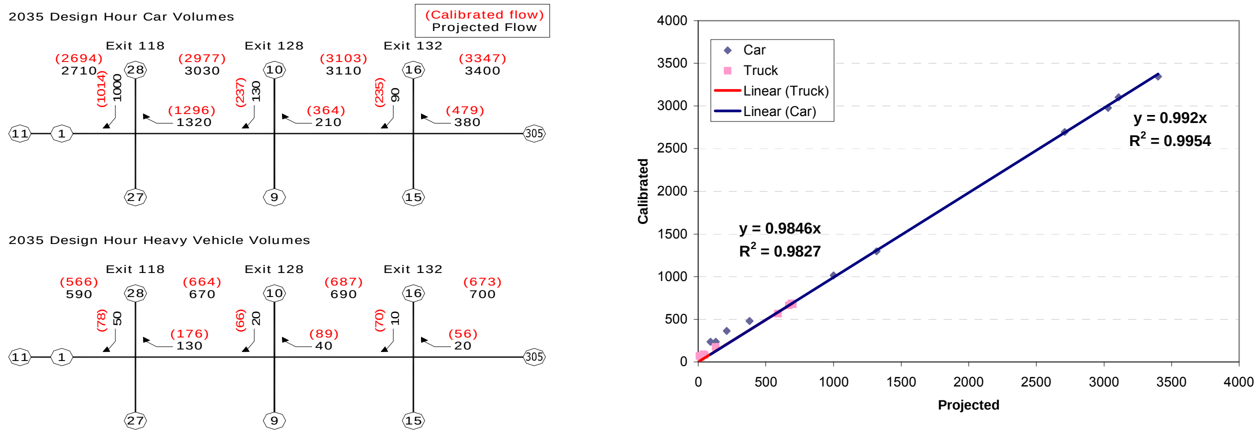

Figure 2: Projected and Calibrated Traffic Volumes (Scatter Plot and Fitted Regression Line)

3.2 Simulation Model Construction

The simulation network construction involved building a network from AutoCAD designs. This design was used to define the horizontal and vertical profile with a high degree of accuracy. Base lane characteristics in terms of capacity, free-flow speed, speed-at-capacity, and jam density were derived using the Highway Capacity Manual (HCM) procedures for a basic freeway section. The impact on lane changing and heavy vehicles on the base roadway parameters was captured using the simulation software. These impacts have been validated in a number of studies (Al-Kaisy et al. 2005; Rakha and Zhang 2004).

Trucks were modelled based on an earlier research effort that characterized the trucks along the study section of I-81 (Rakha and Lucic 2002; Rakha et al. 2001b). The data, which were collected between 1998 and 2000, are summarized in Table 3. Two types of trucks were modeled, namely; truck types 1, 2, 3, 4, and 5 where modeled as Truck Type 1 (67%) and types 6 and 7 where modeled as Truck Type 2 (33 %) as shown in Table 4.

Table 3: I-81 Truck Characteristics

Classification	Truck 1	Truck 2	Truck 3	Truck 4	Truck 5	Truck 6	Truck 7
Mass (Kg)	7500	12500	17500	22500	27500	32500	37500
Length (m)	16	16	16	16	16	16	16
% Mass on Tractive Axle	0.3	0.3	0.3	0.3	0.3	0.3	0.3
Friction Coeff.	0.5	0.5	0.5	0.5	0.5	0.5	0.5
Power (kW)	350	350	350	350	350	350	350
Transmission Efficiency	0.88	0.88	0.88	0.88	0.88	0.88	0.88
Drag Coef.	0.58	0.58	0.58	0.58	0.58	0.58	0.58
Front Area	10.7	10.7	10.7	10.7	10.7	10.7	10.7
Rolling Coef. 1	1.75	1.75	1.75	1.75	1.75	1.75	1.75
Rolling Coef. 2	0.033	0.033	0.033	0.033	0.033	0.033	0.033
Rolling Coef. 3	4.575	4.575	4.575	4.575	4.575	4.575	4.575
% to the total	0.04	0.15	0.17	0.16	0.16	0.27	0.06

Table 4: Modeled Truck Types

Classification	Truck 1	Truck 2
Mass (Kg)	20411	31751
Length (m)	16	16
%Mass on Axle:	0.3	0.3
Friction Coef.	0.5	0.5
Power (kW)	336	261
Transmission Efficiency	0.88	0.88
Drag Coef.	0.58	0.58
Front Area	10.7	10.7
Rolling Coef. 1	1.75	1.75
Rolling Coef. 2	0.033	0.033
Rolling Coef. 3	4.575	4.575
% to the total	0.67	0.33

Light duty vehicles were modelled as light-duty vehicle 3 (LDV3), which is a vehicle of model year 1995 or later, an engine size less than 3.2 L, and an average mileage of less than 83,653 km. The use of different vehicle types would affect the absolute fuel consumption and emission estimates of the various scenarios, but should not affect the relative values given that all scenarios were modeled using the same vehicle composition.

Existing truck climbing lanes were coded. A truck climbing lane is identified when the truck speed is 10 mi/h lower than the regular traffic speed. The truck climbing lanes were located between mileposts 128.1 and 125.0 and between milepost 120.7 and 119.6.

4. EVALUATION OF ALTERNATIVE LANE MANAGEMENT STRATEGIES

The analysis considered four scenarios that involved different strategies for managing truck and general purpose lanes, including the “Do-Nothing” scenario. These strategies included modifications to three sub-sections along I-81, as summarized in Table 5. The scenarios are as follows:

- **Scenario 1 (S1). Do-nothing:** Represents the base case do-nothing scenario.
- **Scenario 2 (S2).** This scenario involves the addition of a single lane along section 2 (milepost 125 to 120.7). In addition, the leftmost lane is restricted to light duty vehicles for the three sub-sections (from milepost 128.1 to 119.6).
- **Scenario 3 (S3).** This scenario involved the addition of a single lane across all three sub-sections (i.e. from milepost 128.1 to 119.6). The two leftmost lanes were restricted to light duty vehicles for sub-sections 1 and 2 while the leftmost lane was restricted to light duty vehicles along the 3-lane sub-section from milepost 125.0 to 120.7 (sub-section 2).
- **Scenario 4 (S4).** This scenario was identical to scenario 3 with the addition of a forth lane along sub-section 2 (from milepost 125.0 to 120.7). The two leftmost lanes were restricted to light duty vehicles for sub-sections 1 and 2 while the leftmost lane was restricted to light duty vehicles along the sub-section 2.

Table 5: Composition of Number of Lanes for Each Scenario

Classification	Milepost		Number of lanes			
	Begin	End	Scenario 1	Scenario 2	Scenario 3	Scenario 4
Section 1	128.1	125.0	3	3	4	4
Section 2	125.0	120.7	2	3	3	4
Section 3	120.7	119.6	3	3	4	4

Having generated the O-D tables for the model years of 2004 through 2035 at 5-year increments, the individual scenarios were simulated using the INTEGRATION microscopic traffic simulation software. Specifically, each scenario was simulated 20 times with a different random number seed for each model year to introduce randomness into the simulation results. Thus, a total of 560 simulation runs were conducted (20 random number seeds x 4 scenarios x 7 model years).

The number of lanes at the network entrance (milepost 133.6 to 128.1) was increased from two lanes to four lanes in order to ensure that the total demand could be loaded onto the study section from milepost 128.1 to 119.6. Simulation runs with two lanes at the entrance section resulted in a bottleneck upstream of milepost 128.1 and thus the flow along this section did not reflect the actual demand; instead it reflected the capacity of the bottleneck. Consequently, the benefits of adding additional lanes along the study section would be minimal given lower demand.

Table 6 shows the average travel time and speed (averaged over the 20 seed runs) for the four scenarios for the different vehicle types. The numbers shown as a percentage are the relative difference between scenario 1 and other scenarios. For example, Scenario 2 produces a 1.6% reduction in travel time when compared to the base case. The results demonstrate that, as would be expected, Scenario 4 produces the largest benefits in terms of reduction in travel time and increase in travel speed. Similarly, Scenario 3 produces benefits over Scenario 2 for light duty vehicles and for overall system-wide benefit. However, because Scenario 3 involves trucks having to shift lanes at the end of the first climbing lane section (at milepost 125.0) the benefits to trucks in Scenario 3 is less than that in Scenario 2. It should be noted that the relative benefits associated with each of the scenarios increases as time progresses given that they have to accommodate higher traffic demand levels. Furthermore, the relative difference across scenarios also increases with time. For example, reductions in average travel times of 5.3%, 7.9%, and 9.3% are achievable in the target 2035 year for Scenarios 2, 3, and 4, respectively.

The average speed across the various scenarios, considering the base year of 2004, ranges between 61.38 and 63.25 mi/h for Scenarios 1 through 4, respectively. Light duty vehicles travel at speeds ranging from 64.7 to 66.6 mi/h while the average speed of the heavy duty trucks is much lower ranging from 46.63 to 47.93 mi/h. These results are consistent with field observations of the existing conditions and thus the simulation results appear to be consistent with field conditions for the base year.

Table 6: Comparison of Scenarios in Terms of Average Travel Time and Speed by Vehicle Types

MOE	Year	All				Cars				Trucks			
		Sc. 1	Sc. 2	Sc. 3	Sc. 4	Sc. 1	Sc. 2	Sc. 3	Sc. 4	Sc. 1	Sc. 2	Sc. 3	Sc. 4
Average Travel Time (min/veh)	2004	11.53	11.35 -1.6%	11.26 -2.3%	11.18 -3.0%	10.69	10.53 -1.5%	10.43 -2.4%	10.38 -2.9%	17.83	17.51 -1.8%	17.53 -1.7%	17.27 -3.1%
	2010	11.80	11.57 -1.9%	11.48 -2.7%	11.38 -3.5%	10.90	10.70 -1.8%	10.58 -2.9%	10.51 -3.6%	18.20	17.79 -2.2%	17.91 -1.6%	17.57 -3.5%
	2015	12.06	11.80 -2.2%	11.69 -3.1%	11.57 -4.0%	11.11	10.88 -2.1%	10.73 -3.4%	10.65 -4.1%	18.49	18.00 -2.6%	18.16 -1.8%	17.79 -3.8%
	2020	12.48	12.18 -2.4%	12.01 -3.8%	11.87 -4.9%	11.43	11.17 -2.2%	10.95 -4.2%	10.86 -5.0%	19.21	18.61 -3.1%	18.75 -2.4%	18.39 -4.3%
	2025	13.20	12.80 -3.0%	12.51 -5.2%	12.32 -6.6%	11.97	11.65 -2.7%	11.30 -5.6%	11.16 -6.7%	20.66	19.77 -4.3%	19.91 -3.6%	19.37 -6.2%
	2030	14.31	13.78 -3.7%	13.37 -6.5%	13.18 -7.9%	12.77	12.36 -3.2%	11.88 -7.0%	11.75 -8.0%	23.12	21.92 -5.2%	21.93 -5.1%	21.36 -7.6%
	2035	16.39	15.52 -5.3%	15.09 -7.9%	14.87 -9.3%	14.48	13.88 -4.1%	13.32 -8.0%	13.21 -8.7%	26.84	24.51 -8.7%	24.71 -7.9%	23.89 -11.0%
Travel Speed (mph)	2004	61.38	62.35 1.6%	62.81 2.3%	63.25 3.0%	64.67	65.66 1.5%	66.27 2.5%	66.62 3.0%	46.43	47.29 1.8%	47.24 1.7%	47.93 3.2%
	2010	60.21	61.38 1.9%	61.86 2.7%	62.41 3.7%	63.65	64.84 1.9%	65.57 3.0%	65.99 3.7%	45.53	46.58 2.3%	46.28 1.6%	47.17 3.6%
	2015	59.11	60.42 2.2%	60.97 3.1%	61.59 4.2%	62.65	63.97 2.1%	64.83 3.5%	65.33 4.3%	44.74	45.96 2.7%	45.57 1.8%	46.50 3.9%
	2020	57.31	58.74 2.5%	59.57 3.9%	60.23 5.1%	61.05	62.45 2.3%	63.70 4.3%	64.26 5.3%	43.08	44.48 3.3%	44.13 2.4%	45.01 4.5%
	2025	54.37	56.07 3.1%	57.33 5.5%	58.23 7.1%	58.45	60.07 2.8%	61.94 6.0%	62.68 7.2%	40.00	41.80 4.5%	41.50 3.8%	42.66 6.6%
	2030	50.31	52.25 3.8%	53.83 7.0%	54.63 8.6%	54.91	56.75 3.4%	59.03 7.5%	59.69 8.7%	35.72	37.67 5.5%	37.66 5.4%	38.66 8.2%
	2035	44.05	46.51 5.6%	47.87 8.7%	48.58 10.3%	48.56	50.67 4.3%	52.79 8.7%	53.23 9.6%	30.76	33.69 9.5%	33.42 8.6%	34.57 12.4%

The impact of the various scenarios on vehicle fuel consumption and emissions indicates that fuel consumption rates are almost constant, as summarized in Table 7. Similar to Table 6, the numbers shown as percentage are the relative difference between each scenario and Scenario 1. In the case of HC emissions Scenario 4 produces the largest decrease in emissions for all vehicles, cars, and trucks. Scenario 3 outperforms Scenario 2 when all vehicles are considered and for light duty vehicles. However, in the case of trucks Scenario 2 outperforms Scenario 3. Similar results are observed for CO emissions; however, system-wide NOx emissions are minimized in Scenarios 2 and 4. When the results are analyzed for light duty vehicles only, Scenario 1 outperforms all the other scenarios, with Scenario 4 being the worst scenario, then 3, then 2. In the case of trucks, both Scenario 2 and 4 outperform Scenario 3 producing similar results.

In terms of crash rates, the study demonstrates significant reductions as a result of the various scenarios. The safety benefits increase as time progresses from the 2004 base year to the 2035 target year. Specifically, reductions in the total number of crashes range from 1.5% to 2.2% to 2.9% for Scenarios 2, 3, and 4 for the 2004 base year, respectively for the 2004 base year. These benefits increase to 4.8%, 7.6%, and 8.9% for Scenarios 2, 3, and 4, respectively for the 2035 target year. A more detailed presentation of the results is presented in Appendix A.

Table 7: Comparison of Scenario in Terms of Fuel Consumption and Emissions by Vehicle Types

MOE	Year	All				Cars				Trucks			
		Sc. 1	Sc. 2	Sc. 3	Sc. 4	Sc. 1	Sc. 2	Sc. 3	Sc. 4	Sc. 1	Sc. 2	Sc. 3	Sc. 4
Fuel (L/veh)	2004	1.98	1.97 -0.5%	1.99 0.3%	1.98 -0.1%	1.53	1.54 0.1%	1.54 0.5%	1.54 0.7%	5.39	5.29 -1.7%	5.38 -0.2%	5.30 -1.6%
	2010	2.01	2.00 -0.5%	2.01 0.2%	2.00 -0.2%	1.54	1.54 0.0%	1.55 0.4%	1.55 0.6%	5.31	5.23 -1.5%	5.30 -0.2%	5.21 -1.9%
	2015	2.03	2.02 -0.6%	2.03 0.0%	2.03 -0.4%	1.55	1.55 -0.2%	1.55 0.3%	1.56 0.5%	5.31	5.23 -1.5%	5.28 -0.5%	5.19 -2.2%
	2020	2.06	2.05 -0.8%	2.06 -0.1%	2.05 -0.7%	1.56	1.56 -0.3%	1.56 0.0%	1.56 0.2%	5.28	5.20 -1.6%	5.26 -0.5%	5.16 -2.3%
	2025	2.11	2.09 -1.1%	2.10 -0.5%	2.09 -1.2%	1.58	1.57 -0.5%	1.57 -0.4%	1.58 -0.3%	5.36	5.24 -2.1%	5.32 -0.7%	5.20 -2.8%
	2030	2.17	2.15 -1.3%	2.15 -1.0%	2.14 -1.5%	1.61	1.59 -0.8%	1.59 -0.9%	1.59 -0.7%	5.45	5.32 -2.3%	5.39 -1.1%	5.29 -2.8%
	2035	2.26	2.23 -1.6%	2.23 -1.2%	2.22 -1.9%	1.65	1.64 -1.0%	1.63 -1.1%	1.64 -1.0%	5.60	5.45 -2.7%	5.52 -1.4%	5.41 -3.3%
HC (g/veh)	2004	1.85	1.77 -4.3%	1.73 -6.2%	1.69 -8.4%	1.19	1.11 -6.3%	1.07 -10.1%	1.04 -12.8%	6.84	6.72 -1.8%	6.77 -1.0%	6.67 -2.5%
	2010	1.94	1.85 -4.5%	1.82 -6.2%	1.77 -8.8%	1.24	1.16 -6.5%	1.12 -10.3%	1.08 -13.5%	6.90	6.76 -1.9%	6.83 -0.9%	6.70 -2.8%
	2015	2.02	1.93 -4.7%	1.90 -6.1%	1.84 -8.9%	1.29	1.20 -6.8%	1.16 -10.1%	1.12 -13.6%	6.96	6.81 -2.2%	6.88 -1.2%	6.75 -3.1%
	2020	2.11	2.02 -4.4%	1.99 -5.5%	1.93 -8.5%	1.33	1.25 -5.9%	1.21 -8.9%	1.16 -12.8%	7.10	6.92 -2.5%	7.00 -1.5%	6.86 -3.4%
	2025	2.22	2.13 -4.3%	2.12 -4.5%	2.05 -8.0%	1.37	1.30 -5.1%	1.28 -6.7%	1.22 -11.0%	7.40	7.15 -3.4%	7.25 -2.1%	7.07 -4.5%
	2030	2.36	2.27 -3.8%	2.27 -3.6%	2.20 -6.9%	1.40	1.35 -3.8%	1.34 -4.3%	1.28 -8.5%	7.84	7.53 -3.9%	7.61 -2.9%	7.43 -5.2%
	2035	2.53	2.42 -4.4%	2.44 -3.4%	2.37 -6.4%	1.44	1.40 -3.3%	1.41 -2.4%	1.36 -6.1%	8.45	7.99 -5.4%	8.09 -4.3%	7.88 -6.8%
CO (g/veh)	2004	251.19	210.97 -16.0%	184.60 -26.5%	168.07 -33.1%	280.36	234.98 -16.2%	205.10 -26.8%	186.52 -33.5%	30.50	29.30 -3.9%	29.48 -3.4%	28.51 -6.5%
	2010	279.93	236.55 -15.5%	208.16 -25.6%	187.89 -32.9%	314.85	265.58 -15.6%	233.12 -26.0%	210.18 -33.2%	31.47	30.01 -4.6%	30.54 -3.0%	29.28 -7.0%
	2015	304.20	257.94 -15.2%	231.25 -24.0%	207.71 -31.7%	344.51	291.64 -15.3%	260.89 -24.3%	234.06 -32.1%	32.29	30.57 -5.4%	31.27 -3.2%	29.90 -7.4%
	2020	324.30	282.59 -12.9%	256.99 -20.8%	229.11 -29.4%	369.72	321.80 -13.0%	292.06 -21.0%	260.05 -29.7%	33.67	31.70 -5.9%	32.56 -3.3%	31.09 -7.7%
	2025	346.19	308.07 -11.0%	291.94 -15.7%	259.16 -25.1%	397.39	353.39 -11.1%	334.40 -15.9%	296.51 -25.4%	35.52	33.08 -6.8%	34.29 -3.4%	32.54 -8.4%
	2030	363.61	334.66 -8.0%	325.14 -10.6%	292.22 -19.6%	420.32	386.80 -8.0%	375.42 -10.7%	337.08 -19.8%	37.42	34.77 -7.1%	35.94 -4.0%	34.17 -8.7%
	2035	384.41	358.88 -6.6%	358.03 -6.9%	327.91 -14.7%	447.57	417.90 -6.6%	416.72 -6.9%	381.39 -14.8%	39.64	36.76 -7.3%	37.70 -4.9%	35.98 -9.2%
NO_x (g/veh)	2004	17.70	17.57 -0.7%	17.81 0.6%	17.68 -0.1%	3.40	3.44 1.1%	3.47 1.9%	3.48 2.3%	125.89	124.53 -1.1%	126.37 0.4%	125.18 -0.6%
	2010	18.18	18.11 -0.4%	18.30 0.7%	18.14 -0.2%	3.38	3.43 1.3%	3.46 2.3%	3.47 2.7%	123.46	122.57 -0.7%	123.91 0.4%	122.51 -0.8%
	2015	18.82	18.76 -0.3%	18.90 0.4%	18.75 -0.4%	3.37	3.42 1.4%	3.45 2.5%	3.47 3.1%	123.08	122.33 -0.6%	123.13 0.0%	121.86 -1.0%
	2020	19.35	19.29 -0.3%	19.44 0.4%	19.28 -0.4%	3.35	3.40 1.5%	3.44 2.8%	3.46 3.4%	121.78	121.00 -0.6%	121.79 0.0%	120.50 -1.0%
	2025	20.30	20.14 -0.8%	20.32 0.1%	20.12 -0.9%	3.33	3.38 1.6%	3.42 2.8%	3.45 3.7%	123.25	121.80 -1.2%	122.83 -0.3%	121.24 -1.6%
	2030	21.39	21.20 -0.9%	21.35 -0.2%	21.21 -0.9%	3.31	3.35 1.4%	3.40 3.0%	3.43 3.8%	125.43	123.83 -1.3%	124.55 -0.7%	123.45 -1.6%
	2035	22.78	22.44 -1.5%	22.65 -0.6%	22.44 -1.5%	3.26	3.31 1.5%	3.37 3.4%	3.40 4.2%	129.33	126.89 -1.9%	127.86 -1.1%	126.39 -2.3%

Table 8: Comparison of Scenarios in Terms of Crash Related MEOs by Vehicle Types

CMOE	Year	All				Cars				Trucks			
		Sc. 1	Sc. 2	Sc. 3	Sc. 4	Sc. 1	Sc. 2	Sc. 3	Sc. 4	Sc. 1	Sc. 2	Sc. 3	Sc. 4
Expected number of Crashes/ Million VMT	2004	1.28	1.26	1.25	1.24	1.21	1.18	1.17	1.16	1.73	1.73	1.74	1.72
			-1.51%	-2.23%	-2.87%		-1.90%	-2.91%	-3.42%		0.20%	0.80%	-0.44%
	2010	1.30	1.28	1.27	1.26	1.22	1.20	1.18	1.17	1.77	1.77	1.79	1.76
			-1.84%	-2.63%	-3.45%		-2.27%	-3.60%	-4.19%		-0.09%	1.37%	-0.41%
	2015	1.33	1.30	1.29	1.27	1.24	1.21	1.19	1.18	1.81	1.81	1.84	1.80
			-2.09%	-3.02%	-3.95%		-2.53%	-4.23%	-4.86%		-0.39%	1.71%	-0.42%
	2020	1.37	1.34	1.32	1.31	1.27	1.24	1.21	1.20	1.91	1.89	1.92	1.89
			-2.30%	-3.87%	-4.85%		-2.68%	-5.13%	-5.84%		-0.93%	0.65%	-1.30%
	2025	1.46	1.41	1.37	1.35	1.33	1.29	1.24	1.23	2.09	2.05	2.06	2.00
			-2.85%	-5.60%	-6.95%		-3.20%	-6.82%	-7.78%		-1.73%	-1.57%	-4.23%
	2030	1.59	1.53	1.48	1.46	1.43	1.38	1.32	1.30	2.35	2.30	2.27	2.21
			-3.48%	-7.05%	-8.26%		-3.97%	-8.27%	-9.01%		-2.01%	-3.38%	-6.02%
	2035	1.83	1.74	1.69	1.67	1.61	1.52	1.47	1.46	2.85	2.74	2.70	2.63
			-4.80%	-7.64%	-8.88%		-5.18%	-8.62%	-9.41%		-3.80%	-5.05%	-7.50%
Expected number of Injury Crashes/ Million VMT	2004	0.61	0.60	0.60	0.59	0.57	0.56	0.56	0.56	0.82	0.82	0.83	0.82
			-1.33%	-1.88%	-2.38%		-1.66%	-2.48%	-2.81%		0.14%	0.78%	-0.48%
	2010	0.62	0.61	0.60	0.60	0.58	0.57	0.56	0.56	0.84	0.84	0.85	0.84
			-1.66%	-2.27%	-2.96%		-2.03%	-3.16%	-3.57%		-0.13%	1.38%	-0.44%
	2015	0.63	0.62	0.61	0.61	0.59	0.57	0.56	0.56	0.86	0.85	0.87	0.86
			-1.95%	-2.67%	-3.45%		-2.34%	-3.80%	-4.24%		-0.45%	1.75%	-0.42%
	2020	0.65	0.63	0.62	0.62	0.60	0.59	0.57	0.57	0.90	0.89	0.91	0.89
			-2.18%	-3.48%	-4.32%		-2.53%	-4.70%	-5.20%		-0.96%	0.88%	-1.16%
	2025	0.68	0.66	0.65	0.64	0.63	0.61	0.59	0.58	0.97	0.96	0.96	0.94
			-2.74%	-5.08%	-6.27%		-3.05%	-6.32%	-7.06%		-1.70%	-1.00%	-3.68%
	2030	0.74	0.71	0.69	0.68	0.67	0.64	0.62	0.61	1.08	1.06	1.05	1.02
			-3.41%	-6.51%	-7.60%		-3.88%	-7.78%	-8.34%		-2.00%	-2.69%	-5.39%
	2035	0.83	0.80	0.78	0.77	0.74	0.70	0.68	0.67	1.28	1.24	1.23	1.19
			-4.43%	-6.97%	-8.17%		-4.86%	-8.07%	-8.76%		-3.30%	-4.00%	-6.60%
Expected number of Fatal Crashes/ Million VMT	2004	0.015	0.016	0.016	0.017	0.016	0.017	0.017	0.017	0.011	0.011	0.011	0.011
			3.53%	5.50%	7.36%		3.42%	5.76%	7.55%		4.58%	2.97%	5.57%
	2010	0.015	0.016	0.016	0.016	0.016	0.016	0.017	0.017	0.011	0.011	0.011	0.011
			3.98%	5.99%	8.35%		3.86%	6.30%	8.63%		5.12%	3.25%	5.88%
	2015	0.014	0.015	0.015	0.016	0.015	0.016	0.016	0.017	0.010	0.011	0.011	0.011
			4.03%	6.40%	9.15%		3.83%	6.70%	9.43%		5.70%	3.89%	6.80%
	2020	0.014	0.015	0.015	0.015	0.015	0.015	0.016	0.016	0.010	0.011	0.011	0.011
			4.36%	6.65%	9.88%		4.22%	7.01%	10.28%		5.42%	3.94%	6.80%
	2025	0.014	0.014	0.014	0.015	0.014	0.015	0.015	0.016	0.010	0.011	0.011	0.011
			4.70%	6.51%	10.40%		4.55%	6.87%	10.87%		5.81%	3.90%	7.05%
	2030	0.013	0.014	0.014	0.015	0.014	0.014	0.015	0.015	0.010	0.011	0.010	0.011
			4.32%	6.26%	10.63%		4.16%	6.69%	11.21%		5.41%	3.38%	6.64%
	2035	0.012	0.013	0.014	0.014	0.013	0.014	0.014	0.015	0.009	0.010	0.010	0.010
			5.93%	9.02%	13.11%		5.46%	9.25%	13.58%		9.04%	7.51%	10.02%

When the results are analyzed for each section, major benefits are realized along the first section of the study section, as demonstrated in Table 9. Again the benefits increase as time progresses. However, unlike the case of the network-wide benefits, the benefits along section 1 are significant in the 2035 target year ranging from a 23% to a 29% reduction in travel time. These savings translate into an increase in overall vehicle speeds in the range of 30% to 40%. These benefits are realized for light duty cars with increases in speeds ranging from 26% to 40% and in heavy duty truck speeds in the range of 28% to 43% for Scenarios 2 through 4. It should be noted that the increase in heavy duty vehicle speeds is least for Scenario 3 given that the trucks have to change lanes at the end of section 1 given the drop from 4 lanes to 3 lanes as vehicles approach section 2. It should be noted that a more detailed presentation of the section by section results is presented in Appendix B.

Table 9: Scenario Comparison for Different MEOs by Vehicle Type along Section 1

MOE	Year	All				Cars				Trucks			
		Sc. 1	Sc. 2	Sc. 3	Sc. 4	Sc. 1	Sc. 2	Sc. 3	Sc. 4	Sc. 1	Sc. 2	Sc. 3	Sc. 4
Average Travel Time (min/veh)	2004	3.51	3.44 -1.95%	3.38 -3.82%	3.35 -4.78%	3.11	3.06 -1.62%	3.00 -3.81%	2.98 -4.29%	5.72	5.55 -2.98%	5.51 -3.72%	5.37 -6.13%
	2010	3.58	3.50 -2.21%	3.43 -4.24%	3.39 -5.39%	3.15	3.10 -1.81%	3.01 -4.55%	2.99 -5.15%	5.80	5.61 -3.28%	5.63 -3.02%	5.47 -5.67%
	2015	3.66	3.55 -2.97%	3.48 -5.01%	3.43 -6.28%	3.21	3.13 -2.64%	3.03 -5.64%	3.01 -6.33%	5.89	5.66 -3.89%	5.71 -3.11%	5.54 -6.00%
	2020	3.79	3.63 -4.10%	3.54 -6.46%	3.48 -8.05%	3.31	3.19 -3.75%	3.06 -7.71%	3.02 -8.70%	6.02	5.71 -5.06%	5.82 -3.32%	5.62 -6.53%
	2025	3.99	3.72 -6.75%	3.62 -9.45%	3.54 -11.43%	3.49	3.28 -6.25%	3.09 -11.51%	3.05 -12.66%	6.23	5.73 -7.97%	5.93 -4.72%	5.69 -8.67%
	2030	4.39	3.82 -12.97%	3.69 -15.78%	3.60 -17.85%	3.82	3.36 -11.98%	3.13 -17.96%	3.09 -19.00%	6.81	5.74 -15.58%	6.03 -11.36%	5.71 -16.03%
	2035	5.10	3.92 -23.22%	3.80 -25.54%	3.63 -28.88%	4.41	3.49 -20.92%	3.20 -27.50%	3.14 -28.70%	8.18	5.77 -29.47%	6.38 -21.94%	5.70 -30.26%
Travel Speed (mph)	2004	59.33	60.51 1.99%	61.69 3.97%	62.31 5.02%	66.95	68.05 1.64%	69.60 3.96%	69.95 4.48%	36.44	37.56 3.07%	37.85 3.86%	38.82 6.53%
	2010	58.21	59.53 2.27%	60.79 4.43%	61.53 5.70%	66.09	67.31 1.84%	69.24 4.77%	69.68 5.43%	35.94	37.16 3.39%	37.06 3.11%	38.10 6.01%
	2015	56.97	58.71 3.06%	59.97 5.27%	60.79 6.70%	64.91	66.67 2.71%	68.78 5.97%	69.29 6.75%	35.38	36.81 4.05%	36.52 3.21%	37.64 6.38%
	2020	55.06	57.41 4.27%	58.86 6.89%	59.88 8.75%	62.97	65.42 3.89%	68.23 8.34%	68.96 9.51%	34.65	36.49 5.33%	35.84 3.43%	37.07 6.98%
	2025	52.20	55.98 7.25%	57.64 10.42%	58.93 12.90%	59.68	63.66 6.68%	67.43 12.99%	68.32 14.48%	33.48	36.38 8.66%	35.14 4.95%	36.66 9.49%
	2030	47.57	54.62 14.82%	56.44 18.64%	57.87 21.63%	54.60	62.00 13.55%	66.50 21.80%	67.36 23.36%	30.66	36.29 18.34%	34.56 12.71%	36.48 18.97%
	2035	40.98	53.24 29.92%	54.90 33.95%	57.47 40.23%	47.36	59.78 26.23%	65.19 37.64%	66.29 39.96%	25.60	36.15 41.18%	32.69 27.70%	36.55 42.78%

The benefits that were observed along section 1 are significantly higher than those observed along section 2 as demonstrated by comparing the results of Table 10 to Table 9. Even though these benefits along section 2 are lower than those of section 1, nevertheless the results demonstrate increases in overall vehicle speeds in the range of 12.8% to 18.3% as a result of the various enhancements along section 2. Light duty vehicles benefit most from these enhancements with increases in travel speeds ranging from 13.2% to 19.6% versus increases in the range 13.2% to 15.2% in the case of heavy duty trucks. Given that Scenarios 2 and 3 involve 3 lanes along section 2 the results are very similar with increases in overall speeds of 12.8% and 12.3%, respectively.

Table 10: Scenario Comparison for Different MEOs by Vehicle Types along Section 2

MOE	Year	All				Cars				Trucks			
		Sc. 1	Sc. 2	Sc. 3	Sc. 4	Sc. 1	Sc. 2	Sc. 3	Sc. 4	Sc. 1	Sc. 2	Sc. 3	Sc. 4
Average Travel Time (min/veh)	2004	3.94	3.68	3.71	3.61	3.76	3.51	3.50	3.43	4.88	4.60	4.84	4.61
			-6.47%	-5.82%	-8.33%		-6.61%	-7.03%	-8.96%		-5.65%	-0.74%	-5.50%
	2010	4.03	3.72	3.76	3.64	3.85	3.55	3.53	3.44	4.99	4.64	4.95	4.64
			-7.68%	-6.84%	-9.85%		-7.83%	-8.34%	-10.57%		-7.02%	-0.86%	-6.96%
	2015	4.12	3.76	3.81	3.66	3.93	3.58	3.56	3.46	5.09	4.67	5.01	4.67
			-8.72%	-7.67%	-11.22%		-8.82%	-9.33%	-12.00%		-8.27%	-1.44%	-8.27%
	2020	4.23	3.81	3.86	3.70	4.02	3.62	3.59	3.48	5.25	4.75	5.10	4.72
			-9.87%	-8.75%	-12.69%		-9.93%	-10.51%	-13.43%		-9.56%	-2.76%	-10.14%
	2025	4.33	3.85	3.93	3.73	4.10	3.65	3.64	3.49	5.41	4.81	5.23	4.79
			-11.10%	-9.40%	-13.99%		-11.08%	-11.26%	-14.83%		-11.15%	-3.43%	-11.48%
	2030	4.41	3.90	3.95	3.74	4.17	3.69	3.67	3.51	5.54	4.87	5.29	4.83
			-11.49%	-10.28%	-15.08%		-11.49%	-12.09%	-15.92%		-12.07%	-4.65%	-12.85%
	2035	4.44	3.94	3.96	3.76	4.21	3.72	3.68	3.52	5.64	4.99	5.32	4.90
			-11.38%	-10.93%	-15.44%		-11.63%	-12.67%	-16.42%		-11.65%	-5.66%	-13.21%
Travel Speed (mph)	2004	61.20	65.43	64.98	66.76	64.00	68.53	68.84	70.30	49.40	52.36	49.77	52.28
			6.92%	6.18%	9.09%		7.08%	7.56%	9.84%		5.99%	0.75%	5.83%
	2010	59.72	64.68	64.10	66.24	62.59	67.91	68.29	69.99	48.27	51.92	48.70	51.88
			8.31%	7.34%	10.92%		8.49%	9.10%	11.81%		7.55%	0.88%	7.48%
	2015	58.41	63.99	63.26	65.80	61.31	67.24	67.62	69.67	47.35	51.62	48.04	51.62
			9.55%	8.30%	12.64%		9.68%	10.29%	13.63%		9.02%	1.47%	9.01%
	2020	56.91	63.14	62.37	65.18	59.96	66.57	67.00	69.26	45.90	50.75	47.21	51.08
			10.95%	9.59%	14.54%		11.02%	11.75%	15.51%		10.57%	2.84%	11.29%
	2025	55.58	62.52	61.35	64.63	58.73	66.05	66.18	68.96	44.51	50.09	46.09	50.28
			12.49%	10.37%	16.27%		12.47%	12.69%	17.41%		12.56%	3.55%	12.97%
	2030	54.68	61.78	60.94	64.39	57.70	65.19	65.63	68.63	43.46	49.43	45.57	49.87
			12.98%	11.46%	17.76%		12.98%	13.75%	18.94%		13.73%	4.87%	14.74%
	2035	54.20	61.16	60.85	64.09	57.18	64.71	65.48	68.41	42.68	48.31	45.24	49.17
			12.83%	12.26%	18.25%		13.16%	14.51%	19.63%		13.19%	5.99%	15.21%

The results of section 3 might appear to be counter intuitive at first glance given that they indicate a reduction in the overall vehicle speeds with an increase in the number of lanes along the study section, as demonstrated in Table 11. These findings are attributed to the fact that the enhancements that are made result in an improvement in traffic stream throughput along sections 1 and 2 and thus an increase in vehicle arrival rate at section 3. This in turn results in a decrease in the vehicle speeds along this section given that more vehicles are able to traverse this section. It should be noted that the results that are presented are for a single hour after 30 minutes of simulation to ensure that steady-state conditions were achieved.

Table 11: Scenario Comparison for Different MEOs by Vehicle Type along Section 3

MOE	Year	All				Cars				Trucks			
		Sc. 1	Sc. 2	Sc. 3	Sc. 4	Sc. 1	Sc. 2	Sc. 3	Sc. 4	Sc. 1	Sc. 2	Sc. 3	Sc. 4
Average Travel Time (min/veh)	2004	1.63	1.65	1.61	1.61	1.45	1.47	1.42	1.42	2.73	2.74	2.73	2.75
			1.00%	-1.75%	-1.67%		1.01%	-2.36%	-2.60%		0.35%	-0.21%	0.43%
	2010	1.67	1.69	1.64	1.63	1.48	1.50	1.44	1.43	2.76	2.76	2.75	2.76
			0.97%	-1.85%	-2.23%		1.15%	-2.52%	-3.23%		0.05%	-0.32%	-0.02%
	2015	1.69	1.73	1.67	1.66	1.50	1.54	1.47	1.45	2.78	2.77	2.76	2.77
			1.91%	-1.67%	-2.28%		2.41%	-2.20%	-3.27%		-0.21%	-0.71%	-0.34%
	2020	1.72	1.77	1.70	1.69	1.52	1.58	1.50	1.48	2.81	2.79	2.78	2.78
			2.76%	-1.29%	-2.23%		3.71%	-1.58%	-3.07%		-0.58%	-1.05%	-0.96%
	2025	1.76	1.82	1.76	1.72	1.56	1.63	1.56	1.51	2.85	2.82	2.81	2.81
			3.20%	-0.29%	-2.46%		4.35%	-0.25%	-3.43%		-1.12%	-1.58%	-1.47%
	2030	1.77	1.88	1.81	1.76	1.57	1.71	1.62	1.56	2.87	2.84	2.83	2.84
			6.56%	2.50%	-0.26%		8.70%	3.46%	-0.65%		-1.16%	-1.53%	-1.03%
	2035	1.79	2.00	1.92	1.80	1.59	1.82	1.74	1.59	2.90	2.91	2.89	2.88
			11.49%	7.01%	0.56%		14.46%	8.89%	0.04%		0.30%	-0.18%	-0.63%
Travel Speed (mph)	2004	58.86	58.28	59.91	59.86	66.12	65.46	67.72	67.88	35.19	35.06	35.26	35.04
			-0.99%	1.78%	1.70%		-1.00%	2.41%	2.67%		-0.35%	0.21%	-0.43%
	2010	57.62	57.07	58.71	58.94	64.90	64.17	66.58	67.07	34.86	34.85	34.98	34.87
			-0.96%	1.88%	2.28%		-1.13%	2.59%	3.34%		-0.05%	0.32%	0.02%
	2015	56.78	55.72	57.75	58.10	64.08	62.57	65.52	66.24	34.66	34.73	34.91	34.78
			-1.87%	1.70%	2.33%		-2.35%	2.25%	3.37%		0.21%	0.71%	0.34%
	2020	55.78	54.29	56.51	57.06	63.10	60.85	64.12	65.10	34.23	34.43	34.60	34.57
			-2.68%	1.31%	2.28%		-3.57%	1.61%	3.17%		0.59%	1.06%	0.97%
	2025	54.66	52.98	54.83	56.03	61.69	59.14	61.87	63.88	33.75	34.13	34.29	34.25
			-3.07%	0.33%	2.52%		-4.12%	0.31%	3.56%		1.13%	1.60%	1.49%
	2030	54.46	51.14	53.20	54.66	61.29	56.43	59.34	61.78	33.50	33.90	34.03	33.85
			-6.10%	-2.32%	0.37%		-7.93%	-3.17%	0.80%		1.18%	1.58%	1.05%
	2035	53.74	48.31	50.72	53.54	60.40	52.95	56.25	60.52	33.19	33.10	33.29	33.42
			-10.10%	-5.63%	-0.38%		-12.33%	-6.86%	0.20%		-0.28%	0.30%	0.69%

In the case of the safety impacts all scenarios result in a decrease in the crash rate for sections 1 and 2, as demonstrated in Table 12. In the case of section 3, however, the results are mixed. Specifically, in 2030 and 2035 scenarios 2 and 3 result in a slight increase in the crash rate along section 3. This increase in crash rate, however, is significantly less than the decrease in crash rate along sections 1 and 2. Consequently, overall there is a decrease in the crash rate.

Table 12: Safety Results by Section

MOE	Year	Section 1				Section 2				Section 3			
		Sc. 1	Sc. 2	Sc. 3	Sc. 4	Sc. 1	Sc. 2	Sc. 3	Sc. 4	Sc. 1	Sc. 2	Sc. 3	Sc. 4
Expected number of Crashes/ Million VMT	2004	1.26	1.23 -1.98%	1.21 -3.75%	1.20 -4.75%	1.22	1.15 -6.43%	1.15 -5.87%	1.12 -8.31%	1.28	1.29 0.95%	1.26 -1.79%	1.26 -1.72%
	2010	1.28	1.25 -2.38%	1.23 -4.20%	1.22 -5.37%	1.25	1.16 -7.63%	1.17 -6.85%	1.13 -9.84%	1.31	1.32 0.98%	1.28 -1.86%	1.28 -2.26%
	2015	1.31	1.27 -3.05%	1.25 -4.97%	1.23 -6.31%	1.28	1.17 -8.63%	1.18 -7.69%	1.14 -11.16%	1.33	1.35 1.92%	1.30 -1.69%	1.30 -2.28%
	2020	1.36	1.30 -4.19%	1.27 -6.58%	1.25 -8.22%	1.32	1.19 -9.75%	1.20 -8.78%	1.15 -12.64%	1.35	1.39 2.77%	1.33 -1.30%	1.32 -2.28%
	2025	1.43	1.33 -6.78%	1.29 -9.51%	1.26 -11.55%	1.35	1.20 -11.04%	1.22 -9.49%	1.16 -14.03%	1.38	1.42 3.14%	1.38 -0.29%	1.35 -2.47%
	2030	1.57	1.37 -12.91%	1.32 -16.04%	1.29 -18.17%	1.37	1.21 -11.44%	1.23 -10.33%	1.16 -15.07%	1.38	1.48 6.70%	1.42 2.64%	1.38 -0.19%
	2035	1.83	1.41 -23.22%	1.36 -25.52%	1.30 -28.90%	1.39	1.23 -11.38%	1.23 -10.99%	1.17 -15.45%	1.40	1.56 11.67%	1.50 7.11%	1.41 0.62%
Expected number of Injury Crashes/ Million VMT	2004	0.600	0.588 -1.93%	0.580 -3.28%	0.575 -4.23%	0.577	0.544 -5.62%	0.549 -4.88%	0.537 -6.82%	0.610	0.616 1.00%	0.602 -1.26%	0.604 -0.98%
	2010	0.611	0.597 -2.33%	0.588 -3.65%	0.582 -4.79%	0.590	0.549 -6.87%	0.555 -5.93%	0.541 -8.35%	0.622	0.628 0.98%	0.613 -1.43%	0.612 -1.56%
	2015	0.623	0.604 -3.01%	0.596 -4.38%	0.587 -5.68%	0.602	0.554 -7.98%	0.561 -6.85%	0.543 -9.75%	0.631	0.642 1.76%	0.622 -1.37%	0.620 -1.70%
	2020	0.644	0.617 -4.16%	0.606 -6.01%	0.595 -7.62%	0.617	0.561 -9.08%	0.567 -8.04%	0.547 -11.28%	0.642	0.658 2.58%	0.635 -1.04%	0.630 -1.77%
	2025	0.677	0.632 -6.71%	0.616 -8.98%	0.603 -10.99%	0.632	0.566 -10.41%	0.575 -8.89%	0.551 -12.70%	0.654	0.673 2.92%	0.653 -0.20%	0.641 -2.03%
	2030	0.742	0.648 -12.62%	0.627 -15.40%	0.612 -17.51%	0.642	0.572 -10.91%	0.579 -9.89%	0.553 -13.84%	0.655	0.698 6.43%	0.673 2.62%	0.656 0.13%
	2035	0.845	0.666 -21.11%	0.649 -23.20%	0.620 -26.62%	0.649 0.00%	0.578 -10.88%	0.580 -10.68%	0.557 -14.24%	0.663	0.738 11.36%	0.710 7.05%	0.669 0.96%
Expected number of Fatal Crashes/ Million VMT	2004	0.015	0.015 0.65%	0.016 6.67%	0.016 7.30%	0.013	0.016 18.58%	0.016 18.44%	0.017 27.95%	0.015	0.015 1.34%	0.016 9.22%	0.016 10.66%
	2010	0.015	0.015 0.01%	0.016 7.90%	0.016 8.14%	0.012	0.015 22.92%	0.015 22.49%	0.017 34.11%	0.014	0.014 -0.24%	0.015 8.28%	0.016 11.14%
	2015	0.014	0.014 0.03%	0.015 9.04%	0.015 9.09%	0.012	0.015 25.78%	0.015 24.86%	0.016 38.71%	0.014	0.014 -3.47%	0.015 6.17%	0.015 9.63%
	2020	0.014	0.013 -1.23%	0.015 9.15%	0.015 9.41%	0.011	0.014 31.04%	0.014 28.38%	0.016 45.79%	0.014	0.013 -3.72%	0.014 4.89%	0.015 9.13%
	2025	0.013	0.013 -2.90%	0.015 9.11%	0.015 9.00%	0.010	0.014 35.89%	0.013 30.30%	0.016 52.91%	0.014	0.013 -4.99%	0.014 2.07%	0.015 6.93%
	2030	0.013	0.012 -4.12%	0.014 9.58%	0.014 8.87%	0.010	0.013 37.70%	0.013 31.51%	0.015 57.32%	0.014	0.013 -5.87%	0.014 1.91%	0.015 6.34%
	2035	0.011	0.012 4.28%	0.014 23.80%	0.014 21.01%	0.010	0.013 37.05%	0.013 31.99%	0.015 58.87%	0.014	0.013 -3.88%	0.014 5.11%	0.015 7.75%

5. BENEFIT-COST ANALYSIS

Economic analysis is a critical component of a comprehensive project or program evaluation methodology that considers all key quantitative and qualitative impacts of highway investments. It allows highway agencies to identify, quantify, and value the economic benefits and costs of highway projects and programs over a multiyear timeframe. With this information, highway agencies are able to make better utilization of scarce resources in their decision process.

The benefit-cost analysis was conducted using the Highway Project Benefit-Cost Analysis System (BCA.Net), which was developed by the Federal Highway Administration (FHWA). This software is a web-based system for highway benefit-cost analysis in support of a project-level decision-making analysis. The software requires a number of data input parameters including: (a) the AADT for the base year (2005), the final near-term year (2010), and the project target year (2035), (b) the percentage trucks for each of the three years along each of the three study sections; (c) the capacity, number of lanes, length, free-flow speed, average grade, operating and maintenance costs, initial Pavement Service Index (PSI), and annual change in PSI for each of the three study sections for the base year; (d) the distribution of traffic demand for each of the three study sections for each of the three years including the percent of AADT in a typical peak and shoulder hour and the directional distribution of traffic demand; (e) the various strategies that are being considered for a specific scenario and the average crash rate for each strategy; (f) the base and alternate cases that are being considered; (g) the scenario-specific truck equivalency, the average vehicle occupancy, the annualization factor, the minimum speed during the peak hour, and the effective elasticity with respect to cost; (h) various social costs including the discount rate, the depreciation rate, the value of time for auto and truck drivers, the monetary value of fatal, injury, and property damage crashes, the base price of gasoline and diesel fuel, oil and emission costs; (i) the oil price index for each year of the analysis period (30 years in this case); and (j) various fuel price policies.

Traffic counts for a typical weekday were obtained from VDOT's permanent count stations in the vicinity of the study section. The counts demonstrate a fairly constant truck volume of approximately 500 veh/h, as illustrated in Figure 3. The light-duty vehicle volume builds up around 6:00 a.m. until it reaches its peak demand around 9:00 a.m. The demand remains high until approximately 6 p.m. before it decays again. Using the vehicle counts the duration of the peak period was computed as 8 h (total volume in excess of 2750 veh/h) and the shoulder period was computed as 10 h (total volume ranging between 1000 and 2750 veh/h). A 2750 veh/h cut-point was selected given that for a truck percentage of 15% and a truck equivalency of 6.0 (mountainous terrain (TRB 2000)) the volume-to-capacity ratio is approximately 100%. Using these values the hourly demand within the peak period was computed as 6.7% of the total AADT while the hourly demand during the shoulder period was computed at 3.9% of the AADT.

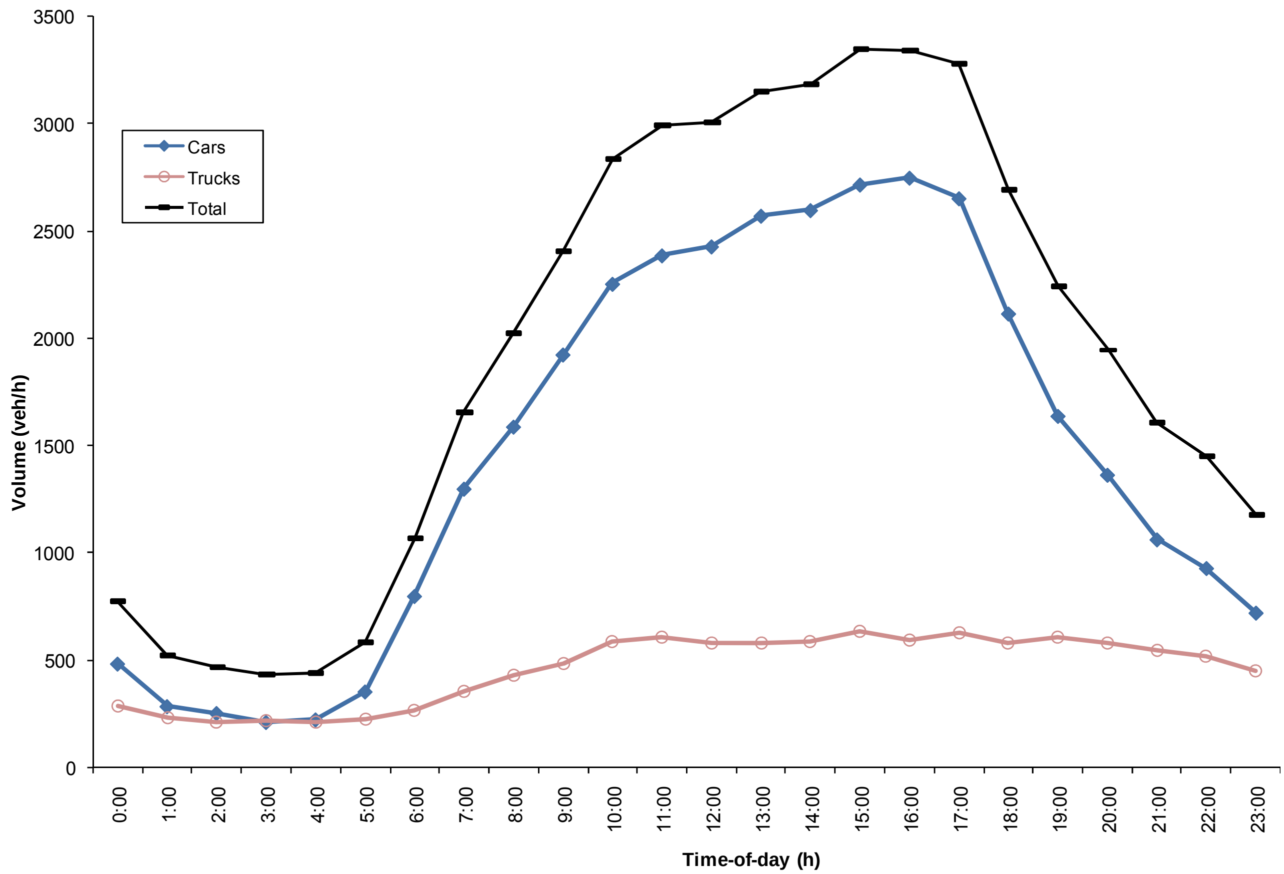

Figure 3: Variation in Light-duty and Truck Volumes by Time-of-day

The crash rates were derived from the INTEGRATION software output for each of the three study sections for each of the four scenarios including the base case scenario. These results were computed for the entire simulation run as opposed to the hourly rates that were reported earlier in Table 12. The specific crash rates are summarized in Table 13.

Table 13: Crash Rates used in Benefit-Cost Analysis

CMOE	Year	Section 1				Section 2				Section 3			
		Sc. 1	Sc. 2	Sc. 3	Sc. 4	Sc. 1	Sc. 2	Sc. 3	Sc. 4	Sc. 1	Sc. 2	Sc. 3	Sc. 4
Crash Rate Per Million VMT	2004	1.25	1.23	1.21	1.20	1.22	1.14	1.15	1.12	1.27	1.28	1.25	1.25
	2010	1.28	1.25	1.23	1.21	1.25	1.15	1.16	1.13	1.30	1.31	1.28	1.27
	2015	1.30	1.27	1.24	1.23	1.27	1.17	1.18	1.13	1.32	1.34	1.30	1.29
	2020	1.34	1.29	1.26	1.24	1.31	1.18	1.19	1.15	1.35	1.38	1.33	1.32
	2025	1.41	1.32	1.28	1.26	1.34	1.19	1.21	1.16	1.38	1.42	1.37	1.34
	2030	1.54	1.36	1.31	1.28	1.36	1.21	1.23	1.17	1.40	1.48	1.43	1.39
	2035	1.80	1.39	1.37	1.30	1.38	1.23	1.24	1.18	1.43	1.57	1.51	1.42

The construction cost estimates for the various scenarios were derived from cost proposals submitted by contractors bidding on the project. A summary of the various input parameters that were used for the analysis and the source of the data used to derive these parameters are presented in Table 14 and Table 15.

It should be noted that the analysis considered an interest rate of 5%, which is the mid-range of typical values reported in the literature (ranges between 3 to 7%) (FHWA 2003). This discount rate assumes an inflation rate of 0%. FHWA (FHWA 2003) indicates that "*in the case of economic analysis of investments by a public agency, it is best to forecast the life-cycle costs and benefits of a project without inflation (i.e. in real or base year dollars). Inflation is very hard to predict, particularly more than a few years into the future. More importantly, if inflation is added to benefits and costs projected for future years, it will only have to be removed again before these benefits and costs can be compared in the form of dollars of any given base year*."

The various variable values that were considered in the analysis were as follows:

- **Travel demand and traffic composition:** scenario-specific truck equivalencies of 3.0 were used. These values were modified for section 1 and 2 using the HCM procedures using a grade of 4%. The average vehicle occupancy was assumed to be 1.1, the annualization factor was assumed to be 365 days, the minimum speed during the peak hour was considered to be 10 mi/h, and the effective elasticity with respect to cost considered to be -0.1. These values represent the default values.

- **Social costs:** the value of time for auto and truck passengers was assumed to be $16.31/h and $29.5/h, respectively (ODOT 2006), the base year price of oil was considered at $2.2/qt, gasoline at $2.2/gal, diesel fuel at $2.2/gal, and fuel tax of $0.5/gal (EIA 2008). The safety benefits were computed considering three crash types: (a) Crashes involving at least one fatality ($3.9 million); (b) Crashes involving at least one injury but no fatalities ($80 thousand); (c) Crashes limited to property damage only ($5.8 thousand). These values are premised on official U.S. DOT guidance, and include emergency services, lost productivity, and associated costs (FHWA 2007a).

- **Oil price index:** the study assumed a 35% increase from the base year price for 2008 and 10% for each other year of the analysis period (30 years in this case). This captures the surge of fuel prices in 2008.

Table 14: Benefit-Cost Analysis Input Parameter Summary

Input Parameter	Base Year (2005)			Final Near-Term Year (2010)			Project Target Year (2035)			Source
	Sect. 1	Sect. 2	Sect. 3	Sect. 1	Sect. 2	Sect. 3	Sect. 1	Sect. 2	Sect. 3	
AADT	35,380			40,084			67,425			VDOT traffic counts
Duration Peak Period (h)	8			8			8			Figure 3
Duration Shoulder Period (h)	10			10			10			Figure 3
Percent Truck	41.4	14.2	41.4	41.4	14.6	41.4	41.4	16.6	41.4	VDOT traffic counts

Table 15: Section Specific Benefit-Cost Analysis Input Parameter Summary

Input Parameter	Section 1	Section 2	Section 3	Source
Base Year (2005) Number of lanes	3	2	3	Field Observation
Free Flow Speed (mph)	70	70	70	Field Observation
Maximum Flow Rate (veh/hr/lane)	2400	2400	2400	(TRB 2000)
Length (miles)	3.47	4.01	1.6	VDOT Design Plan
Average Percent Grade	0.02	0.01	0.04	VDOT Design Drawings
Operating and Maintenance Cost (thous. $/facility-mile)	4.5	3.0	4.5	(Wu et al. 2008)
Pavement Service Index (PSI)	4.5	4.5	4.5	(FHWA 2007a)
Pavement Deterioration (Annual change in PSI)	0.1	0.1	0.1	(FHWA 2007a)
Costs of Improvement / Maintenance Construction Cost (thous. $/lane-mile)	11,988.5	10,213.9	10,213.9	VDOT
Rehabilitation Cost ($/lane-mile)	362,043			(Wu et al. 2008)
Operating and Maintenance Cost ($/lane-mile)	1,515			(Wu et al. 2008)

The results, which are presented in Table 16, indicate that all three scenarios offer cost-effective benefits in comparison to the base (do nothing) scenario. Specifically, the addition of a single lane along section 2 (scenario 2) offers a benefit-cost ratio of 5.35. The addition, of a truck climbing lane that extends across all three sections (scenario 3) offers a benefit-cost ratio of 2.30, while adding an additional fourth lane along section 2 in addition to what was proposed in scenario 3 (scenario 4) results in a benefit cost ratio of 1.60. The results indicate that the majority of benefits arise from travel time savings followed by safety savings.

It should be emphasized that the results for scenario 2 demonstrate the need to increase the number of lanes along section 2 regardless of what is done in terms for increasing the number of all purpose lanes along the other two sections (sections 1 and 3).

Table 16: Summary Benefit-Cost Analysis Results

Variable	Scenario 2	Scenario 3	Scenario 4
Travel time savings, thous. PV$	191968.1	192395.3	192538.1
Vehicle operating cost savings, thous. PV$	-5539.0	-6579.4	-6833.8
Safety benefits, thous. PV$	164.9	1403.0	1403.1
Environmental benefits, thous. PV$	-35.2	-36.6	-36.8
Project residual value, thous. PV$	2094.1	4962.2	7204.4
Disbenefit of traffic disruption from construction, thous. PV$	0.0	0.0	0.0
Total benefits, thous. PV$	188652.9	192144.6	194275.0
Of this, benefits to new users, thous. PV$	9565.4	9565.4	9554.5
Total costs, thous. PV$	35237.6	83718.2	121595.5
Net benefits, thous. PV$	153415.3	108426.4	72679.6
Benefit-cost ratio	5.35	2.30	1.60
Rate of return, percent	16.33	9.86	7.61

6. CONCLUSIONS

The average light-duty and heavy-duty vehicle speeds produced by the simulation model were found to be consistent with field observations for the base condition, demonstrating the validity of the simulation results. Three scenarios were considered including: (a) adding a single lane to section 2 to increase it from 2 to 3 lanes (from milepost 125.0 to 120.7); (b) adding a single lane to sections 1, 2, and 3 (from milepost 128.1 to 119.6); (c) combining (a) and (b) to result in 4 lanes from milepost 128.1 to 119.6. The three scenarios in addition to the base case do-nothing scenario were simulated using the INTEGRATION microscopic traffic simulation software. Each scenario was simulated 20 times with different random number seeds considering 7 year horizons for a total of 560 simulation runs (20 random number seeds x 4 scenarios x 7 model years). Average results across all 20 simulations were considered for the analysis.

The results of the analysis indicate that all three scenarios produce travel time, energy, and HC, CO, CO_2 emission, and crash savings relative to the base do-nothing scenario. These benefits increase as the travel demand increases with the progression of time from the base 2004 year to the horizon year of 2035.

A benefit-cost analysis was conducted and the results demonstrate that the most cost effective upgrade is to add a third lane to section 2 (benefit-cost ratio of 5.35) followed by the addition of a single lane to sections 1 through

3 (benefit-cost ratio of 2.30). The addition of a fourth lane to section 2 in addition to an additional lane to sections 1 through 3 still offers benefits with a benefit-cost ratio of 1.60.

REFERENCES

(2005). "Truck Only Lanes Eyed for I-81. http://www.washtimes.com/metro/20031125-094642-9290r.htm." The Washington Times.

AASHTO. (1994). *A Policy on Geometric Design of Highways and Streets*, American Association of State Highway and Transportation Officials, Washington DC.

Ahn, K., Rakha, H., and Trani, A. (2004). "Microframework for modeling of high-emitting vehicles." *Transportation Research Record.* (1880), 39-49.

Ahn, K., Rakha, H., Trani, A., and Van Aerde, M. (2001). "Estimating vehicle fuel consumption and emissions based on instantaneous speed and acceleration levels." *Journal of Transportation Engineering*, 128(2), 182-190.

Al-Kaisy, A., Jung, Y., and Rakha, H. (2005). "Developing passenger car equivalency factors for heavy vehicles during congestion." *Journal of Transportation Engineering*, 131(7), 514-523.

Avgoustis, A., Rakha, H., and Van Aerde, M. "Framework for estimating network-wide safety Impacts of intelligent transportation systems." *Intelligent Transportation Systems Safety and Security Conference* Miami.

Cate, M., and Urbanik, T. (2004). "Another View of Truck Lane Restrictions." Transportation Research Board, Washington D.C.

Dion, F., Rakha, H., and Kang, Y.-S. (2004). "Comparison of delay estimates at under-saturated and over-saturated pre-timed signalized intersections." *Transportation Research Part B-Methodological*, 38(2), 99-122.

EIA. (2008). "http://www.eia.doe.gov/oil_gas/petroleum/info_glance/petroleum.html ", Energy Information Administration.

FHWA. (2003). "Economic Analysis Primer."

FHWA. (2007a). "BCA.Net - Highway Project Benefit-Cost Analysis System User's Manual."

FHWA. (2007b). "I-81 Corridor Improvement Study: Tier 1 Final Report." Richmond, VA.

Hellinga, B. R., and Van Aerde, M. "Estimating dynamic O-D demands for a freeway corridor using loop detector data." Halifax, NS, Canada, 185-198.

Hoel, L. A., and Peek, J. L. (1999). "A Simulation Analysis of Traffic Flow Elements for Restricted Truck Lanes on Interstate Highways in Virginia." Charlottesville, VA.

ODOT. (2006). "The Value of Travel-Time: Estimates of the Hourly Value of Time for Vehicles in Oregon 2005." Oregon Department of Transportation, Economics & Policy Analysis Unit.

Park, S., and Rakha, H. (2006). "Energy and Environmental Impacts of Roadway Grades." *Transportation Research Record*, 1987, 148-160.

Rakha, H. (1990). "An Evaluation of the Benefits of User and System Optimised Route Guidance Strategies," Queen's University, Kingston.

Rakha, H., and Ahn, K. (2004). "Integration modeling framework for estimating mobile source emissions." *Journal of Transportation Engineering*, 130(2), 183-193.

Rakha, H., Ahn, K., and Trani, A. (2003). "Microscopic modeling of vehicle start emissions." *Transportation Research Record.* (1842), 29-38

Rakha, H., Ahn, K., and Trani, A. (2004). "Development of VT-Micro model for estimating hot stabilized light duty vehicle and truck emissions." *Transportation Research, Part D: Transport & Environment*, 9(1), 49-74.

Rakha, H., and Crowther, B. (2002). "Comparison of Greenshields, Pipes, and Van Aerde car-following and traffic stream models." *Transportation Research Record.* (1802), 248-262

Rakha, H., and Crowther, B. (2003). "Comparison and calibration of FRESIM and INTEGRATION steady-state car-following behavior." *Transportation Research*, 37A, 1-27.

Rakha, H., Flintsch, A. M., Ahn, K., El-Shawarby, I., and Arafeh, M. (2005a). "Evaluating alternative truck management strategies along interstate 81." *Transportation Research Record*, n 1925, 76-86.

Rakha, H., Kang, Y.-S., and Dion, F. (2001a). "Estimating vehicle stops at undersaturated and oversaturated fixed-time signalized intersections." *Transportation Research Record*, n 1776, 128-137

Rakha, H., and Lucic, I. (2002). "Variable power vehicle dynamics model for estimating maximum truck acceleration levels." *Journal of Transportation Engineering*, 128(5), 412-419.

Rakha, H., Lucic, I., Demarchi, S. H., Setti, J. R., and Van Aerde, M. (2001b). "Vehicle dynamics model for predicting maximum truck acceleration levels." *Journal of Transportation Engineering*, 127(5), 418-425.

Rakha, H., Medina, A., Sin, H., Dion, F., Van Aerde, M., and Jenq, J. (2000a). "Traffic signal coordination across jurisdictional boundaries: Field evaluation of efficiency, energy, environmental, and safety impacts." *Transportation Research Record*, n 1727, 42-51

Rakha, H., Paramahamsan, H., and Van Aerde, M. (2005b). "Comparison of Static Maximum Likelihood Origin-Destination Formulations." Transportation and Traffic Theory: Flow, Dynamics and Human Interaction, Proceedings of the 16th International Symposium on Transportation and Traffic Theory (ISTTT16), 693-716.

Rakha, H., Van Aerde, M., Ahn, K., and Trani, A. A. (2000b). "Requirements for evaluating traffic signal control impacts on energy and emissions based on instantaneous speed and acceleration measurements." *Transportation Research Record*, n 1738, 56-67

Rakha, H., Van Aerde, M., Bloomberg, L., and Huang, X. (1998). "Construction and calibration of a large-scale microsimulation model of the Salt Lake area." *Transportation Research Record*, n 1644, 93-102.

Rakha, H., and Yu, B. (2004). "Truck performance curves reflective of truck and pavement characteristics." *Journal of Transportation Engineering*, 130(6), 753-767.

Rakha, H., and Zhang, Y. (2004). "INTEGRATION 2.30 framework for modeling lane-changing behavior in weaving sections." *Transportation Research Record*.(1883), 140-149.

TRB. (2000). *Highway Capacity Manual 2000*, Transportation Research Board.

TXDOT. (2004). "Managed-Lanes http://managed-lanes.tamu.edu."

Van Aerde, M., Hellinga, B. R., and MacKinnon, G. "QUEENSOD: A Method for Estimating Time Varying Origin-Destination Demands For Freeway Corridors/Networks." *72nd Annual Meeting of the Transportation Research Board*, Washington D.C.

Van Aerde, M., and Rakha, H. (2007a). "INTEGRATION © Release 2.30 for Windows: User's Guide – Volume I: Fundamental Model Features." M. Van Aerde & Assoc., Ltd., Blacksburg.

Van Aerde, M., and Rakha, H. (2007b). "INTEGRATION © Release 2.30 for Windows: User's Guide – Volume II: Advanced Model Features." M. Van Aerde & Assoc., Ltd., Blacksburg.

Van Aerde, M., Rakha, H., and Paramahamsan, H. (2003). "Estimation of Origin-Destination Matrices: Relationship between Practical and Theoretical Considerations." *Transportation Research Record* 1831, 122-130

Van Aerde, M., and Yagar, S. (1988a). "Dynamic Integrated Freeway/Traffic Signal Networks: A Routeing-Based Modelling Approach." *Transportation Research*, 22A(6), 445-453.

Van Aerde, M., and Yagar, S. (1988b). "Dynamic Integrated Freeway/Traffic Signal Networks: Problems and Proposed Solutions." *Transportation Research*, 22A(6), 435-443.

Van Zuylen, J. H., and Willumsen, L. G. (1980). "The most likely trip matrix estimated from traffic counts." *Transportation Research*, 14B, 281-293.

VDOT. (2004). "http://www.Virginiadot.org/projects."

VDOT. (2005). "I-81 Corridor Improvement Study. Tier 1 Final Environmental Impact Statement." Richmond, VA.

Willumsen, L. G. (1978). "Estimation of an O-D matrix from traffic counts: A review." Institute for Transport Studies, Working paper no. 99, Leeds University.

Wu, Z., Flintsch, G., and Chowdhury, T. (2008). "Hybrid Multi-Objective Optimization Model for Regional Pavement Preservation Resource Allocation." 87th Annual Meeting of the Transportation Research Board, Washington D.C.

APPENDIX A: SUMMARY RESULTS FOR ENTIRE NETWORK

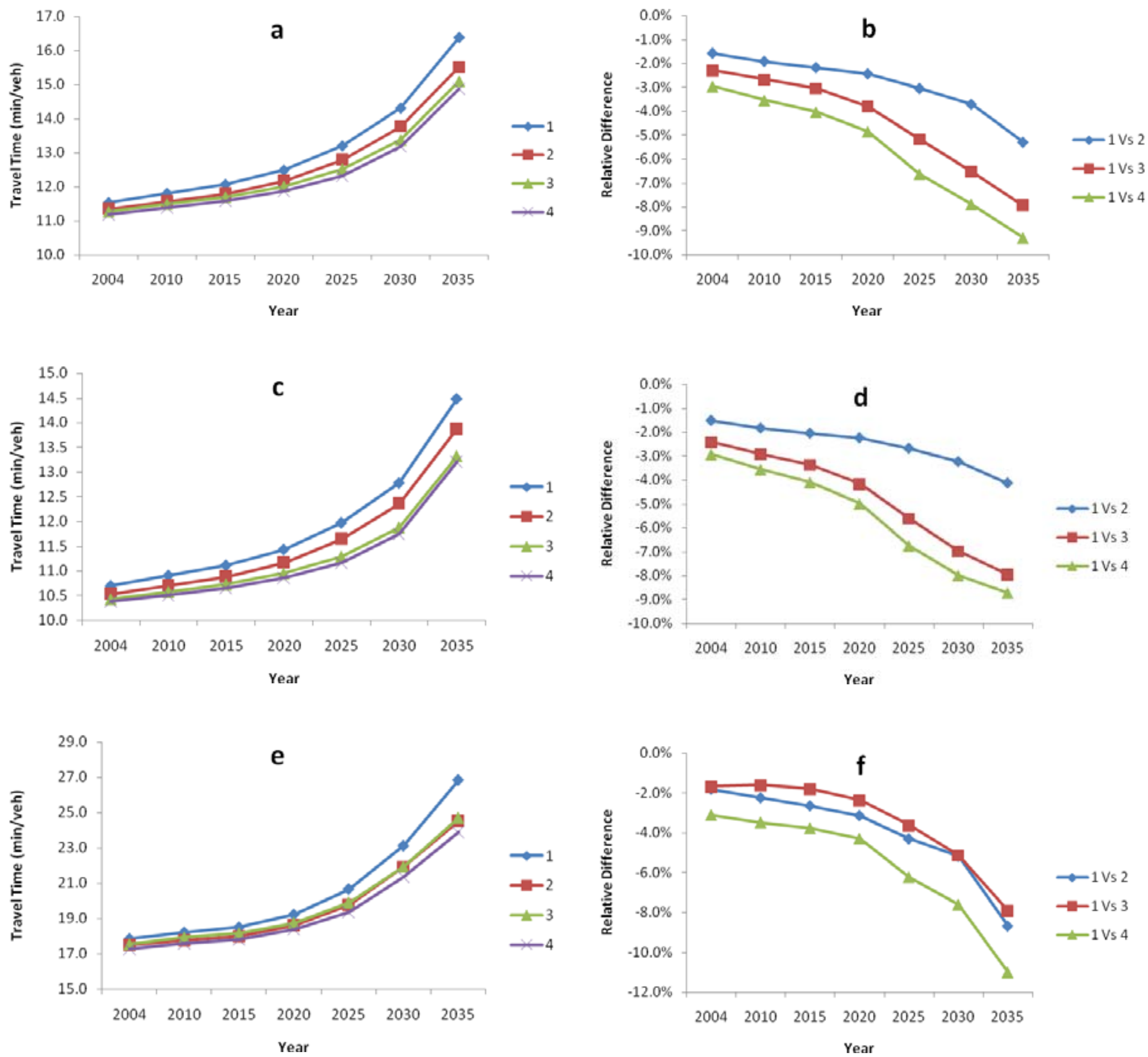

Figure 4: Comparison of scenarios in terms of Travel Time and Travel Time relative difference by vehicle type. (a, b) All vehicles, (c, d) Cars, and (e, f) Trucks.

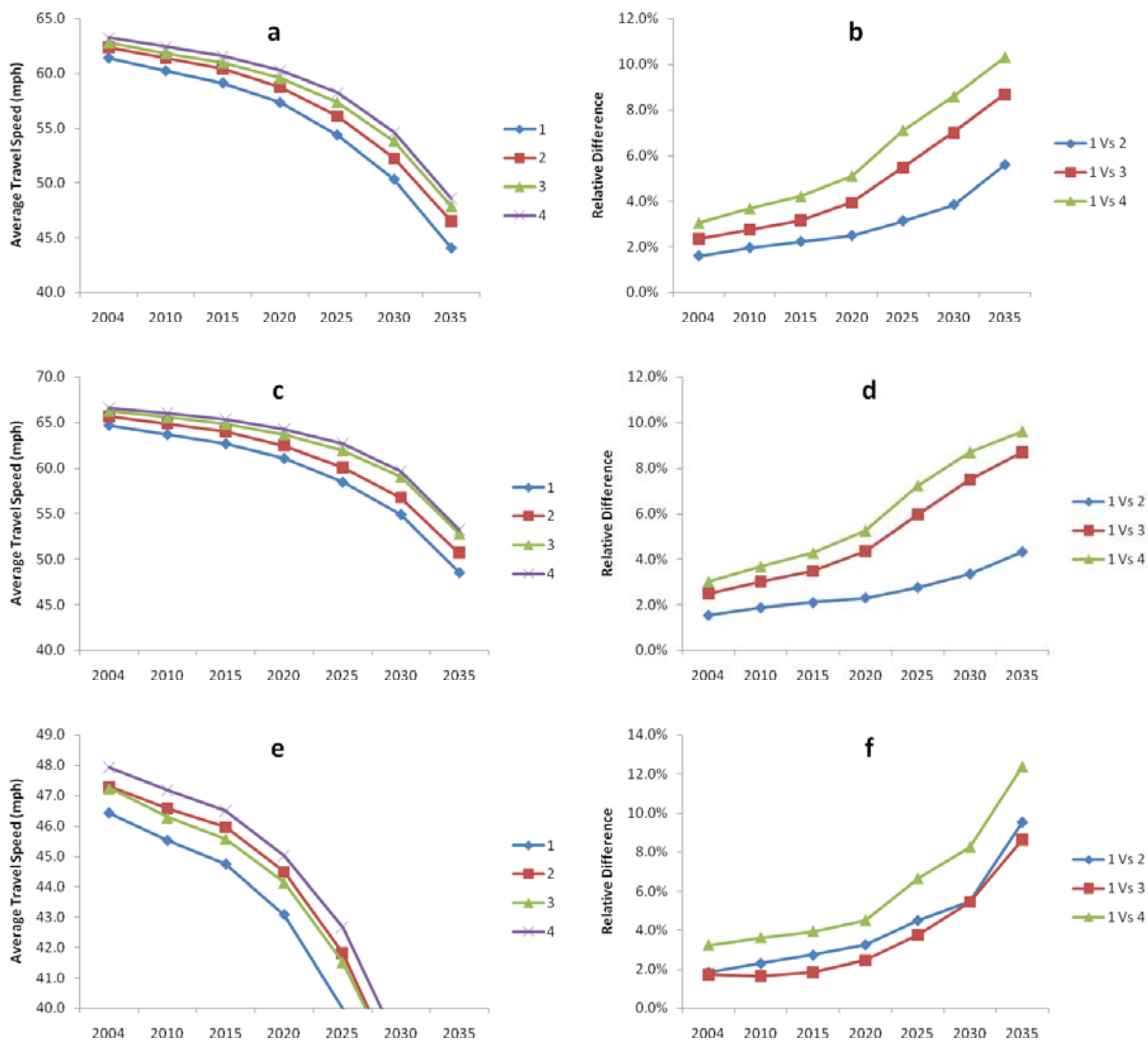

Figure 5: Comparison of scenario in terms of Average Travel Speed and Average Travel Speed relative difference by vehicle type. (a, b) All vehicles, (c, d) Cars, and (e, f) Trucks.

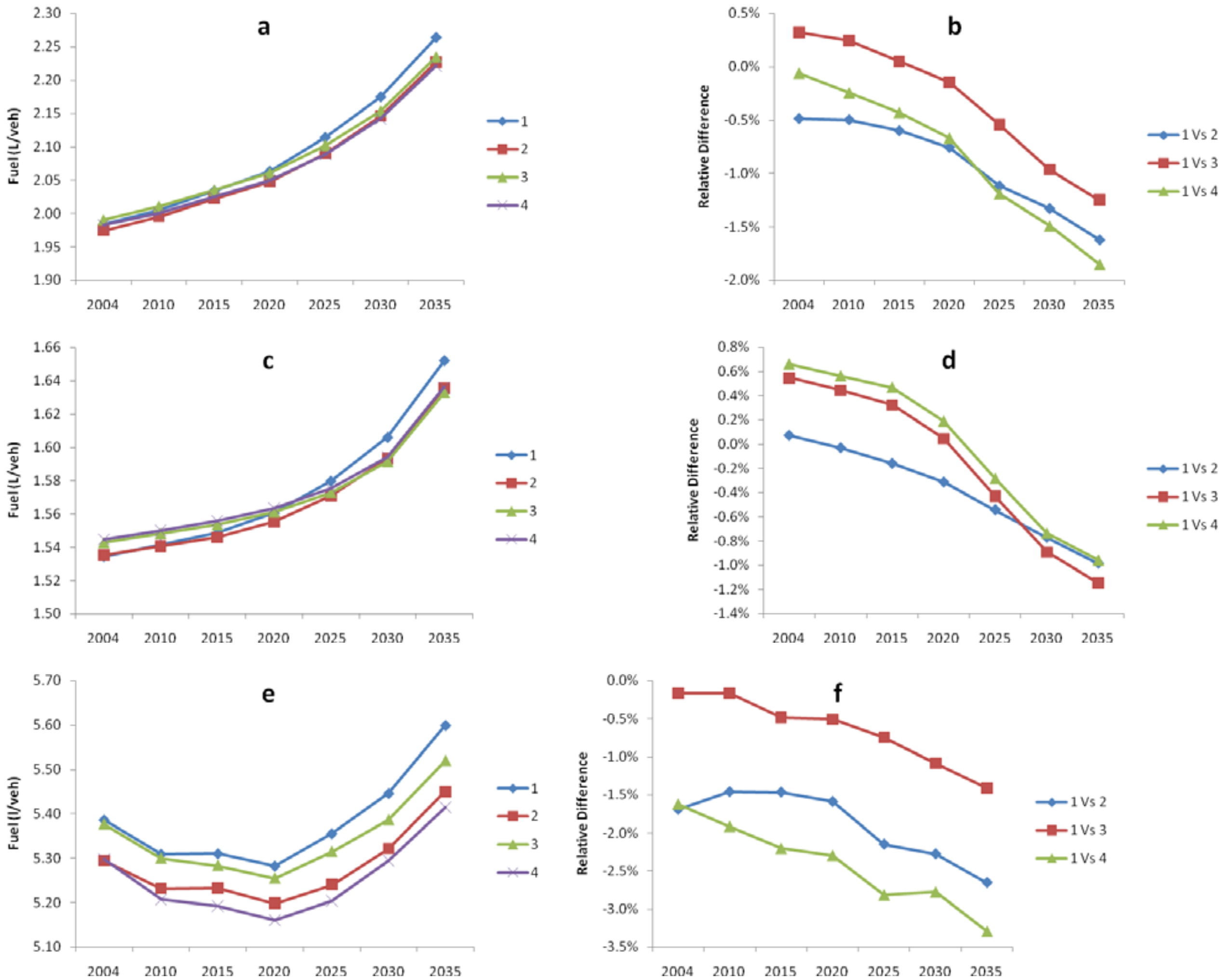

Figure 6: Comparison of scenario in terms of Average Fuel comsumption and Average Fuel comsumption relative difference by vehicle type. (a, b) All vehicles, (c, d) Cars, and (e, f) Trucks.

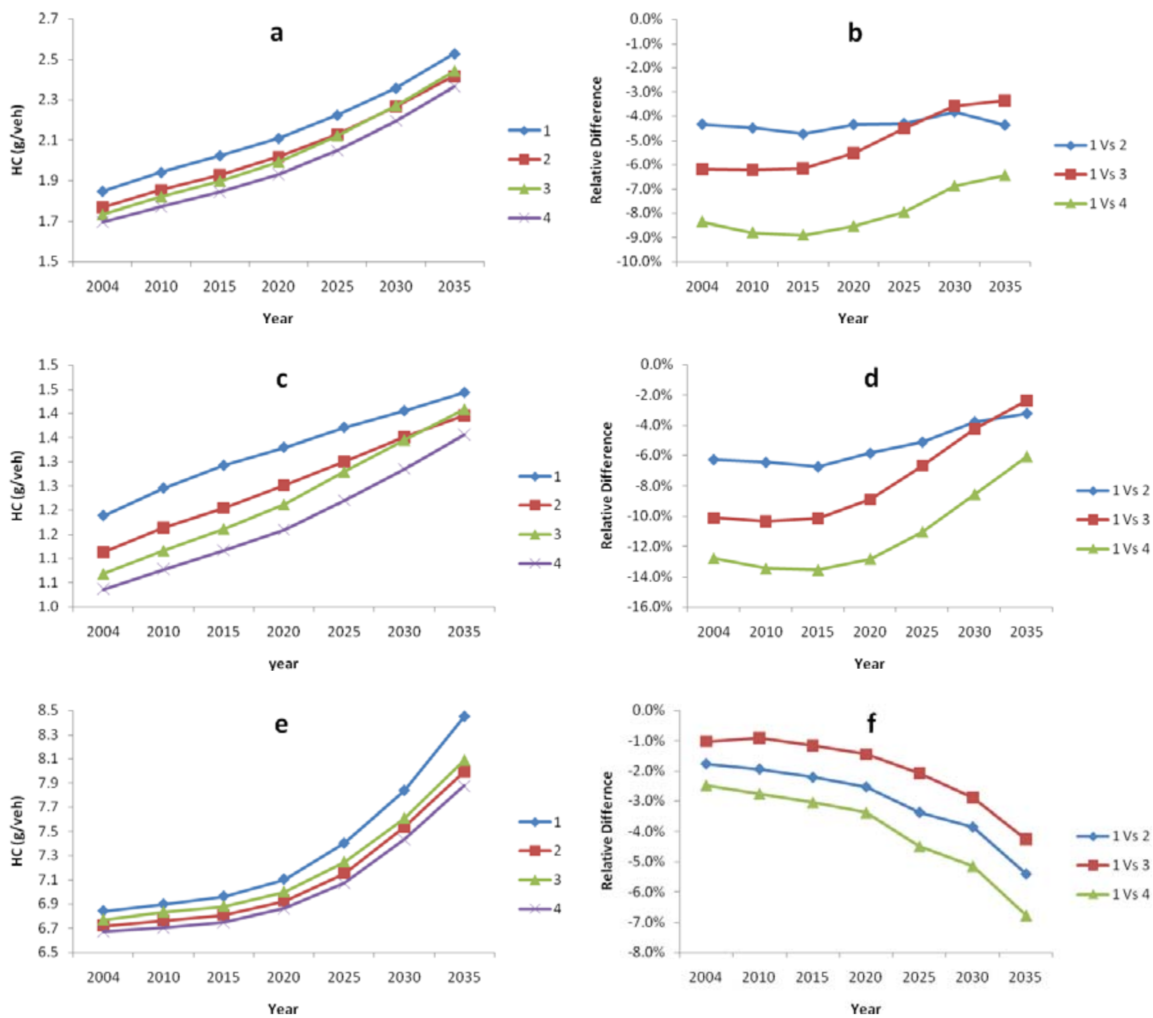

Figure 7: Comparison of scenario in terms of average HC emission and average HC emission relative difference by vehicle type. (a, b) All vehicles, (c, d) Cars, and (e, f) Trucks.

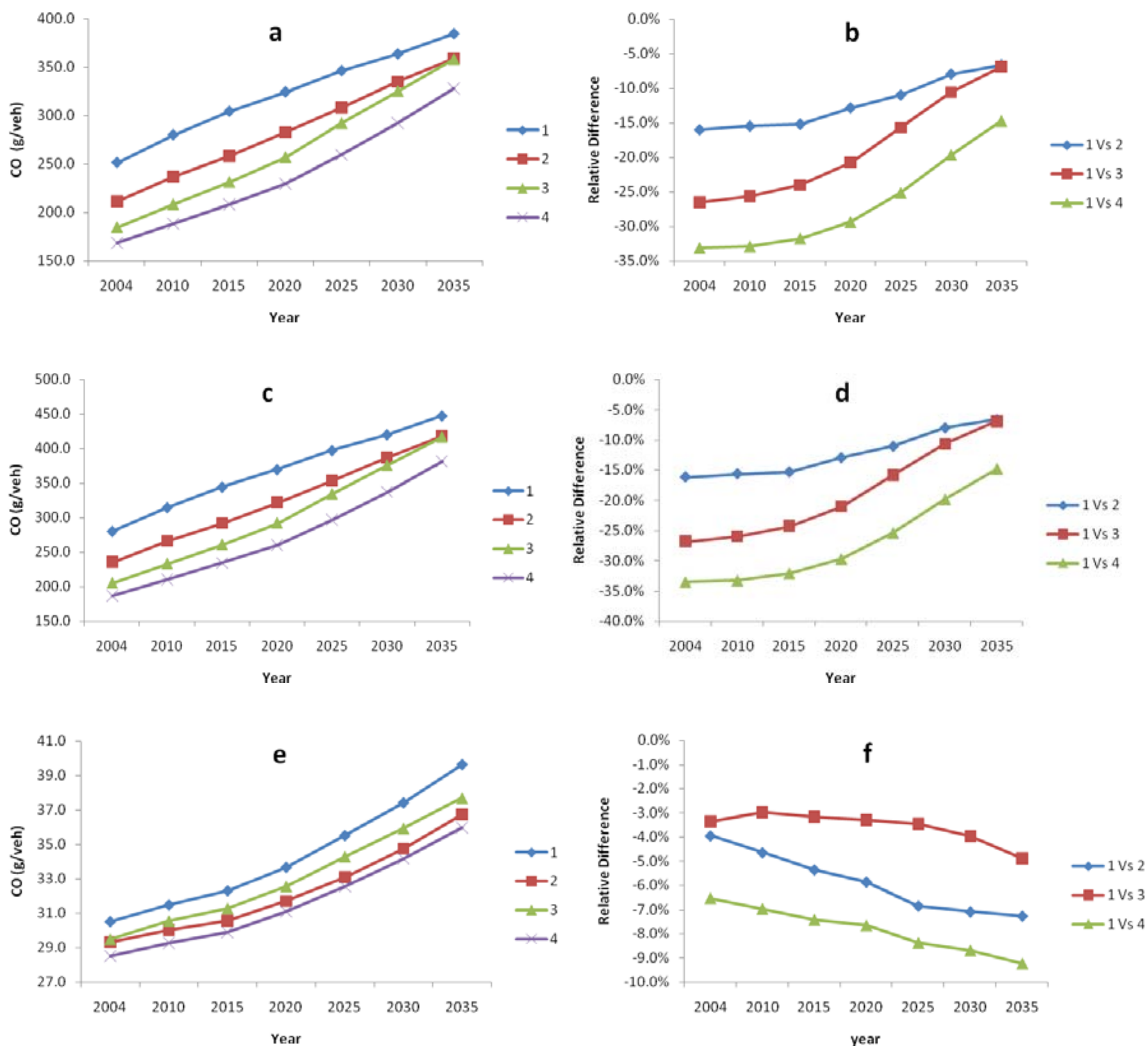

Figure 8: Comparison of scenario in terms of average CO emission and average CO emission relative difference by vehicle type. (a, b) All vehicles, (c, d) Cars, and (e, f) Trucks.

Table 17: Comparison of scenario in terms of crash related MEOs by vehicle types

MOE	Year	All				Cars				Trucks			
		Sc. 1	Sc. 2	Sc. 3	Sc. 4	Sc. 1	Sc. 2	Sc. 3	Sc. 4	Sc. 1	Sc. 2	Sc. 3	Sc. 4
Expected number of No Damage Crashes/ Million VMT	2004	0.053	0.052	0.052	0.052	0.048	0.047	0.047	0.047	0.084	0.083	0.084	0.082
			-1.19%	-1.10%	-1.28%		-1.21%	-1.43%	-1.11%		-1.09%	0.09%	-1.91%
	2010	0.053	0.052	0.053	0.052	0.048	0.047	0.047	0.047	0.086	0.085	0.087	0.085
			-1.70%	-1.59%	-1.99%		-1.80%	-2.39%	-2.06%		-1.37%	1.06%	-1.75%
	2015	0.054	0.053	0.053	0.053	0.048	0.047	0.047	0.047	0.088	0.087	0.090	0.087
			-2.39%	-2.09%	-2.65%		-2.55%	-3.28%	-2.98%		-1.90%	1.60%	-1.62%
	2020	0.056	0.054	0.054	0.054	0.049	0.047	0.047	0.047	0.091	0.089	0.093	0.090
			-2.77%	-2.81%	-3.47%		-3.02%	-4.45%	-4.17%		-2.05%	1.95%	-1.44%
	2025	0.057	0.055	0.055	0.054	0.050	0.048	0.047	0.047	0.093	0.090	0.095	0.091
			-3.43%	-3.83%	-4.65%		-3.80%	-5.96%	-5.79%		-2.39%	2.10%	-1.47%
	2030	0.060	0.057	0.057	0.056	0.053	0.050	0.048	0.048	0.095	0.093	0.097	0.093
			-4.53%	-5.41%	-6.34%		-5.17%	-7.91%	-7.82%		-2.83%	1.32%	-2.37%
	2035	0.061	0.059	0.058	0.057	0.054	0.051	0.049	0.049	0.095	0.095	0.099	0.094
			-3.12%	-4.50%	-5.96%		-4.45%	-7.80%	-8.12%		0.34%	4.16%	-0.27%
Expected number of Minor Damage Crashes/ Million VMT	2004	0.51	0.49	0.48	0.47	0.47	0.44	0.43	0.42	0.76	0.76	0.77	0.76
			-3.79%	-6.05%	-7.78%		-4.86%	-7.84%	-9.69%		0.37%	0.94%	-0.32%
	2010	0.53	0.51	0.49	0.48	0.49	0.46	0.44	0.43	0.78	0.78	0.79	0.78
			-4.18%	-6.56%	-8.66%		-5.31%	-8.67%	-10.91%	0.00%	1.29%	-0.32%	
	2015	0.55	0.53	0.51	0.50	0.51	0.48	0.46	0.45	0.80	0.80	0.82	0.80
			-4.17%	-6.98%	-9.28%		-5.28%	-9.37%	-11.75%		-0.20%	1.54%	-0.46%
	2020	0.59	0.56	0.54	0.53	0.54	0.51	0.48	0.47	0.87	0.87	0.87	0.85
			-4.18%	-8.16%	-10.48%		-5.23%	-10.39%	-13.00%		-0.71%	-0.77%	-2.12%
	2025	0.66	0.63	0.59	0.57	0.59	0.56	0.52	0.50	1.03	1.01	0.98	0.95
			-4.65%	-10.66%	-13.60%		-5.59%	-12.56%	-15.67%		-1.89%	-5.07%	-7.53%
	2030	0.77	0.73	0.68	0.66	0.67	0.63	0.58	0.56	1.26	1.24	1.17	1.14
			-4.76%	-11.85%	-14.25%		-5.86%	-13.61%	-16.09%		-1.91%	-7.29%	-9.49%
	2035	1.01	0.93	0.88	0.86	0.84	0.77	0.73	0.71	1.76	1.66	1.59	1.56
			-7.50%	-12.48%	-14.16%		-8.13%	-13.57%	-15.30%		-6.10%	-10.08%	-11.65%
Expected number of Moderate Damage Crashes/ Million VMT	2004	0.418	0.417	0.418	0.418	0.401	0.400	0.401	0.402	0.523	0.524	0.527	0.521
			-0.17%	0.00%	-0.02%		-0.24%	-0.16%	0.05%		0.18%	0.80%	-0.36%
	2010	0.420	0.418	0.419	0.419	0.401	0.399	0.398	0.400	0.533	0.532	0.541	0.531
			-0.39%	-0.23%	-0.28%		-0.47%	-0.62%	-0.28%		-0.03%	1.51%	-0.30%
	2015	0.422	0.419	0.420	0.420	0.401	0.397	0.396	0.398	0.544	0.542	0.554	0.543
			-0.74%	-0.49%	-0.57%		-0.82%	-1.07%	-0.66%		-0.39%	1.92%	-0.20%
	2020	0.426	0.422	0.422	0.422	0.402	0.398	0.395	0.397	0.558	0.553	0.568	0.555
			-1.00%	-0.92%	-1.00%		-1.00%	-1.64%	-1.14%		-0.98%	1.88%	-0.45%
	2025	0.433	0.427	0.426	0.425	0.407	0.401	0.396	0.398	0.570	0.562	0.580	0.565
			-1.47%	-1.62%	-1.80%		-1.48%	-2.57%	-2.05%		-1.43%	1.84%	-0.90%
	2030	0.446	0.435	0.434	0.433	0.417	0.407	0.401	0.404	0.585	0.573	0.592	0.574
			-2.34%	-2.67%	-2.92%		-2.45%	-3.78%	-3.23%		-1.98%	1.20%	-1.85%
	2035	0.448	0.441	0.440	0.436	0.419	0.410	0.405	0.405	0.583	0.583	0.601	0.579
			-1.58%	-1.85%	-2.74%		-2.05%	-3.34%	-3.36%		-0.02%	3.12%	-0.67%

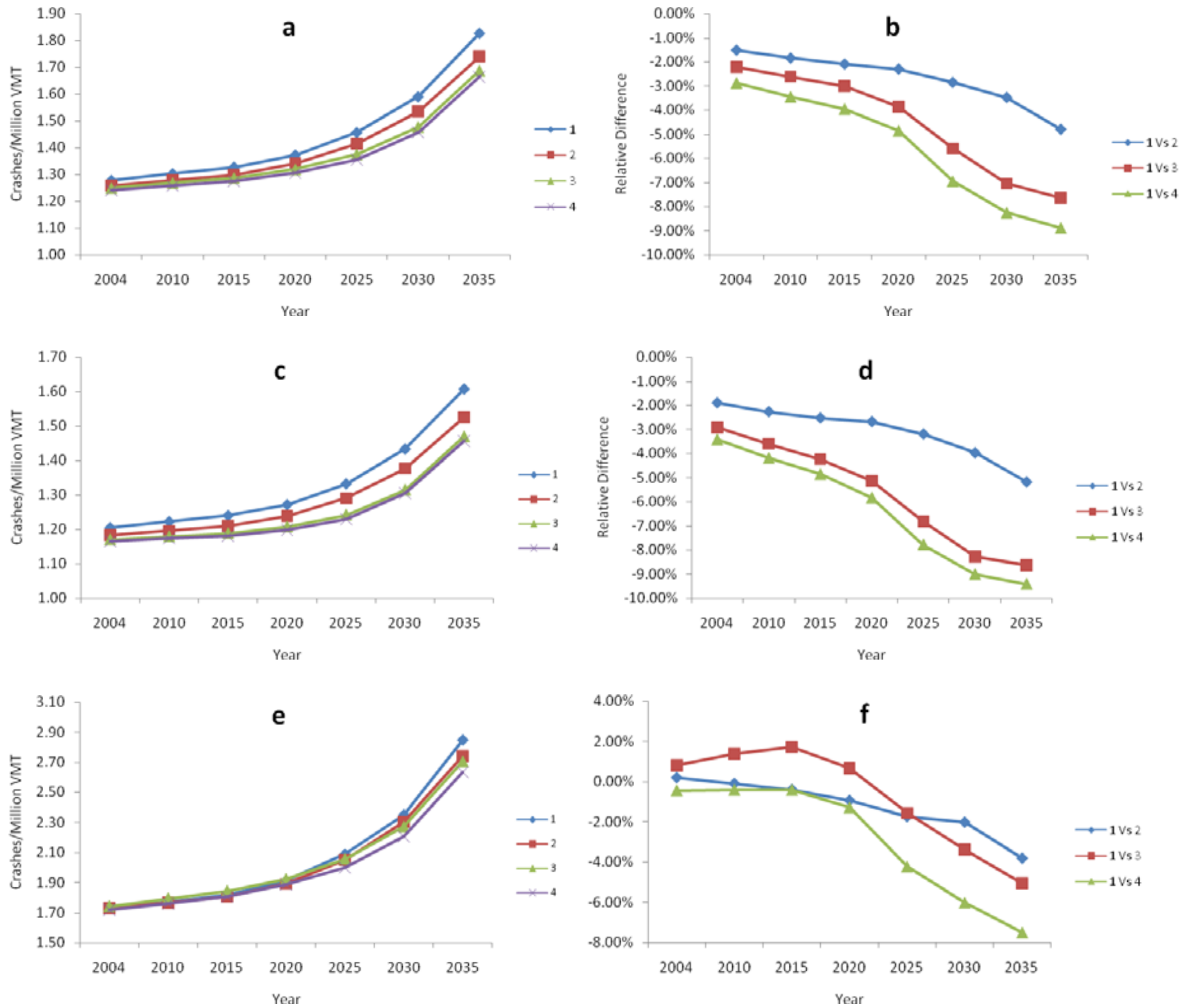

Figure 9: Comparison of scenario in terms of number of crahes/ million VMT and number of crahes/ million VMT relative difference by vehicle type. (a, b) All vehicles, (c, d) Cars, and (e, f) Trucks.

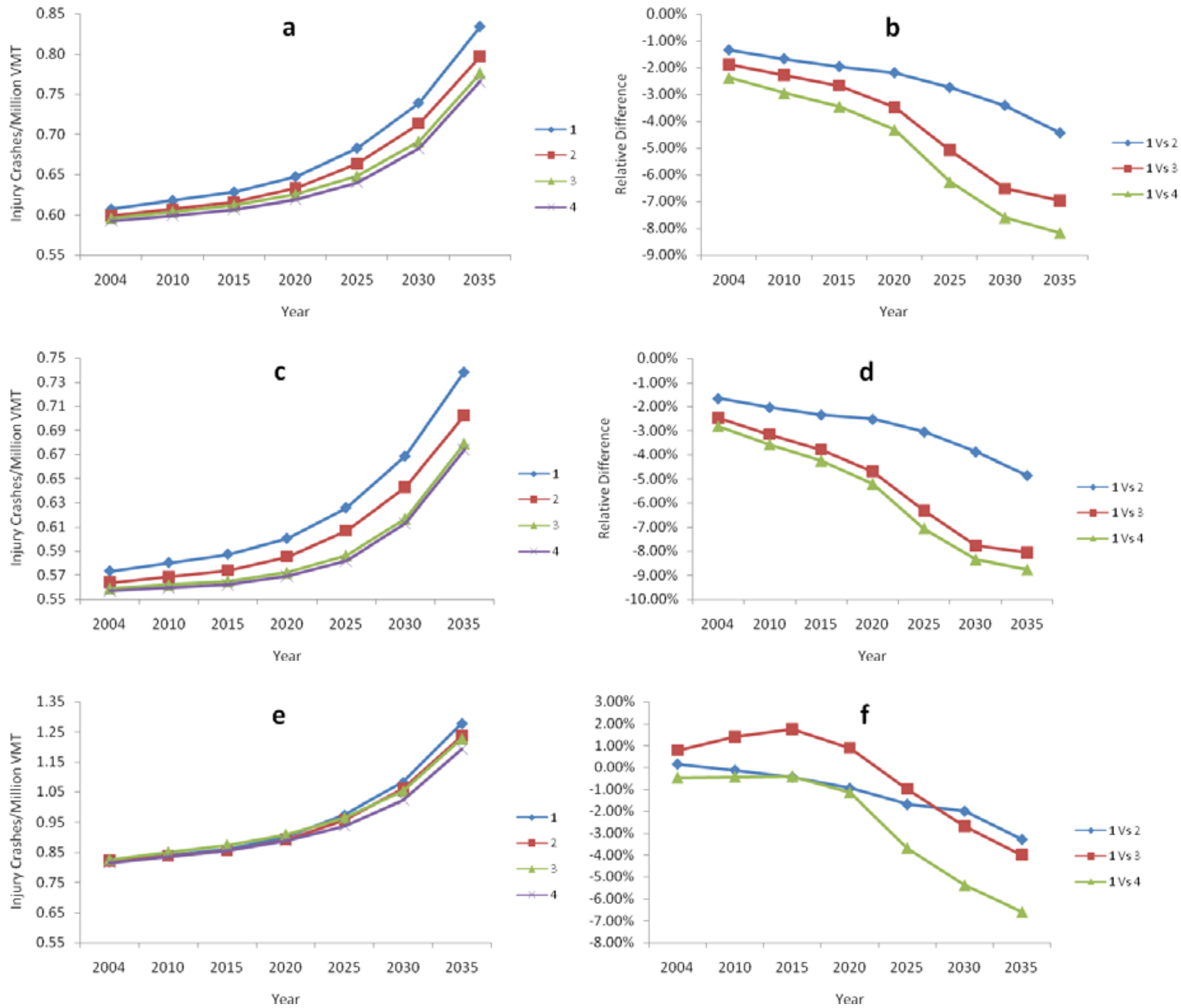

Figure 10: Comparison of scenario in terms of number of injury crahes/ million VMT and number of injury crahes/ million VMT relative difference by vehicle type. (a, b) All vehicles, (c, d) Cars, and (e, f) Trucks.

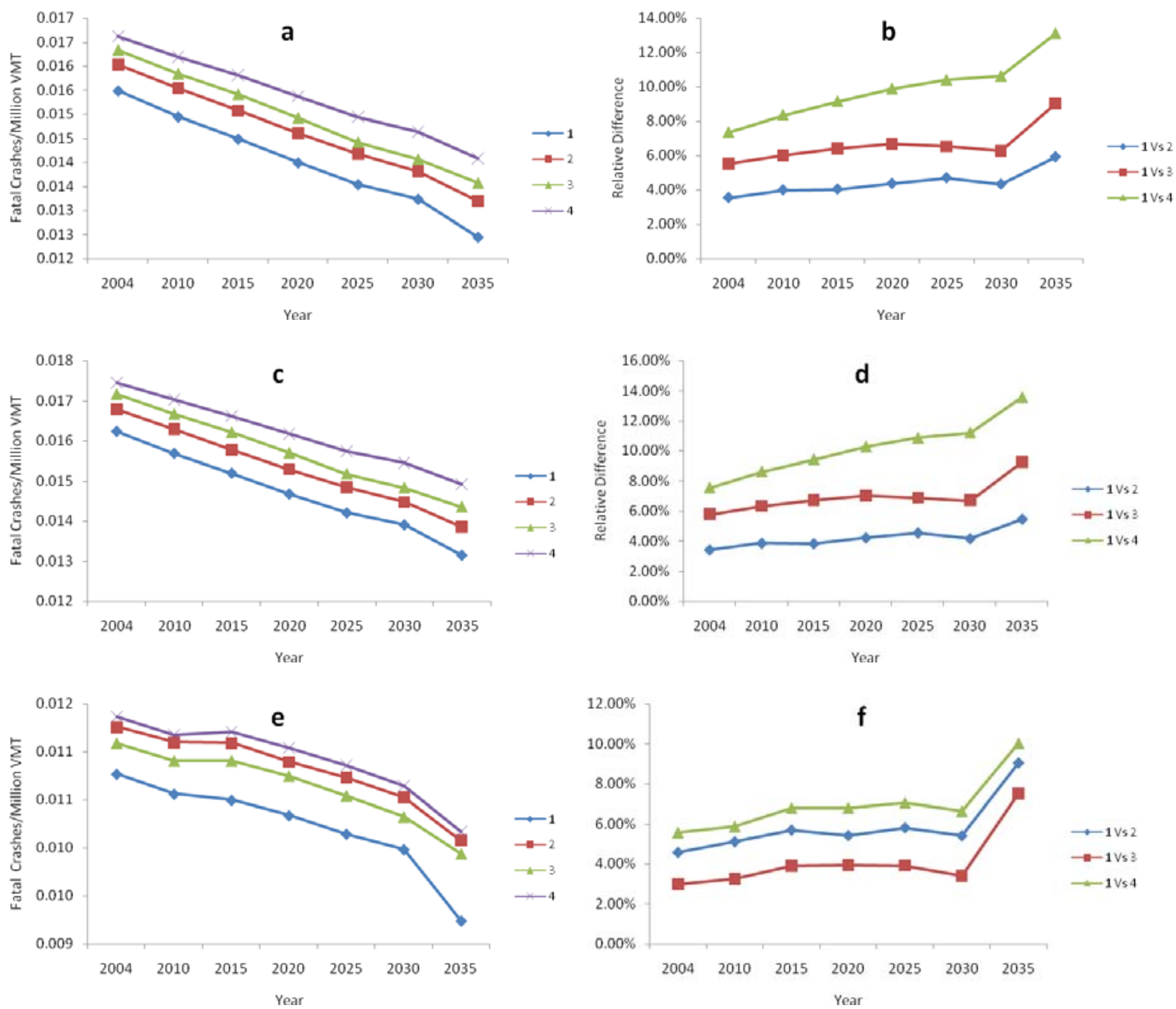

Figure 11: Comparison of scenario in terms of number of fatal crahes/ million VMT and number of fatal crahes/ million VMT relative difference by vehicle type. (a, b) All vehicles, (c, d) Cars, and (e, f) Trucks.

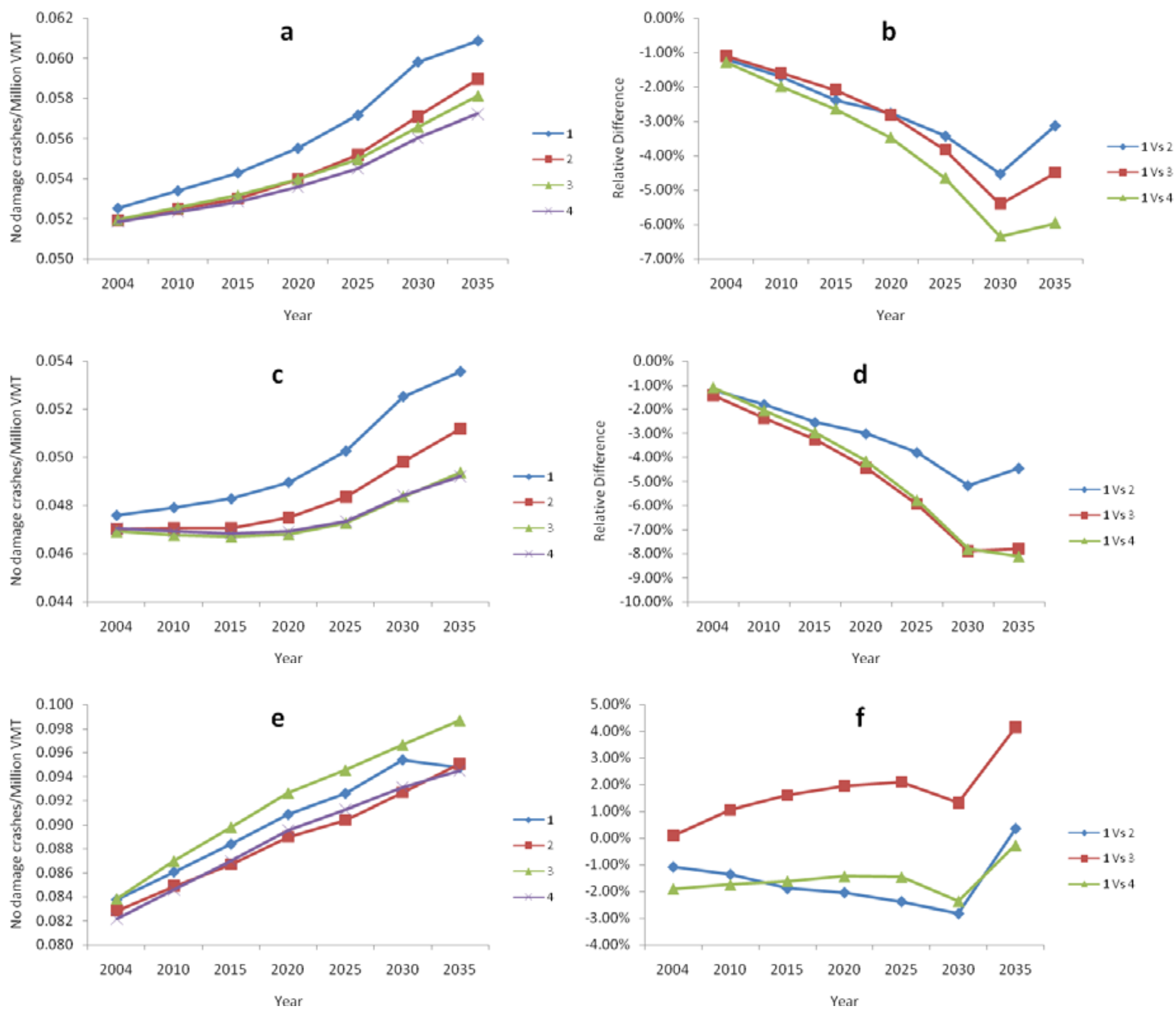

Figure 12: Comparison of scenario in terms of number of no damage crahes/ million VMT and number of no damage crahes/ million VMT relative difference by vehicle type. (a, b) All vehicles, (c, d) Cars, and (e, f) Trucks.

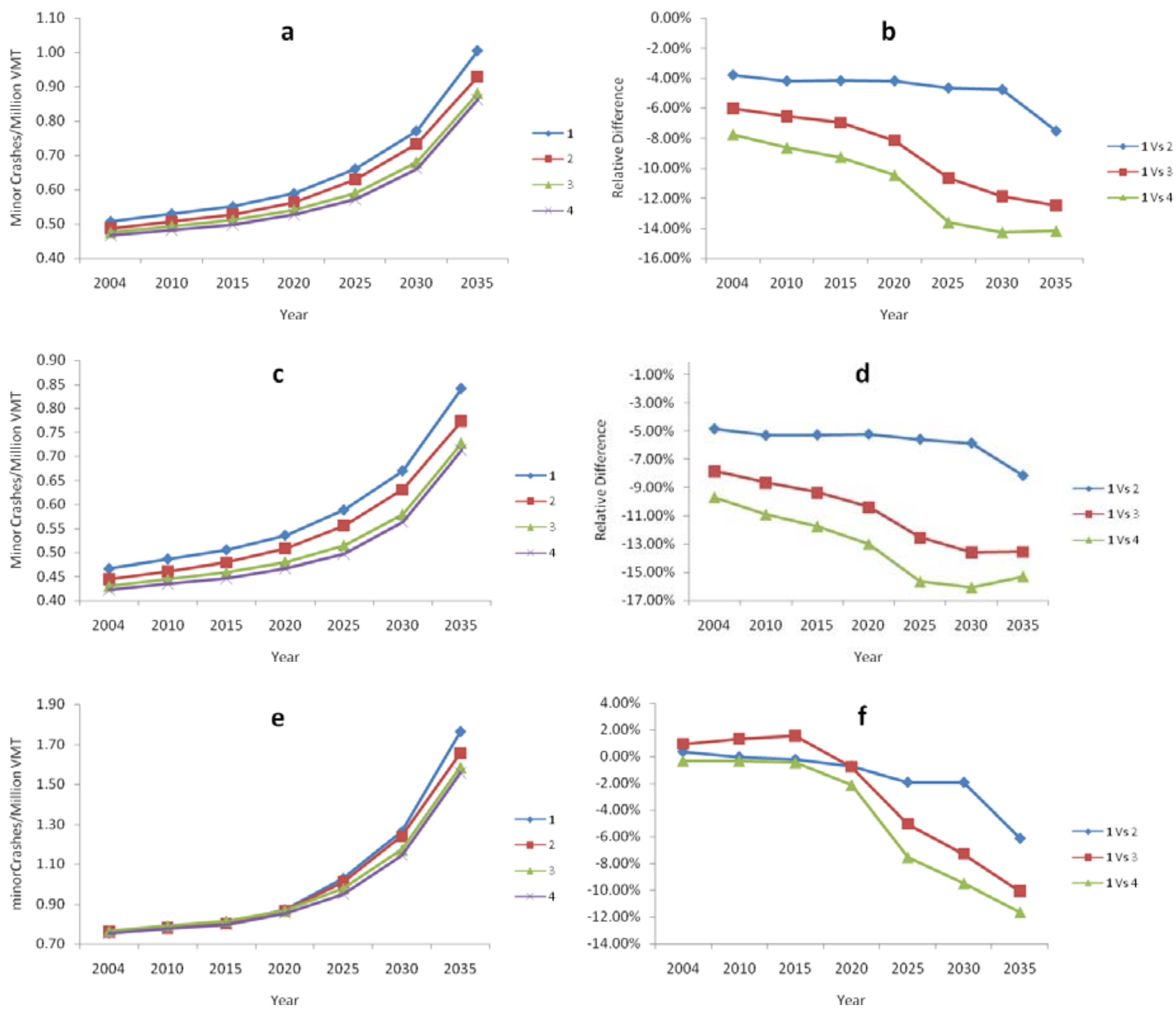

Figure 13: Comparison of scenario in terms of number of minor damage crahes/ million VMT and number of minor damage crahes/ million VMT relative difference by vehicle type. (a, b) All vehicles, (c, d) Cars, and (e, f) Trucks.

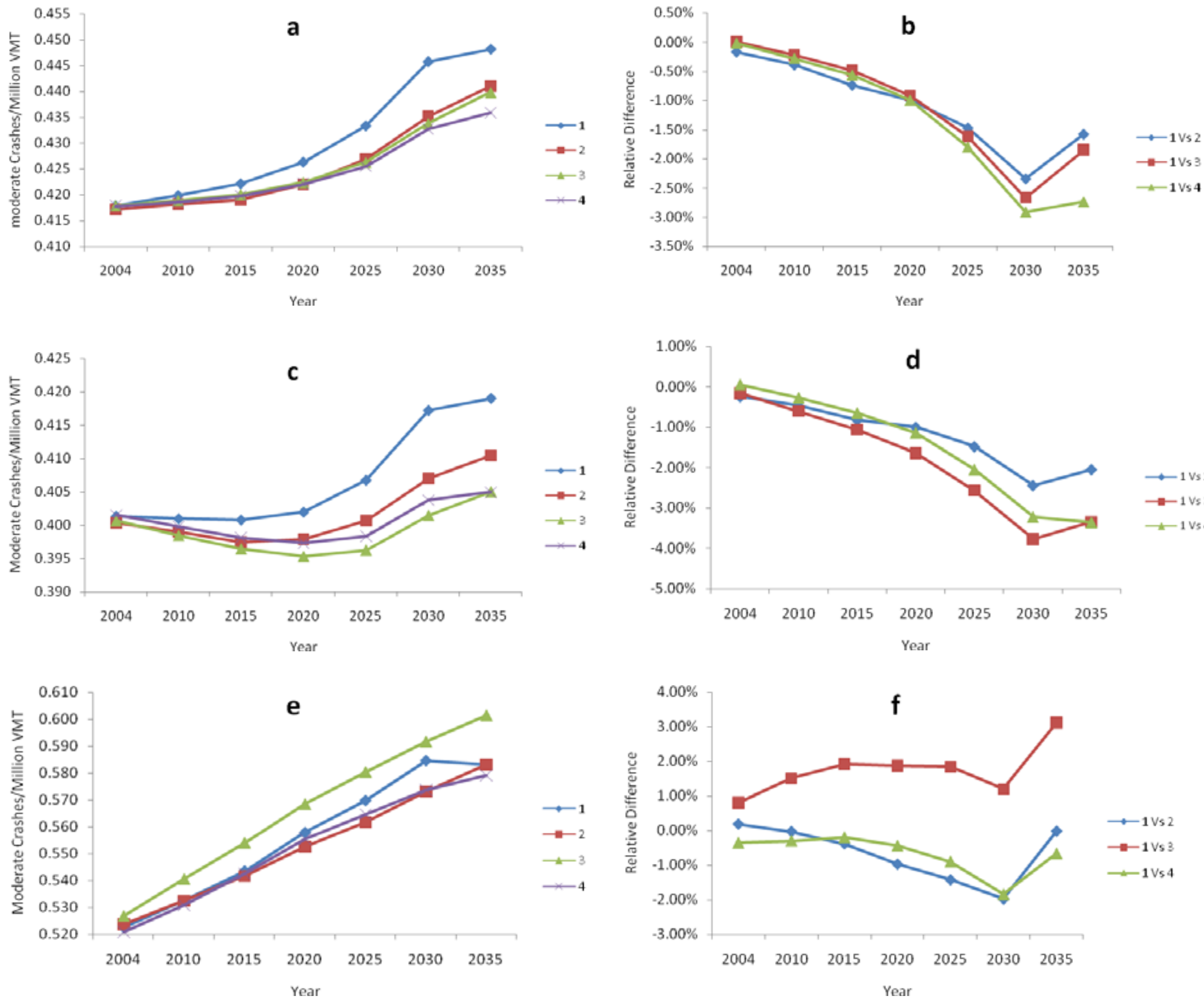

Figure 14: Comparison of scenario in terms of number of moderate damage crahes/ million VMT and number of moderate damage crahes/ million VMT relative difference by vehicle type. (a, b) All vehicles, (c, d) Cars, and (e, f) Trucks.

APPENDIX B: SUMMARY RESULTS BY SECTION

Table 18: Comparison of scenario in terms of different MEOs by vehicle type for section 1

MOE	Year	All				Cars				Trucks			
		Sc. 1	Sc. 2	Sc. 3	Sc. 4	Sc. 1	Sc. 2	Sc. 3	Sc. 4	Sc. 1	Sc. 2	Sc. 3	Sc. 4
Average Travel Time (min/veh)	2004	3.51	3.44	3.38	3.35	3.11	3.06	3.00	2.98	5.72	5.55	5.51	5.37
			-1.95%	-3.82%	-4.78%		-1.62%	-3.81%	-4.29%		-2.98%	-3.72%	-6.13%
	2010	3.58	3.50	3.43	3.39	3.15	3.10	3.01	2.99	5.80	5.61	5.63	5.47
			-2.21%	-4.24%	-5.39%		-1.81%	-4.55%	-5.15%		-3.28%	-3.02%	-5.67%
	2015	3.66	3.55	3.48	3.43	3.21	3.13	3.03	3.01	5.89	5.66	5.71	5.54
			-2.97%	-5.01%	-6.28%		-2.64%	-5.64%	-6.33%		-3.89%	-3.11%	-6.00%
	2020	3.79	3.63	3.54	3.48	3.31	3.19	3.06	3.02	6.02	5.71	5.82	5.62
			-4.10%	-6.46%	-8.05%		-3.75%	-7.71%	-8.70%		-5.06%	-3.32%	-6.53%
	2025	3.99	3.72	3.62	3.54	3.49	3.28	3.09	3.05	6.23	5.73	5.93	5.69
			-6.75%	-9.45%	-11.43%		-6.25%	-11.51%	-12.66%		-7.97%	-4.72%	-8.67%
	2030	4.39	3.82	3.69	3.60	3.82	3.36	3.13	3.09	6.81	5.74	6.03	5.71
			-12.97%	-15.78%	-17.85%		-11.98%	-17.96%	-19.00%		-15.58%	-11.36%	-16.03%
	2035	5.10	3.92	3.80	3.63	4.41	3.49	3.20	3.14	8.18	5.77	6.38	5.70
			-23.22%	-25.54%	-28.88%		-20.92%	-27.50%	-28.70%		-29.47%	-21.94%	-30.26%
Travel Speed (mph)	2004	59.33	60.51	61.69	62.31	66.95	68.05	69.60	69.95	36.44	37.56	37.85	38.82
			1.99%	3.97%	5.02%		1.64%	3.96%	4.48%		3.07%	3.86%	6.53%
	2010	58.21	59.53	60.79	61.53	66.09	67.31	69.24	69.68	35.94	37.16	37.06	38.10
			2.27%	4.43%	5.70%		1.84%	4.77%	5.43%		3.39%	3.11%	6.01%
	2015	56.97	58.71	59.97	60.79	64.91	66.67	68.78	69.29	35.38	36.81	36.52	37.64
			3.06%	5.27%	6.70%		2.71%	5.97%	6.75%		4.05%	3.21%	6.38%
	2020	55.06	57.41	58.86	59.88	62.97	65.42	68.23	68.96	34.65	36.49	35.84	37.07
			4.27%	6.89%	8.75%		3.89%	8.34%	9.51%		5.33%	3.43%	6.98%
	2025	52.20	55.98	57.64	58.93	59.68	63.66	67.43	68.32	33.48	36.38	35.14	36.66
			7.25%	10.42%	12.90%		6.68%	12.99%	14.48%		8.66%	4.95%	9.49%
	2030	47.57	54.62	56.44	57.87	54.60	62.00	66.50	67.36	30.66	36.29	34.56	36.48
			14.82%	18.64%	21.63%		13.55%	21.80%	23.36%		18.34%	12.71%	18.97%
	2035	40.98	53.24	54.90	57.47	47.36	59.78	65.19	66.29	25.60	36.15	32.69	36.55
			29.92%	33.95%	40.23%		26.23%	37.64%	39.96%		41.18%	27.70%	42.78%

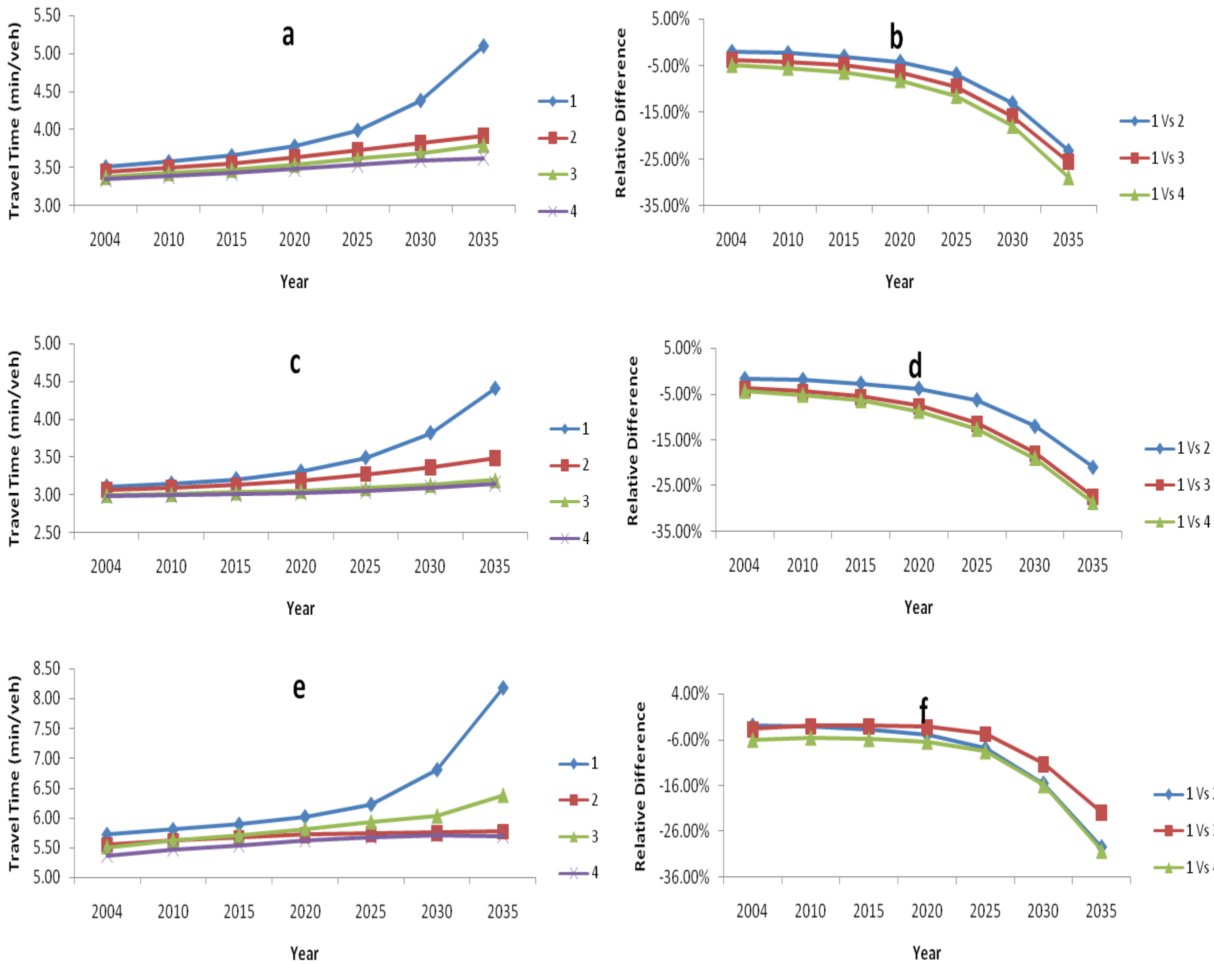

Figure 15: Comparison of scenario in terms of Travel Time and Travel Time relative difference by vehicle type fort section 1. (a, b) All vehicles, (c, d) Cars, and (e, f) Trucks.

Table 19: Comparison of scenario in terms of different MEOs by vehicle type for section 2.

MOE	Year	All				Cars				Trucks			
		Sc. 1	Sc. 2	Sc. 3	Sc. 4	Sc. 1	Sc. 2	Sc. 3	Sc. 4	Sc. 1	Sc. 2	Sc. 3	Sc. 4
Average Travel Time (min/veh)	2004	3.94	3.68	3.71	3.61	3.76	3.51	3.50	3.43	4.88	4.60	4.84	4.61
			-6.47%	-5.82%	-8.33%		-6.61%	-7.03%	-8.96%		-5.65%	-0.74%	-5.50%
	2010	4.03	3.72	3.76	3.64	3.85	3.55	3.53	3.44	4.99	4.64	4.95	4.64
			-7.68%	-6.84%	-9.85%		-7.83%	-8.34%	-10.57%		-7.02%	-0.86%	-6.96%
	2015	4.12	3.76	3.81	3.66	3.93	3.58	3.56	3.46	5.09	4.67	5.01	4.67
			-8.72%	-7.67%	-11.22%		-8.82%	-9.33%	-12.00%		-8.27%	-1.44%	-8.27%
	2020	4.23	3.81	3.86	3.70	4.02	3.62	3.59	3.48	5.25	4.75	5.10	4.72
			-9.87%	-8.75%	-12.69%		-9.93%	-10.51%	-13.43%		-9.56%	-2.76%	-10.14%
	2025	4.33	3.85	3.93	3.73	4.10	3.65	3.64	3.49	5.41	4.81	5.23	4.79
			-11.10%	-9.40%	-13.99%		-11.08%	-11.26%	-14.83%		-11.15%	-3.43%	-11.48%
	2030	4.41	3.90	3.95	3.74	4.17	3.69	3.67	3.51	5.54	4.87	5.29	4.83
			-11.49%	-10.28%	-15.08%		-11.49%	-12.09%	-15.92%		-12.07%	-4.65%	-12.85%
	2035	4.44	3.94	3.96	3.76	4.21	3.72	3.68	3.52	5.64	4.99	5.32	4.90
			-11.38%	-10.93%	-15.44%		-11.63%	-12.67%	-16.42%		-11.65%	-5.66%	-13.21%
Travel Speed (mph)	2004	61.20	65.43	64.98	66.76	64.00	68.53	68.84	70.30	49.40	52.36	49.77	52.28
			6.92%	6.18%	9.09%		7.08%	7.56%	9.84%		5.99%	0.75%	5.83%
	2010	59.72	64.68	64.10	66.24	62.59	67.91	68.29	69.99	48.27	51.92	48.70	51.88
			8.31%	7.34%	10.92%		8.49%	9.10%	11.81%		7.55%	0.88%	7.48%
	2015	58.41	63.99	63.26	65.80	61.31	67.24	67.62	69.67	47.35	51.62	48.04	51.62
			9.55%	8.30%	12.64%		9.68%	10.29%	13.63%		9.02%	1.47%	9.01%
	2020	56.91	63.14	62.37	65.18	59.96	66.57	67.00	69.26	45.90	50.75	47.21	51.08
			10.95%	9.59%	14.54%		11.02%	11.75%	15.51%		10.57%	2.84%	11.29%
	2025	55.58	62.52	61.35	64.63	58.73	66.05	66.18	68.96	44.51	50.09	46.09	50.28
			12.49%	10.37%	16.27%		12.47%	12.69%	17.41%		12.56%	3.55%	12.97%
	2030	54.68	61.78	60.94	64.39	57.70	65.19	65.63	68.63	43.46	49.43	45.57	49.87
			12.98%	11.46%	17.76%		12.98%	13.75%	18.94%		13.73%	4.87%	14.74%
	2035	54.20	61.16	60.85	64.09	57.18	64.71	65.48	68.41	42.68	48.31	45.24	49.17
			12.83%	12.26%	18.25%		13.16%	14.51%	19.63%		13.19%	5.99%	15.21%

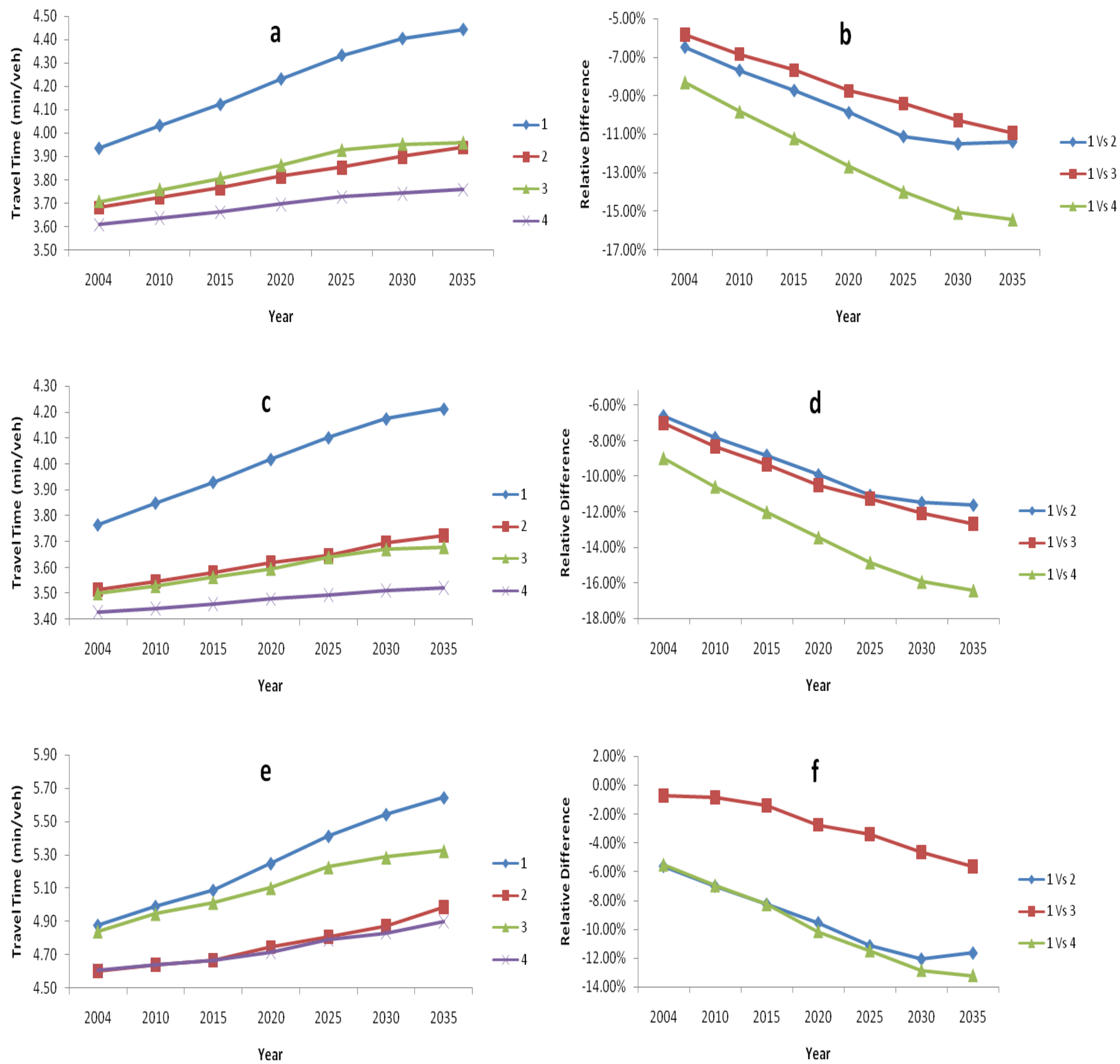

Figure 16: Comparison of scenario in terms of Travel Time and Travel Time relative difference by vehicle type fort section 2. (a, b) All vehicles, (c, d) Cars, and (e, f) Trucks.

Table 20: Comparison of scenario in terms of different MEOs by vehicle type for section 3.

MOE	Year	All				Cars				Trucks			
		Sc. 1	Sc. 2	Sc. 3	Sc. 4	Sc. 1	Sc. 2	Sc. 3	Sc. 4	Sc. 1	Sc. 2	Sc. 3	Sc. 4
Average Travel Time (min/veh)	2004	1.63	1.65	1.61	1.61	1.45	1.47	1.42	1.42	2.73	2.74	2.73	2.75
			1.00%	-1.75%	-1.67%		1.01%	-2.36%	-2.60%		0.35%	-0.21%	0.43%
	2010	1.67	1.69	1.64	1.63	1.48	1.50	1.44	1.43	2.76	2.76	2.75	2.76
			0.97%	-1.85%	-2.23%		1.15%	-2.52%	-3.23%		0.05%	-0.32%	-0.02%
	2015	1.69	1.73	1.67	1.66	1.50	1.54	1.47	1.45	2.78	2.77	2.76	2.77
			1.91%	-1.67%	-2.28%		2.41%	-2.20%	-3.27%		-0.21%	-0.71%	-0.34%
	2020	1.72	1.77	1.70	1.69	1.52	1.58	1.50	1.48	2.81	2.79	2.78	2.78
			2.76%	-1.29%	-2.23%		3.71%	-1.58%	-3.07%		-0.58%	-1.05%	-0.96%
	2025	1.76	1.82	1.76	1.72	1.56	1.63	1.56	1.51	2.85	2.82	2.81	2.81
			3.20%	-0.29%	-2.46%		4.35%	-0.25%	-3.43%		-1.12%	-1.58%	-1.47%
	2030	1.77	1.88	1.81	1.76	1.57	1.71	1.62	1.56	2.87	2.84	2.83	2.84
			6.56%	2.50%	-0.26%		8.70%	3.46%	-0.65%		-1.16%	-1.53%	-1.03%
	2035	1.79	2.00	1.92	1.80	1.59	1.82	1.74	1.59	2.90	2.91	2.89	2.88
			11.49%	7.01%	0.56%		14.46%	8.89%	0.04%		0.30%	-0.18%	-0.63%
Travel Speed (mph)	2004	58.86	58.28	59.91	59.86	66.12	65.46	67.72	67.88	35.19	35.06	35.26	35.04
			-0.99%	1.78%	1.70%		-1.00%	2.41%	2.67%		-0.35%	0.21%	-0.43%
	2010	57.62	57.07	58.71	58.94	64.90	64.17	66.58	67.07	34.86	34.85	34.98	34.87
			-0.96%	1.88%	2.28%		-1.13%	2.59%	3.34%		-0.05%	0.32%	0.02%
	2015	56.78	55.72	57.75	58.10	64.08	62.57	65.52	66.24	34.66	34.73	34.91	34.78
			-1.87%	1.70%	2.33%		-2.35%	2.25%	3.37%		0.21%	0.71%	0.34%
	2020	55.78	54.29	56.51	57.06	63.10	60.85	64.12	65.10	34.23	34.43	34.60	34.57
			-2.68%	1.31%	2.28%		-3.57%	1.61%	3.17%		0.59%	1.06%	0.97%
	2025	54.66	52.98	54.83	56.03	61.69	59.14	61.87	63.88	33.75	34.13	34.29	34.25
			-3.07%	0.33%	2.52%		-4.12%	0.31%	3.56%		1.13%	1.60%	1.49%
	2030	54.46	51.14	53.20	54.66	61.29	56.43	59.34	61.78	33.50	33.90	34.03	33.85
			-6.10%	-2.32%	0.37%		-7.93%	-3.17%	0.80%		1.18%	1.58%	1.05%
	2035	53.74	48.31	50.72	53.54	60.40	52.95	56.25	60.52	33.19	33.10	33.29	33.42
			-10.10%	-5.63%	-0.38%		-12.33%	-6.86%	0.20%		-0.28%	0.30%	0.69%

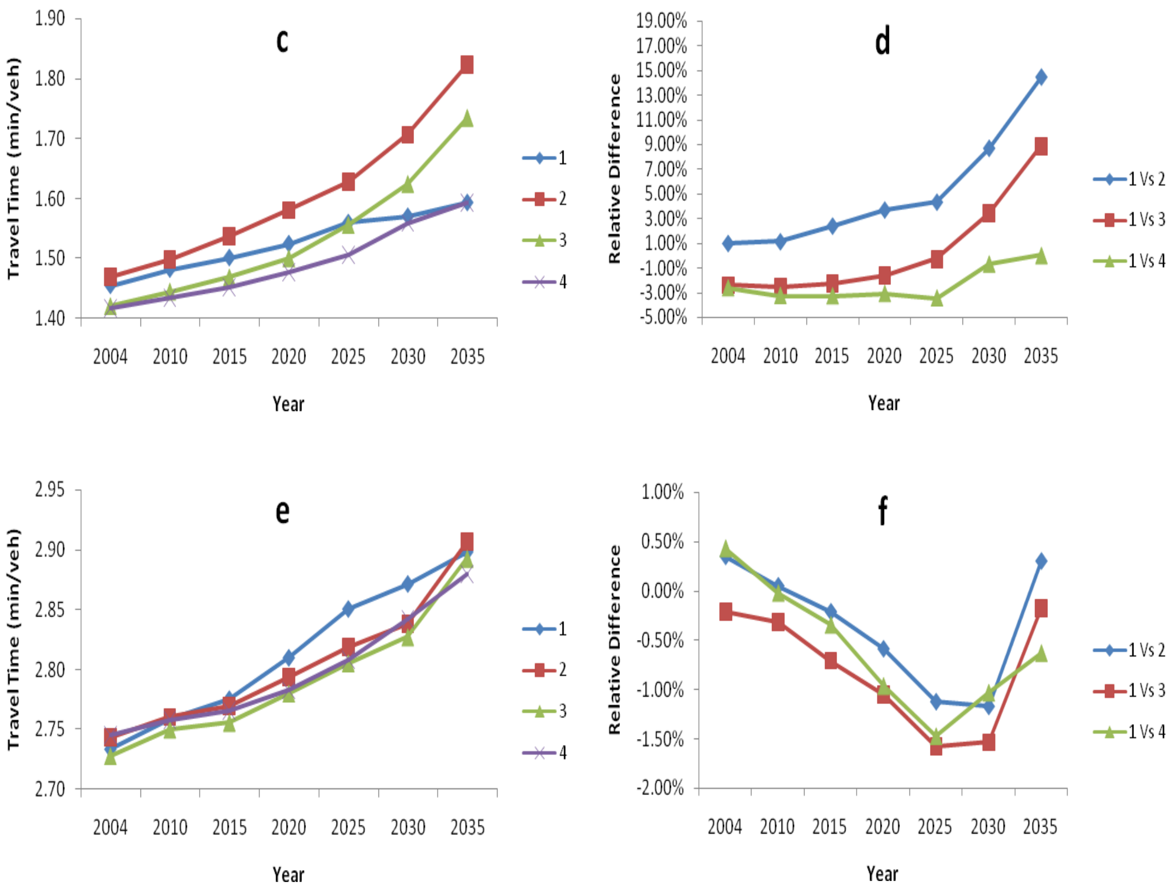

Figure 17: Comparison of scenario in terms of Travel Time and Travel Time relative difference by vehicle type fort section 3. (a, b) All vehicles, (c, d) Cars, and (e, f) Trucks.

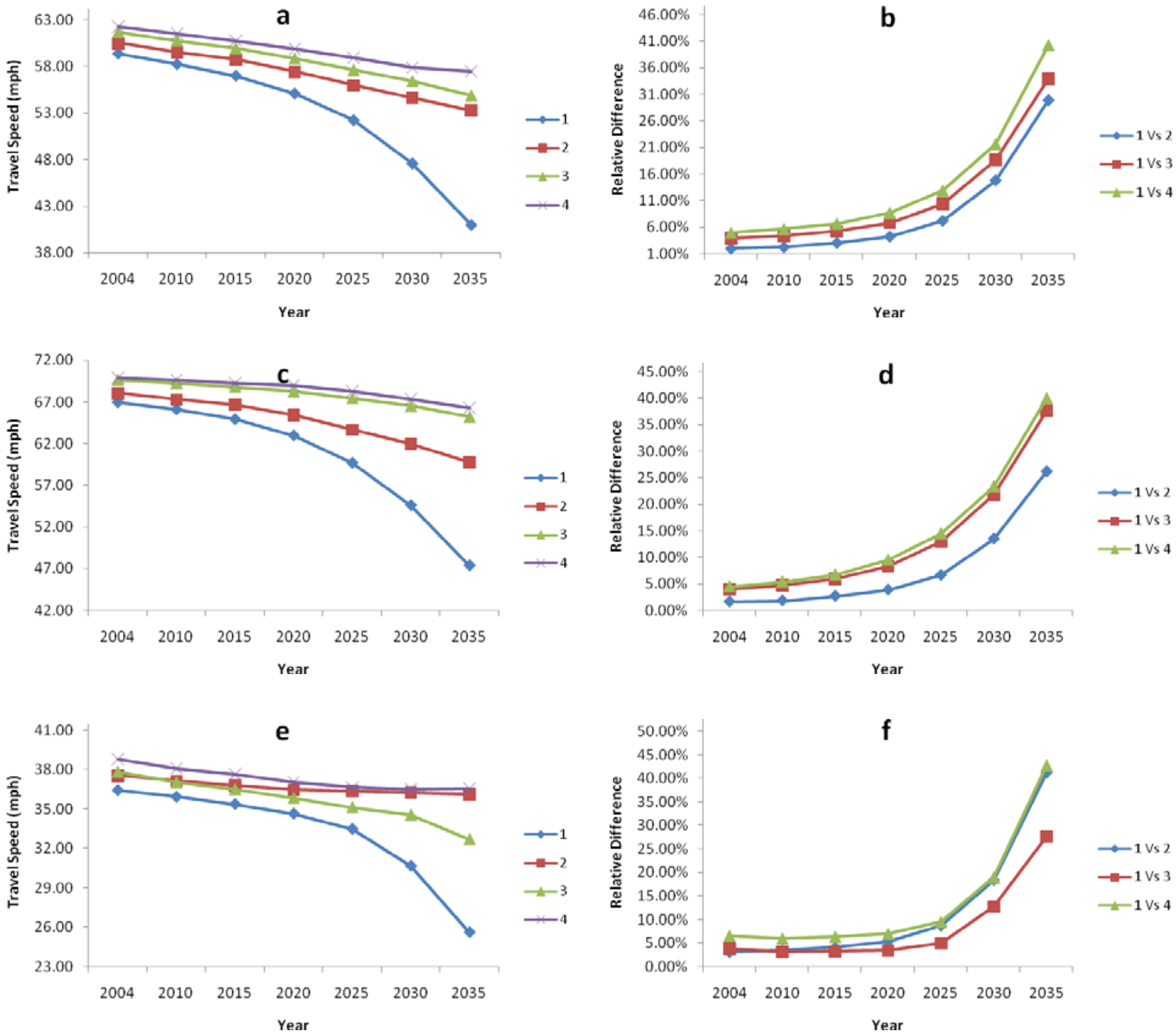

Figure 18: Comparison of scenario in terms of Travel Speed and Travel Speed relative difference by vehicle type for section 1. (a, b) All vehicles, (c, d) Cars, and (e, f) Trucks.

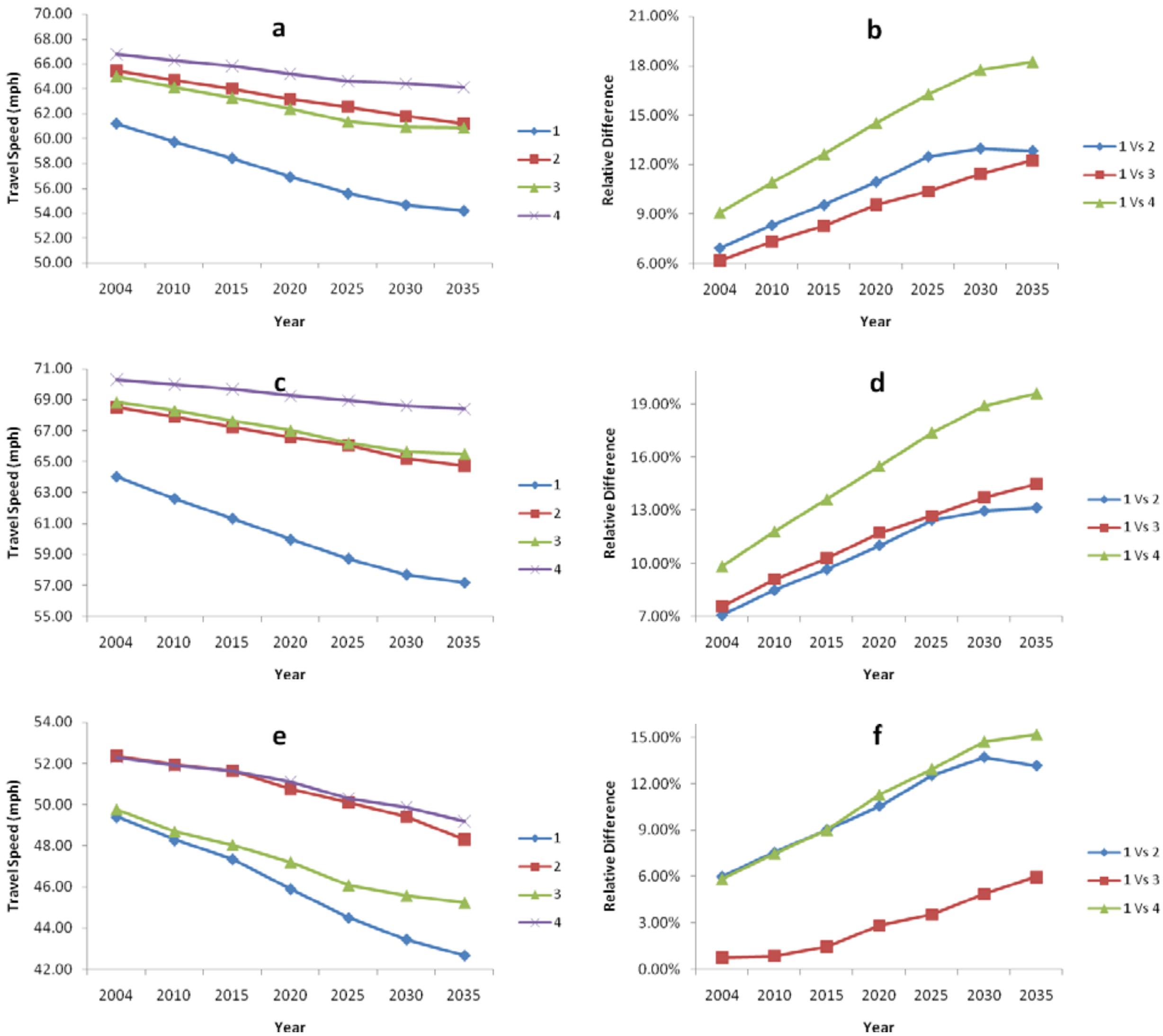

Figure 19: Comparison of scenario in terms of Travel Speed and Travel Speed relative difference by vehicle type for section 2. (a, b) All vehicles, (c, d) Cars, and (e, f) Trucks.

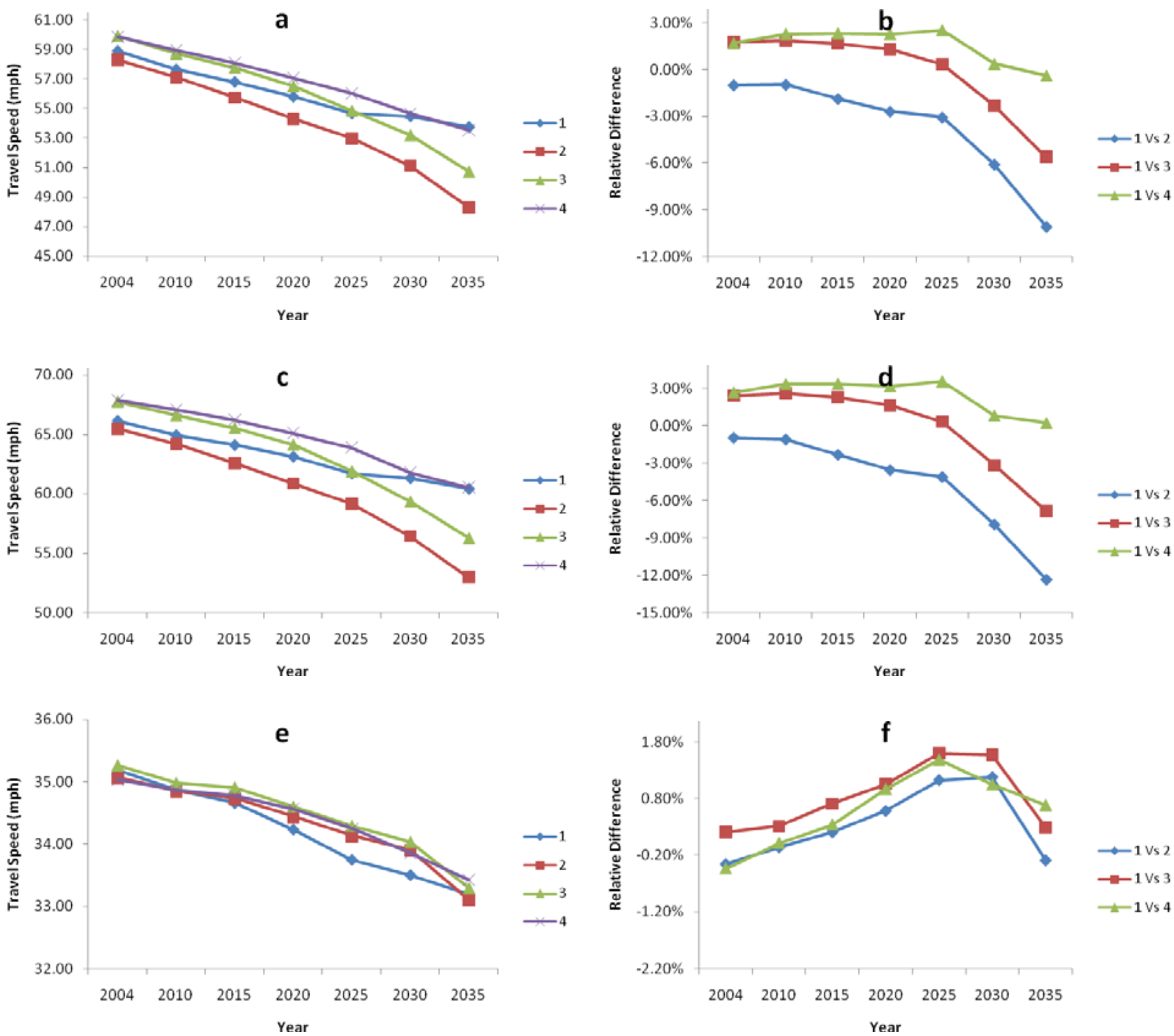

Figure 20: Comparison of scenario in terms of Travel Speed and Travel Speed relative difference by vehicle type for section 3. (a, b) All vehicles, (c, d) Cars, and (e, f) Trucks.

Table 21: Fuel Consumption and HC Emissions by Section

MOE	Year	Section 1				Section 2				Section 3			
		Sc. 1	Sc. 2	Sc. 3	Sc. 4	Sc. 1	Sc. 2	Sc. 3	Sc. 4	Sc. 1	Sc. 2	Sc. 3	Sc. 4
Fuel (liter/mil/veh)	2004	0.189	0.186	0.188	0.185	0.163	0.163	0.166	0.165	0.211	0.210	0.211	0.212
			-1.82%	-0.78%	-2.16%		-0.17%	1.72%	0.96%		-0.28%	0.27%	0.59%
	2010	0.191	0.188	0.190	0.187	0.164	0.163	0.167	0.165	0.212	0.212	0.213	0.213
			-1.86%	-0.75%	-2.09%		-0.54%	1.65%	0.76%		-0.44%	0.15%	0.45%
	2015	0.194	0.190	0.192	0.189	0.165	0.163	0.167	0.166	0.214	0.212	0.214	0.215
			-2.07%	-0.86%	-2.22%		-1.01%	1.34%	0.41%		-0.69%	-0.13%	0.27%
	2020	0.197	0.193	0.195	0.192	0.166	0.164	0.168	0.166	0.216	0.214	0.215	0.216
			-2.19%	-1.03%	-2.47%		-1.69%	0.80%	-0.38%		-1.03%	-0.49%	-0.18%
	2025	0.201	0.195	0.197	0.195	0.167	0.163	0.168	0.166	0.217	0.214	0.216	0.217
			-2.72%	-1.60%	-3.05%		-2.53%	0.42%	-1.00%		-1.34%	-0.67%	-0.25%
	2030	0.206	0.198	0.200	0.197	0.166	0.162	0.167	0.165	0.217	0.214	0.215	0.216
			-3.98%	-2.94%	-4.45%		-2.44%	0.23%	-0.90%		-1.25%	-0.57%	-0.21%
	2035	0.212	0.200	0.202	0.198	0.166	0.162	0.166	0.165	0.217	0.217	0.217	0.218
			-5.76%	-4.70%	-6.70%		-1.93%	0.25%	-0.35%		-0.18%	-0.04%	0.18%
HC (g/mil/veh)	2004	196.5	184.4	170.4	164.0	151.0	130.7	139.1	127.4	216.1	203.1	192.0	191.8
			-6.17%	-13.26%	-16.56%	0.00%	-13.44%	-7.90%	-15.63%		-5.99%	-11.15%	-11.25%
	2010	203.5	192.9	177.1	170.3	156.2	133.9	144.0	130.6	227.2	208.2	200.3	197.7
			-5.18%	-12.96%	-16.29%	0.00%	-14.25%	-7.79%	-16.39%		-8.34%	-11.84%	-12.98%
	2015	210.1	198.5	183.5	176.3	159.3	136.1	148.0	132.9	234.7	211.3	206.3	201.9
			-5.50%	-12.64%	-16.08%	0.00%	-14.58%	-7.10%	-16.57%	0.00%	-9.96%	-12.08%	-13.95%
	2020	217.6	206.8	191.4	182.5	160.6	139.2	151.3	135.5	240.0	211.7	213.0	205.2
			-4.93%	-12.02%	-16.12%	0.00%	-13.35%	-5.78%	-15.63%	0.00%	-11.77%	-11.25%	-14.51%
	2025	225.4	212.0	200.0	190.2	158.1	139.6	154.1	137.6	242.4	210.2	218.5	206.5
			-5.93%	-11.24%	-15.59%	0.00%	-11.69%	-2.52%	-12.97%	0.00%	-13.28%	-9.85%	-14.82%
	2030	233.7	217.4	209.4	199.5	152.0	139.4	152.3	136.8	242.3	205.4	219.5	205.7
			-6.97%	-10.42%	-14.64%	0.00%	-8.27%	0.21%	-10.00%	0.00%	-15.21%	-9.39%	-15.09%
	2035	246.7	219.4	221.9	206.7	147.4	140.0	147.5	138.0	244.3	205.0	222.1	207.8
			-11.05%	-10.04%	-16.22%	0.00%	-5.02%	0.11%	-6.36%	0.00%	-16.09%	-9.09%	-14.93%

Table 22: CO and NOx Emissions by Section

MOE	Year	Section 1				Section 2				Section 3			
		Sc. 1	Sc. 2	Sc. 3	Sc. 4	Sc. 1	Sc. 2	Sc. 3	Sc. 4	Sc. 1	Sc. 2	Sc. 3	Sc. 4
CO (g/mil/veh)	2004	28060	22736 -19%	14735 -47%	12514 -55%	19359	7540 -61%	9977 -48%	4761 -75%	30223	25010 -17%	17129 -43%	17053 -44%
	2010	29297	24904 -15%	15441 -47%	13087 -55%	20953	8275 -61%	11017 -47%	5197 -75%	34149	26021 -24%	19319 -43%	18166 -47%
	2015	30620	25792 -16%	16580 -46%	14049 -54%	21481	8652 -60%	12073 -44%	5402 -75%	36523	26409 -28%	21168 -42%	18899 -48%
	2020	31670	27518 -13%	17493 -45%	14155 -55%	20443	9187 -55%	12437 -39%	5606 -73%	37624	25208 -33%	23149 -38%	18977 -50%
	2025	32894	28331 -14%	19386 -41%	15675 -52%	17999	9073 -50%	12792 -29%	5743 -68%	38412	23780 -38%	25598 -33%	18569 -52%
	2030	33156	29598 -11%	22104 -33%	18674 -44%	15808	9752 -38%	12661 -20%	5971 -62%	39846	22591 -43%	27368 -31%	19236 -52%
	2035	34544	30141 -13%	26948 -22%	22396 -35%	14223	9677 -32%	10709 -25%	6322 -56%	40696	20450 -50%	27760 -32%	18917 -54%
NO_x (g/mil/veh)	2004	1629	1588 -2.5%	1614 -0.9%	1570 -3.6%	1458	1460 0.1%	1488 2.0%	1466 0.5%	1705	1720 0.9%	1719 0.8%	1737 1.9%
	2010	1696	1654 -2.5%	1682 -0.8%	1639 -3.4%	1479	1489 0.7%	1521 2.8%	1499 1.3%	1765	1779 0.8%	1780 0.8%	1797 1.8%
	2015	1757	1714 -2.4%	1744 -0.8%	1703 -3.1%	1513	1524 0.7%	1556 2.8%	1537 1.6%	1816	1830 0.8%	1825 0.5%	1847 1.7%
	2020	1834	1793 -2.2%	1828 -0.3%	1785 -2.6%	1539	1548 0.5%	1587 3.1%	1562 1.5%	1873	1881 0.4%	1874 0.1%	1899 1.4%
	2025	1902	1855 -2.4%	1899 -0.2%	1859 -2.2%	1543	1547 0.3%	1606 4.1%	1573 1.9%	1894	1905 0.6%	1899 0.2%	1931 2.0%
	2030	1974	1900 -3.7%	1960 -0.7%	1919 -2.7%	1482	1516 2.3%	1569 5.9%	1545 4.3%	1854	1877 1.2%	1866 0.6%	1906 2.8%
	2035	2024	1916 -5.3%	1991 -1.6%	1927 -4.8%	1441	1508 4.6%	1547 7.3%	1543 7.0%	1865	1936 3.8%	1892 1.5%	1943 4.2%

Table 23: Safety Impacts by Section

MOE	Year	Section 1				Section 2				Section 3			
		Sc. 1	Sc. 2	Sc. 3	Sc. 4	Sc. 1	Sc. 2	Sc. 3	Sc. 4	Sc. 1	Sc. 2	Sc. 3	Sc. 4
Expected number of Crashes/ Million VMT	2004	1.26	1.23 -1.98%	1.21 -3.75%	1.20 -4.75%	1.22	1.15 -6.43%	1.15 -5.87%	1.12 -8.31%	1.28	1.29 0.95%	1.26 -1.79%	1.26 -1.72%
	2010	1.28	1.25 -2.38%	1.23 -4.20%	1.22 -5.37%	1.25	1.16 -7.63%	1.17 -6.85%	1.13 -9.84%	1.31	1.32 0.98%	1.28 -1.86%	1.28 -2.26%
	2015	1.31	1.27 -3.05%	1.25 -4.97%	1.23 -6.31%	1.28	1.17 -8.63%	1.18 -7.69%	1.14 -11.16%	1.33	1.35 1.92%	1.30 -1.69%	1.30 -2.28%
	2020	1.36	1.30 -4.19%	1.27 -6.58%	1.25 -8.22%	1.32	1.19 -9.75%	1.20 -8.78%	1.15 -12.64%	1.35	1.39 2.77%	1.33 -1.30%	1.32 -2.28%
	2025	1.43	1.33 -6.78%	1.29 -9.51%	1.26 -11.55%	1.35	1.20 -11.04%	1.22 -9.49%	1.16 -14.03%	1.38	1.42 3.14%	1.38 -0.29%	1.35 -2.47%
	2030	1.57	1.37 -12.91%	1.32 -16.04%	1.29 -18.17%	1.37	1.21 -11.44%	1.23 -10.33%	1.16 -15.07%	1.38	1.48 6.70%	1.42 2.64%	1.38 -0.19%
	2035	1.83	1.41 -23.22%	1.36 -25.52%	1.30 -28.90%	1.39	1.23 -11.38%	1.23 -10.99%	1.17 -15.45%	1.40	1.56 11.67%	1.50 7.11%	1.41 0.62%
Expected number of Injury Crashes/ Million VMT	2004	0.600	0.588 -1.93%	0.580 -3.28%	0.575 -4.23%	0.577	0.544 -5.62%	0.549 -4.88%	0.537 -6.82%	0.610	0.616 1.00%	0.602 -1.26%	0.604 -0.98%
	2010	0.611	0.597 -2.33%	0.588 -3.65%	0.582 -4.79%	0.590	0.549 -6.87%	0.555 -5.93%	0.541 -8.35%	0.622	0.628 0.98%	0.613 -1.43%	0.612 -1.56%
	2015	0.623	0.604 -3.01%	0.596 -4.38%	0.587 -5.68%	0.602	0.554 -7.98%	0.561 -6.85%	0.543 -9.75%	0.631	0.642 1.76%	0.622 -1.37%	0.620 -1.70%
	2020	0.644	0.617 -4.16%	0.606 -6.01%	0.595 -7.62%	0.617	0.561 -9.08%	0.567 -8.04%	0.547 -11.28%	0.642	0.658 2.58%	0.635 -1.04%	0.630 -1.77%
	2025	0.677	0.632 -6.71%	0.616 -8.98%	0.603 -10.99%	0.632	0.566 -10.41%	0.575 -8.89%	0.551 -12.70%	0.654	0.673 2.92%	0.653 -0.20%	0.641 -2.03%
	2030	0.742	0.648 -12.62%	0.627 -15.40%	0.612 -17.51%	0.642	0.572 -10.91%	0.579 -9.89%	0.553 -13.84%	0.655	0.698 6.43%	0.673 2.62%	0.656 0.13%
	2035	0.845	0.666 -21.11%	0.649 -23.20%	0.620 -26.62%	0.649 0.00%	0.578 -10.88%	0.580 -10.68%	0.557 -14.24%	0.663	0.738 11.36%	0.710 7.05%	0.669 0.96%
Expected number of Fatal Crashes/ Million VMT	2004	0.015	0.015 0.65%	0.016 6.67%	0.016 7.30%	0.013	0.016 18.58%	0.016 18.44%	0.017 27.95%	0.015	0.015 1.34%	0.016 9.22%	0.016 10.66%
	2010	0.015	0.015 0.01%	0.016 7.90%	0.016 8.14%	0.012	0.015 22.92%	0.015 22.49%	0.017 34.11%	0.014	0.014 -0.24%	0.015 8.28%	0.016 11.14%
	2015	0.014	0.014 0.03%	0.015 9.04%	0.015 9.09%	0.012	0.015 25.78%	0.015 24.86%	0.016 38.71%	0.014	0.014 -3.47%	0.015 6.17%	0.015 9.63%
	2020	0.014	0.013 -1.23%	0.015 9.15%	0.015 9.41%	0.011	0.014 31.04%	0.014 28.38%	0.016 45.79%	0.014	0.013 -3.72%	0.014 4.89%	0.015 9.13%
	2025	0.013	0.013 -2.90%	0.015 9.11%	0.015 9.00%	0.010	0.014 35.89%	0.013 30.30%	0.016 52.91%	0.014	0.013 -4.99%	0.014 2.07%	0.015 6.93%
	2030	0.013	0.012 -4.12%	0.014 9.58%	0.014 8.87%	0.010	0.013 37.70%	0.013 31.51%	0.015 57.32%	0.014	0.013 -5.87%	0.014 1.91%	0.015 6.34%
	2035	0.011	0.012 4.28%	0.014 23.80%	0.014 21.01%	0.010	0.013 37.05%	0.013 31.99%	0.015 58.87%	0.014	0.013 -3.88%	0.014 5.11%	0.015 7.75%

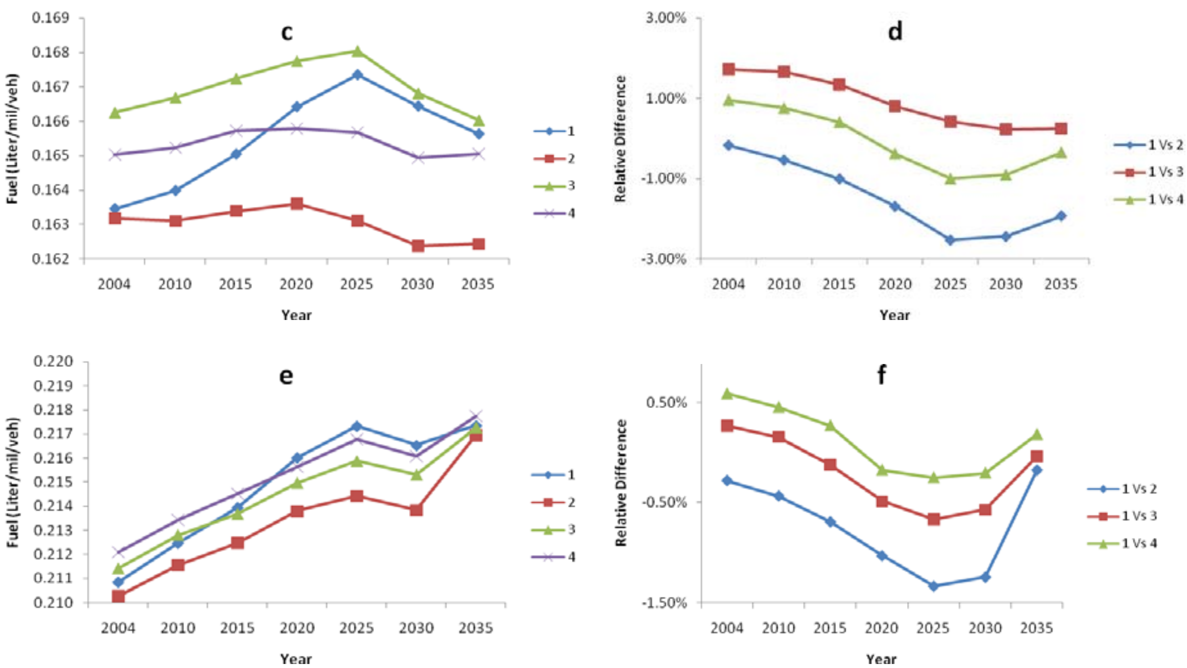

Figure 21: Comparison of scenario in terms of Fuel consumption and Fuel consumption relative difference by section. (a, b) Section 1, (c, d) Section 2, and (e, f) Section 3.

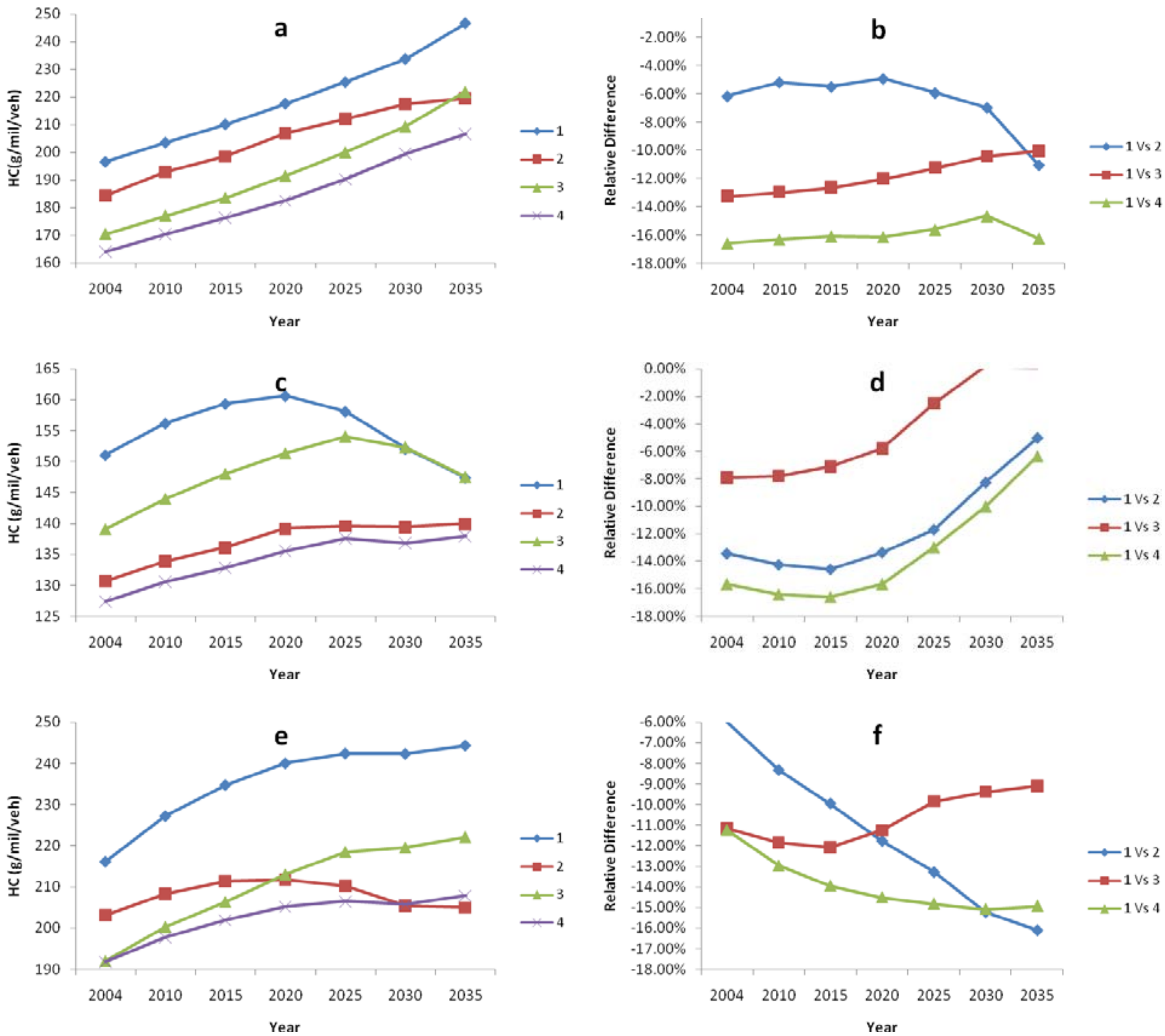

Figure 22: Comparison of scenario in terms of HC emission and HC emission relative difference by section. (a, b) Section 1, (c, d) Section 2, and (e, f) Section 3.

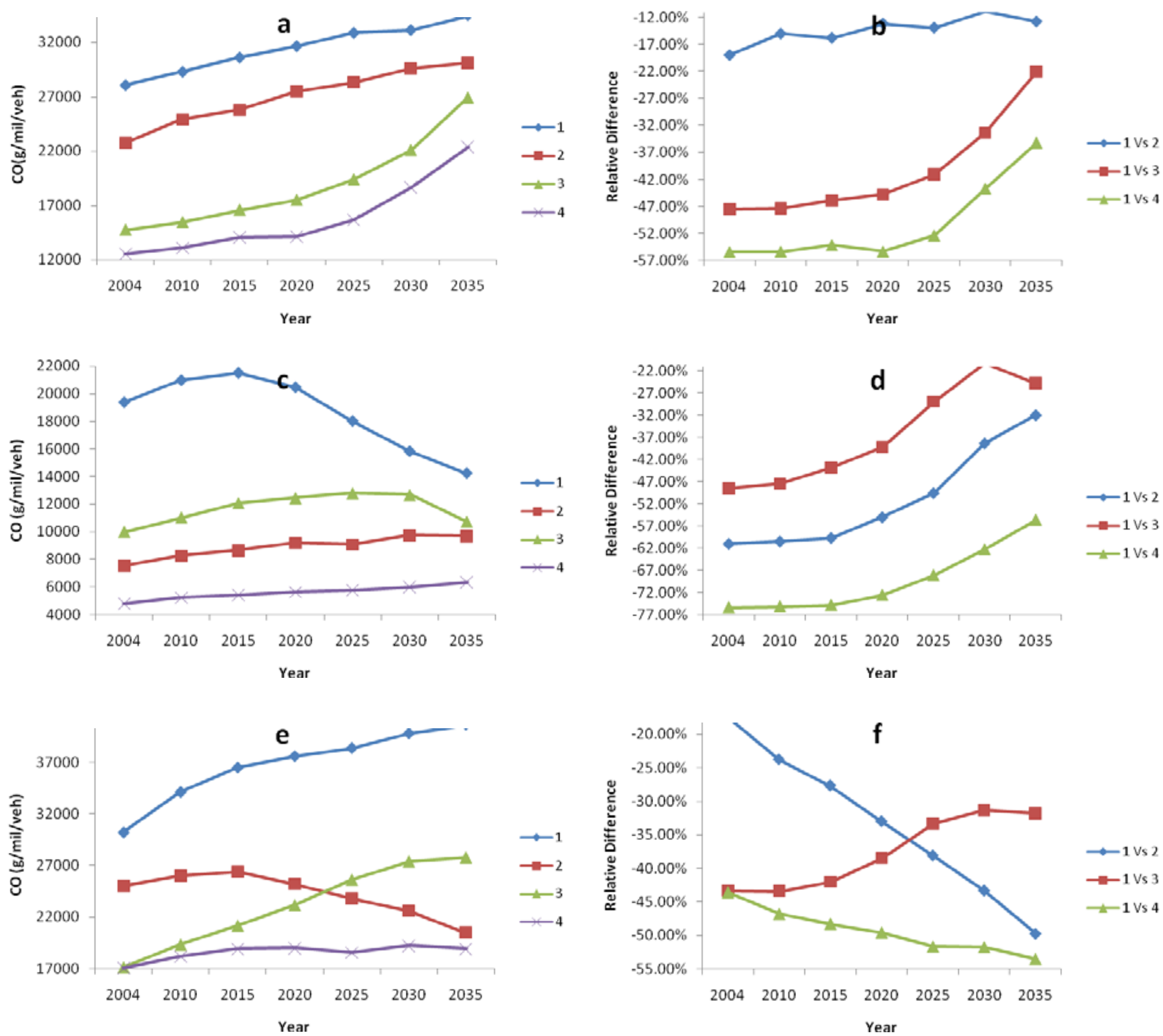

Figure 23: Comparison of scenario in terms of CO emission and CO emission relative difference by section. (a, b) Section 1, (c, d) Section 2, and (e, f) Section 3.

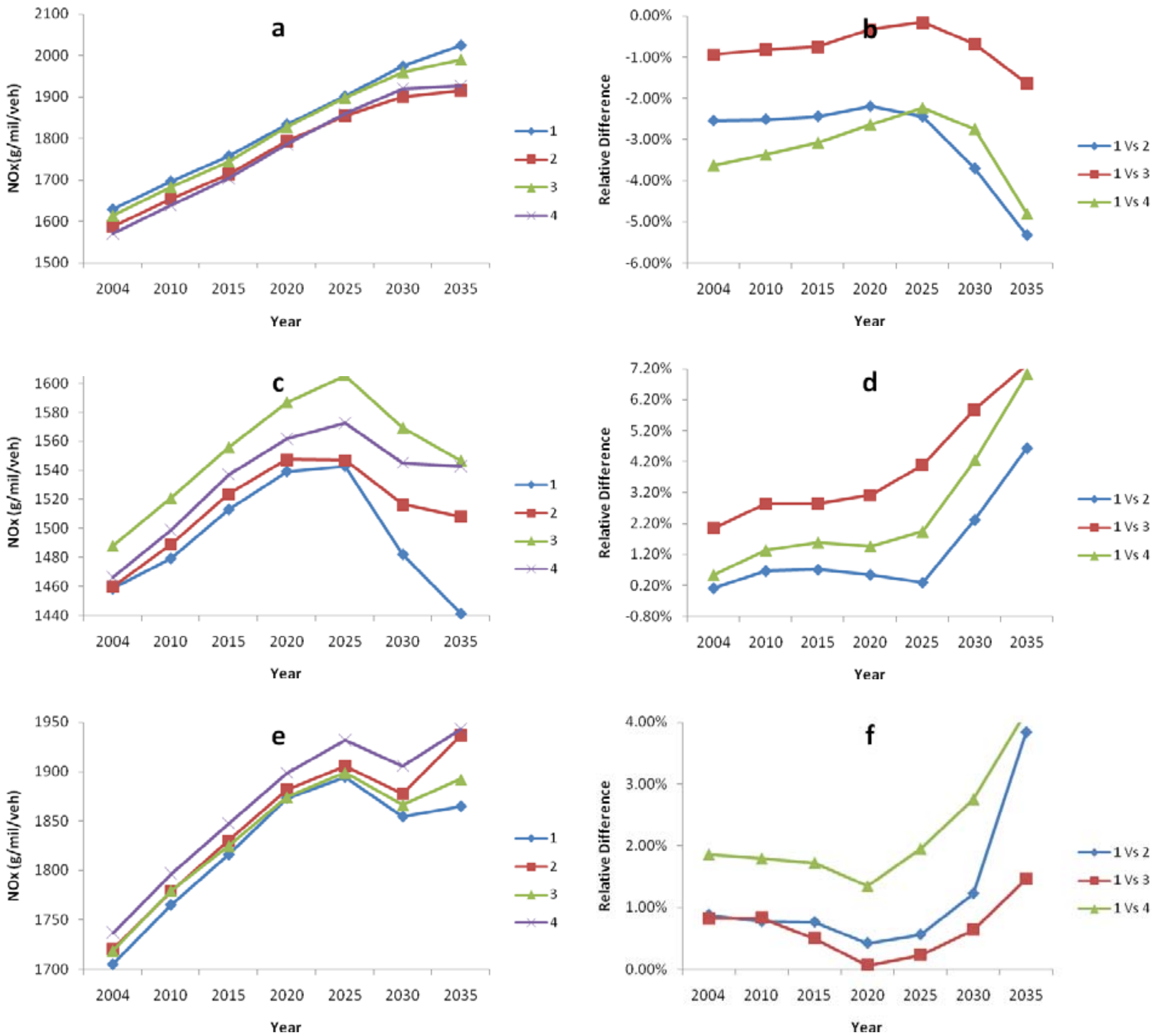

Figure 24: Comparison of scenario in terms of NO_x emission and NO_x emission relative difference by section. (a, b) Section 1, (c, d) Section 2, and (e, f) Section 3.

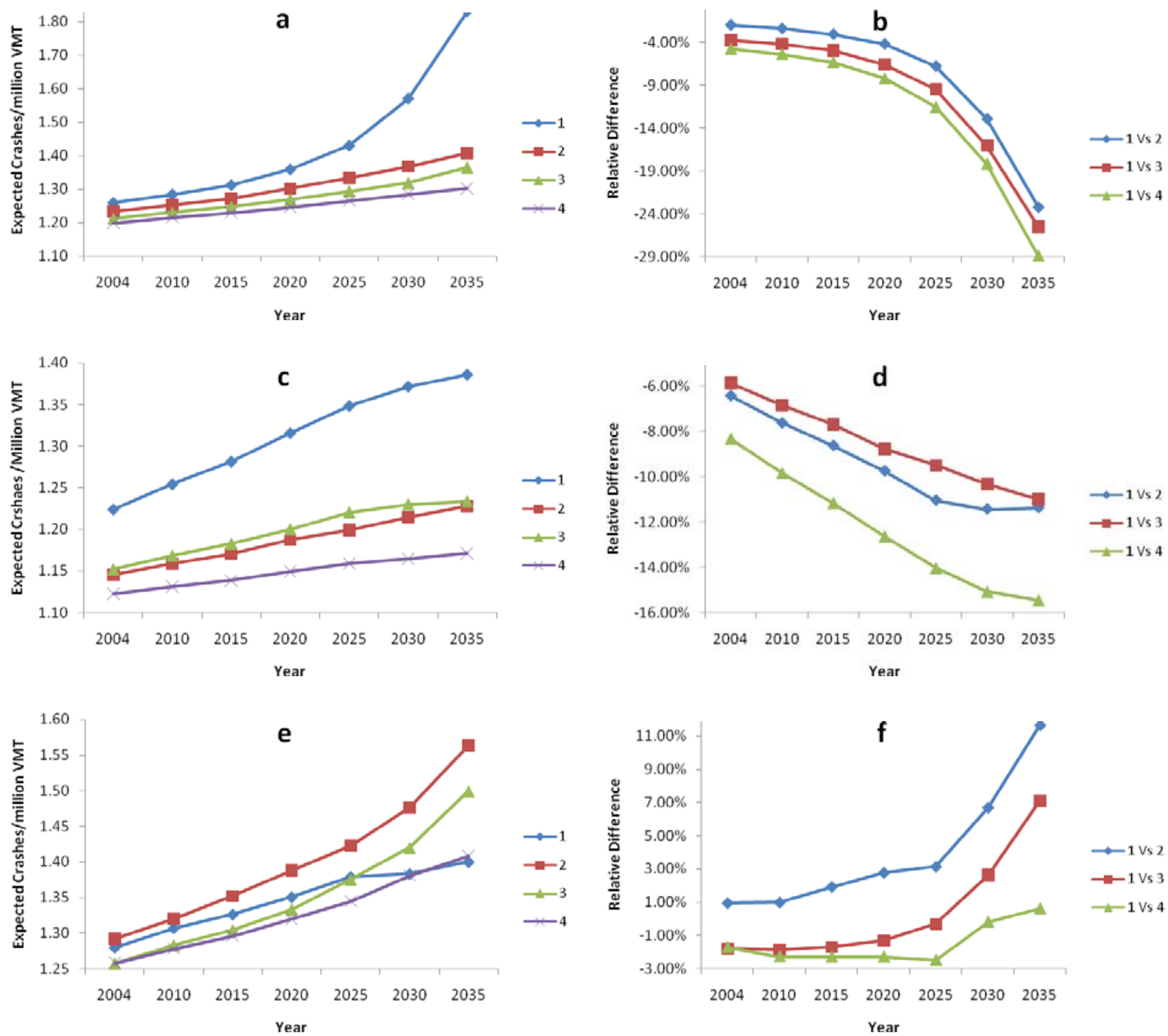

Figure 25: Comparison of scenario in terms of expected number of crashes and expected number of crashes relative difference by section. (a, b) Section 1, (c, d) Section 2, and (e, f) Section 3.

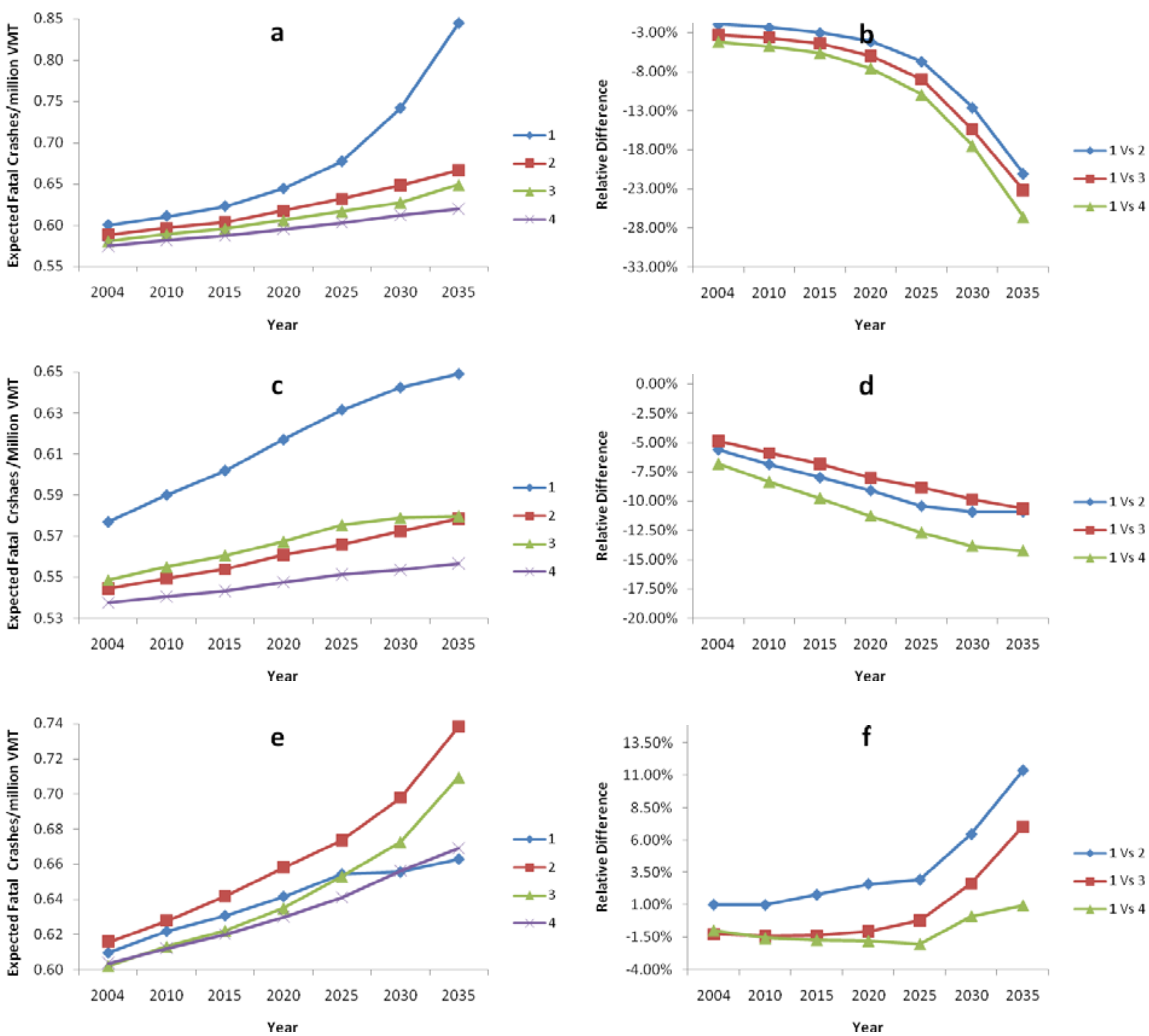

Figure 26: Comparison of scenario in terms of expected number of Injury crashes and expected number of Injury crashes relative difference by section. (a, b) Section 1, (c, d) Section 2, and (e, f) Section 3.

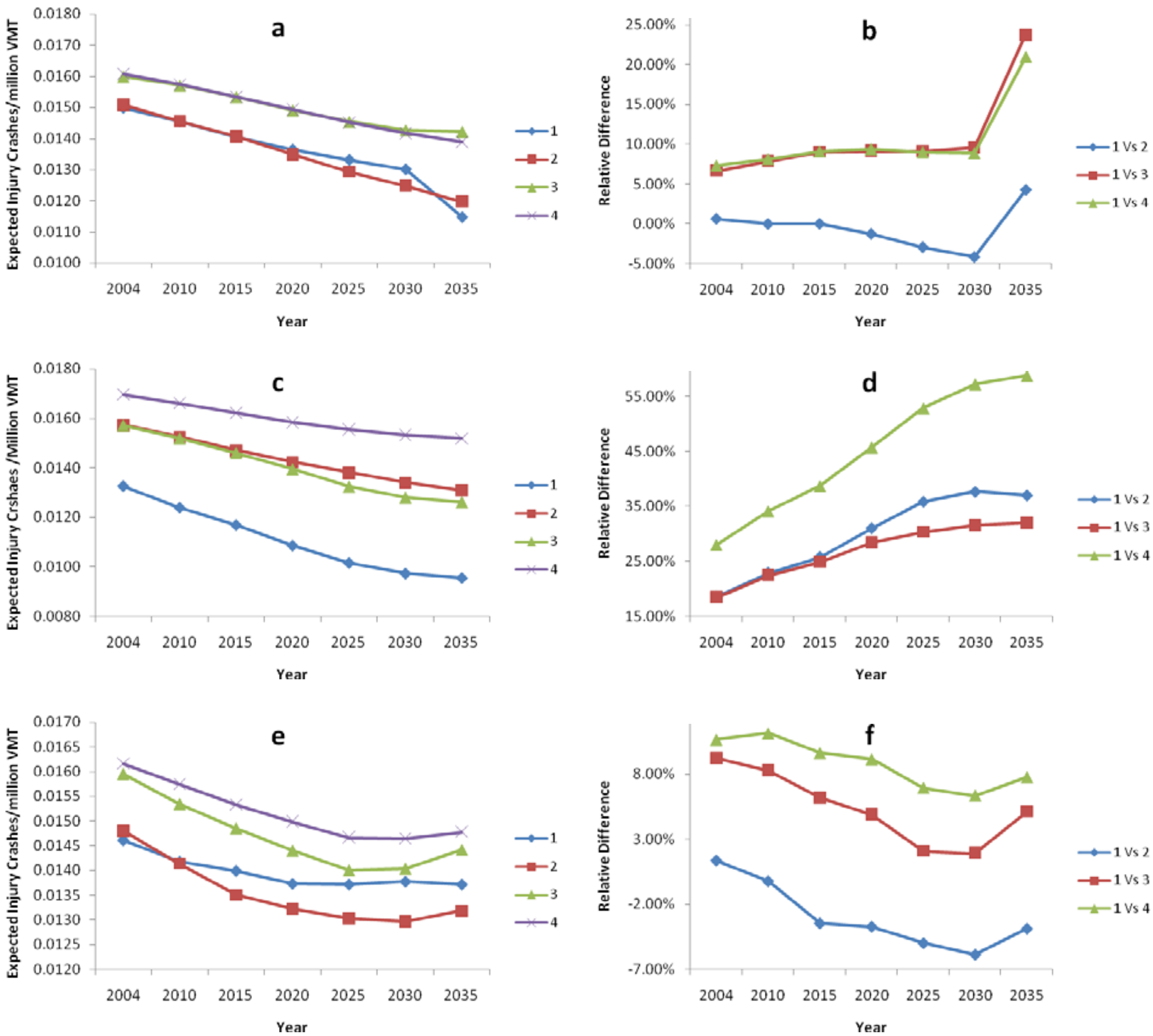

Figure 27: Comparison of scenario in terms of expected number of Fatal crashes and expected number of Injury crashes relative difference by section. (a, b) Section 1, (c, d) Section 2, and (e, f) Section 3.

APPENDIX C: THE INTEGRATION MODELING FRAMEWORK FOR ESTIMATING MOBILE SOURCE EMISSIONS

By: Hesham Rakha* and Kyoungho Ahn†

Abstract

Transportation network improvements are commonly evaluated by estimating average speeds from a transportation/traffic model and converting them into emission estimates using an environmental model such as MOBILE or EMFAC. Unfortunately, recent research has demonstrated that average speed, and perhaps even simple estimates of the amount of delay and the number of vehicle stops on a roadway, is insufficient to fully capture the environmental impacts of Intelligent Transportation System (ITS) strategies such as adaptive traffic signal control. Specifically, for the same average speed, one can observe widely different instantaneous speed and acceleration profiles, each resulting in very different fuel consumption and emission levels. In an attempt to address this limitation, the paper presents the INTEGRATION model framework for quantifying the environmental impacts of ITS alternatives. The model combines car-following, vehicle dynamics, lane changing, energy, and emission models to estimate mobile source emissions directly from instantaneous speed and acceleration levels. The validity of the model is demonstrated using sample test scenarios that include traveling at a constant speed, traveling at variable speeds, stopping at a stop sign, and traveling along a signalized arterial. The study also demonstrates that an adjustment in driver aggressiveness can provide environmental benefits that are equivalent to the benefits of adaptive traffic signal control.

1. Introduction

With the introduction of Intelligent Transportation Systems (ITS), there is a need to evaluate and compare alternative ITS and non-ITS investments. In comparing alternatives, a number of Measures of Effectiveness (MOEs) are typically considered, such as vehicle delay, stops, fuel consumption, emissions, and accident risk. The assessment of the fuel consumption and emission impacts of alternative investments requires a highly sophisticated evaluation tool in order to capture both the microscopic dynamics of vehicle-to-vehicle and vehicle-to-control interaction, as well as model the intricacies of vehicle fuel consumption and emissions that result from these vehicle dynamics.

Consequently, the assessment of the energy and emission impacts of alternative investments can be viewed as a two-level process. The first level is the microscopic behavior of traffic, which includes a system of car-following and lane changing models. This behavior is utilized to characterize vehicle speed and acceleration behavior. At the second level, the energy and emissions of hydrocarbons (HC), carbon monoxide (CO), and nitrogen oxides (NO_x) are computed based on instantaneous speed and acceleration estimates that were derived from the first level. It should be noted that research is underway to develop models for carbon dioxide (CO_2) and particulate matter (PM).

The system of car-following models captures both steady state and non-steady state longitudinal vehicle behavior along a roadway section. The steady state behavior is characterized by vehicles traveling at identical cruising speeds ($du/dt=0$). The non-steady state behavior characterizes how vehicles move from one steady state to another, which involves either vehicle decelerations or accelerations. Alternatively, lane-changing behavior describes the lateral behavior of vehicles along a roadway segment. Lane changing behavior affects the vehicle car-following behavior especially at high intensity lane changing locations such as merge, diverge, and weaving sections.

The objective of this paper is to demonstrate how the combination of these two integrated processes (traffic simulation model and an energy and emission model) can be utilized to evaluate alternative ITS initiatives. It

* Assistant Professor, Charles Via Department of Civil and Environmental Engineering. Virginia Tech Transportation Institute, 3500 Transportation Research Plaza (0536), Blacksburg, VA 24061. Tel: (540) 231-1505. Fax: (540) 231-1555. E-mail: hrakha@vt.edu.

† Research Scientist, Virginia Tech Transportation Institute, 3500 Transportation Research Plaza (0536), Blacksburg, VA 24061. E-mail: kahn@vt.edu.

also describes the approach that is implemented within the INTEGRATION microscopic traffic assignment and simulation software and demonstrates the feasibility of the proposed approach using a number of traffic signal control examples. These examples are presented in order to show the flexibility, feasibility, and validity of the INTEGRATION framework rather than to present specific results. It should be noted that a comparison of the INTEGRATION framework to other microscopic simulation models is beyond the scope of this paper.

2. Traffic Modeling

The combined use of traffic modeling in conjunction with energy and emission modeling can be utilized for the evaluation of environmental impacts of ITS and non-ITS deployments. The approach described in this paper utilizes the INTEGRATION microscopic traffic assignment and simulation software for traffic modeling (Van Aerde and Yagar, 1988a and b; M. Van Aerde & Assoc. Ltd., 2002a and b). The INTEGRATION model, which was developed over the past two decades, has not only been validated against standard traffic flow theory (Rakha and Van Aerde, 1996; Rakha and Crowther, 2002), but has also been utilized for the evaluation of real-life applications (Rakha *et al*., 1998; Rakha *et al*., 2000). Further enhancements to the INTEGRATION model have been incorporated in order to model vehicle dynamics more accurately. These enhancements are based on research described elsewhere (Rakha *et al*., 2001; Rakha and Lucic, 2002). This section provides a brief description of the INTEGRATION model and the enhancements that have been implemented in the latest version of the model (Version 2.10) to provide the reader with a basic understanding of the traffic-modeling component of the proposed framework. The following section describes how energy and emission models were developed using field data, and how these models were incorporated within the INTEGRATION software in order to develop a fully integrated mobile emission evaluation tool. It should be noted that the energy and emission models that are described have been enhanced to include high emitting vehicles, effect of vehicle starts on vehicle emissions, and different types of vehicles. Subsequent publications will describe these efforts separately.

The manner in which the INTEGRATION model represents traffic flow can be best presented by discussing how a typical vehicle initiates its trip, selects its speed, changes lanes, and transitions from one speed to another.

2.1 Initiation of Vehicle Trips

Prior to initiating the actual simulation logic, the individual vehicles that are to be loaded onto the network must be generated. Vehicle types, such as passenger cars and trucks, can be pre-assigned by modifying the model input files. As most available O-D (Origin-Destination) information is macroscopic in nature, INTEGRATION permits the traffic demand to be specified as a time series histogram of O-D departure rates for each possible O-D pair within the entire network. The actual generation of individual vehicles satisfies the time-varying macroscopic departure rates that were specified by the modeler within the model's input data files. This model simply disaggregates an externally specified time-varying O-D demand matrix into a series of individual vehicle departures prior to the start of the simulation. These departure rates can be fully random (negative exponential time headway distribution), fully uniform, or partially uniform and random.

As the externally specified demand file is disaggregated, each of the individual vehicle departures is tagged with its desired departure time, trip origin, and trip destination, as well as a unique vehicle number. This unique vehicle number can subsequently be utilized to trace a particular vehicle along the entire path towards its destination. It can also be utilized to verify that subsequent turning movements of vehicles at network diverges are assigned according to the actual vehicle destinations, rather than arbitrary turning movement probabilities as is the case in many other microscopic models that are not assignment-based.

The calibration of O-D demand is achieved using a maximum likelihood approach, the details of which are beyond the scope of this paper but are provided in the literature (Van Aerde *et al*., 2003). It should be noted that this approach has been successfully applied in numerous modeling studies (Rakha *et al*., 1998; Rakha *et al*., 2000).

2.2 Steady State Car-Following Behavior

When the simulation clock reaches a particular vehicle's scheduled departure time, an attempt is made to enter that vehicle into the network at its origin zone. From this point, the vehicle proceeds along its trip towards its final destination in a link-by-link fashion. Once the vehicle has selected which lane to enter, INTEGRATION computes the vehicle's desired initial speed on the basis of the distance headway between the vehicle and the vehicle immediately downstream within the same lane. This computation is based on a link-specific microscopic car-following relationship that is calibrated macroscopically to yield the appropriate target aggregate speed-flow attributes for that particular link. The steady state car-following model, which was proposed by Van Aerde (1995) and Van Aerde and Rakha (1995), combines the Pipes and Greenshields models into a single-regime model (Rakha and Crowther, 2002), as demonstrated in Equation 1. Specifically, the first two terms constitute the Pipes steady state model (Pipes, 1953), and the third term constitutes the Greenshields steady state model (Greenshields, 1935). This combination provides a functional form that includes four parameters that require calibration using field data (constants c_1, c_2, c_3 and the roadway free-speed u_f). The first two terms of the relationship provide the linear increase in vehicle speed as a function of the distance headway, and the third term introduces curvature to the model and ensures that the vehicle speed does not exceed the free-speed. The addition of the third term allows the model to operate with a speed-at-capacity that does not necessarily equal the free-speed, as is the case with the Pipes model. The Pipes model is proven to be inconsistent with a variety of field data from different facility types, as illustrated in Figure 28. Alternatively, the Van Aerde model overcomes the main shortcoming of the Greenshields model, which assumes that the speed-flow relationship is parabolic, and again is inconsistent with field data from a variety of facility types, as demonstrated in Figure 28. A detailed comparison of the Van Aerde, Pipes, and Greenshields models is described by Rakha and Crowther (2002).

$$h = c_1 + c_3 u + \frac{c_2}{u_f - u} \qquad [1]$$

Equations 2 through 5 are utilized to compute the c_1, c_2, and c_3 constants based on four parameters; free-speed, speed-at-capacity, capacity, and jam density (Rakha and Crowther, 2002). These parameters can be calibrated to loop detector data (Van Aerde and Rakha, 1995) or can be input based on typical values.

Once the vehicle's speed is computed, the vehicle's position is updated every 0.1 seconds to reflect the distance that it travels during each previous 0.1 seconds. The vehicle's headway and speed is then re-computed.

$$m = \frac{2u_c - u_f}{(u_f - u_c)^2} \qquad [2]$$

$$c_2 = \frac{1}{k_j\left(m + \frac{1}{u_f}\right)} \qquad [3]$$

$$c_1 = mc_2 \qquad [4]$$

$$c_3 = \frac{-c_1 + \frac{u_c}{q_c} - \frac{c_2}{u_f - u_c}}{u_c} \qquad [5]$$

2.3 Vehicle Decelerations

INTEGRATION provides separate deceleration and acceleration logic. The deceleration logic recognizes speed differentials between the vehicle that is making desired speed decisions and the vehicle ahead of it. It is simplest to first describe how this logic applies to a vehicle approaching a stationary object. In this case, a vehicle will first estimate the excess headway between itself and the vehicle ahead of it. This excess headway is defined as the residual distance that remains when the currently available headway is reduced by the minimum headway (jam density headway). Based on the residual headway, the vehicle computes the time it has to comfortably decelerate from its current speed to the speed of the object/vehicle in front of it. For constant deceleration rates, this time is equal to the residual headway divided by the average speed of the initial and final speeds of the following vehicle. The following vehicle computes the required deceleration rate as the speed differential divided by the deceleration time.

Alternatively, if the lead vehicle is actually moving, the following vehicle would attempt to decelerate at a constant rate in such a manner as to attain the speed of the lead vehicle over a distance equal to the spacing of vehicles minus the jam density headway. Of course, by the time the following vehicle reached this location, the lead vehicle would have already moved ahead on the highway, resulting in an asymptotic deceleration of the following vehicle to the lead vehicle's speed, rather than a constant deceleration. Similarly, if the lead vehicle were accelerating, the following vehicle would only continue to decelerate until it was traveling at the same speed of the lead vehicle. From this point onward, the following vehicle would likely begin to accelerate again, as the increasing gap to the lead vehicle would cause the following vehicle to perceive increasing desired speeds.

2.4 Vehicle Accelerations

The INTEGRATION model updates vehicle speeds every 0.1 seconds based on the distance headway and speed differential between the subject vehicle and the vehicle immediately ahead of it. Unfortunately, using this type of car-following model can result in unrealistically high vehicle accelerations. Consequently, the model constrains vehicle accelerations using a vehicle dynamics model that estimates the maximum vehicle acceleration (Rakha *et al*., 2001; Rakha and Lucic, 2002). Two important points are worth noting. First, the INTEGRATION framework currently captures a total of 25 default vehicle types including light-duty cars, light-duty trucks, and heavy-duty trucks. In addition, 25 user-specific vehicle parameters can be input to the model. Second, the level of acceleration can be varied utilizing a user-defined acceleration reduction factor. Consequently, the impact of different acceleration levels can be analyzed, as will be demonstrated later in the paper.

The model computes the maximum acceleration based on the resultant force, as indicated in Equation 6. Given that acceleration is the second derivative of distance with respect to time, Equation 6 resolves to a second-order Ordinary Differential Equation (ODE) of the form indicated in Equation 7.

$$a = \frac{F - R}{M} \quad [6]$$

$$\ddot{x} = f(\dot{x}, x) \quad [7]$$

$$R = R_a + R_r + R_g \quad [8]$$

The state-of-practice vehicle dynamics models estimate the vehicle tractive effort using Equation 9 with a maximum value based on Equation 10, demonstrated in Equation 11. Equation 10 accounts for the maximum friction force that can be maintained between the tires of the vehicle's tractive axle and the roadway surface. The use of Equation 11 ensures that the tractive effort does not approach infinity at low vehicle speeds.

Equation 9 indicates that the tractive force F_t is a function of the ratio between the vehicle speed u and the engine power P. The model assumes the vehicle power to be constant and equal to the maximum potential power. It considers two main sources of power loss that degrade the tractive effort produced by the truck engine: losses in the engine and losses in the transmission system with an engine efficiency of 0.89 to 0.94, depending on the type of transmission (Society of Automotive Engineers, 1996). Equations 10 and 11 ensure that the tractive force does not exceed the maximum sustainable force between the vehicle tires and the pavement surface.

$$F_t = 3600\ \eta\ \frac{P}{u} \quad [9]$$

$$F_{\max} = 9.8066\ M_{ta}\ \mu \quad [10]$$

$$F = \min(F_t, F_{\max}) \quad [11]$$

2.5 Lane Changing Logic

The above presentation of a vehicle's selection of its desired speed, required deceleration, and potential acceleration rate considers that vehicles stay primarily in their own lane. Unfortunately, many of the complications within traffic flow theory arise when vehicles change lanes, either voluntarily or when required.

INTEGRATION's discretionary lane-changing logic is predominant when a vehicle is traveling on a multi-lane facility and is out of the influence area of downstream diverges or lane drops. Under these conditions, vehicles are essentially free to travel in any lane unless the user provides a bias towards a specific lane or group of lanes. When a vehicle travels under these conditions on a multi-lane facility without any other vehicles ahead of it, INTEGRATION's default logic provides incentives for vehicles to migrate towards the middle lane. This incentive leaves the left-most lane open for any faster vehicles to get around the vehicle in question and also keeps the vehicle away from the right shoulder lane, where vehicles entering the highway might merge in.

As soon as multiple vehicles become present on the highway, simulated vehicles tend to spread themselves across the multiple lanes, with slower vehicles moving to the right and faster vehicles moving to the left. This logic is especially important when slow-moving trucks are present on the highway, as they should move to the right in order to allow faster vehicles or faster trucks to move around them to the left. However, vehicles generally attempt to move towards lanes that provide them with the longest headway, for longer headways will result in longer desired speeds. The potential for a vehicle to move from its current lane into a lane with a longer headway is examined once every 0.1 seconds, with respect to the lanes immediately adjacent to the current lane. In addition, the potential to move to any other lanes on the facility, not necessarily adjacent to the current lane, is examined once every second.

In deciding whether to move to an adjacent lane with a longer headway, the vehicle considers both an absolute and a relative improvement threshold. This threshold represents the minimum improvement that is needed for a vehicle to consider a lane change and to guard between frequent oscillations between two lanes that provide virtually identical headways. Once a vehicle has identified that a lane change may be desirable, it considers the availability of an acceptable gap in that lane. Such availability depends upon the distance that is available in the desired lane both ahead of and behind the vehicle. Both distances ensure that, at a minimum, sufficient space is available to physically hold the vehicle and, ideally, some additional buffer. This additional buffer is speed dependent.

In summary, INTEGRATION considers discretionary lane changes in two stages. Every 0.1 seconds it considers whether a discretionary lane change is desirable. If a change is desirable, it determines if such a lane change is possible given the availability of a suitable gap. The combination of these decisions results in a spreading of vehicles across all available lanes for roadway sections outside of the influence of lane drops or diverges.

When a lane drop or diverge is being approached, vehicles will be forced to consider the model's mandatory and discretionary lane-changing logic. The transition from discretionary to mandatory lane-changing logic occurs gradually as the influence area of the lane-drop or diverge area is penetrated further. The management of this transition is best visualized by considering the presence of both virtual softwalls and hardwalls on the roadway. Specifically, the softwall represents the first point in space where a vehicle becomes aware of a pending mandatory lane change, and the hardwall represents the absolute last point in space before which a mandatory lane change must occur.

During the transition from the softwall to the hardwall, the mandatory lane change logic gradually phases in and has four effects. First, vehicles that pass the softwall will not be able to make any discretionary lane changes that are opposite to the direction of the required mandatory lane change. Second, once the softwall is passed, the additional advantage that the current lane must provide (in order to remain preferred over the lane in which the mandatory logic requires to be utilized) is gradually increased (eventually to the point where no advantage will be sufficient to resist the incentive to change lanes). Third, once the softwall is passed, vehicles are gradually prohibited from passing vehicles that are on the same side as the direction of their mandatory lane change requirement. Finally, as a vehicle transitions from the softwall to the hardwall, the vehicle will be required to gradually come to a stop.

The first rule prohibits vehicles from moving into a lane that is temporarily preferred but that will very shortly become heavily penalized. The second rule ensures that, when possible, vehicles move towards the direction of the mandatory lane change before the hardwall is reached. The third rule ensures that when vehicles are queued up in a turning base or an off-ramp, the vehicles join the queue. The fourth rule ensures that vehicles, even when unable to initially find a gap, will not miss their exit, off-ramp, turn lane, or turn bay.

As part of the lane-changing logic within INTEGRATION, a vehicle occupies both the lane it is changing from and the lane it is changing to for the duration of the lane change maneuver. In doing so, the INTEGRATION model can capture capacity losses that occur at on-ramp, off-ramp, and weaving sections.

3. Energy and Emission Modeling

Having estimated the vehicle speed and acceleration levels, the next step is to compute the vehicle fuel consumption and emission rates. This section describes the VT-Micro model (Version 1.0) that was developed to estimate light-duty hot stabilized vehicle fuel consumption and emission rates. Initially, the data that were utilized to develop the models are described followed by a description of the models.

It should be noted that different energy and emission models could be incorporated fairly easily, given the modular design of the INTEGRATION framework. Currently, research is underway to develop VT-Micro Version 2.0 by expanding energy and emission models using 101 light-duty vehicles and light-duty trucks to capture the effects of different vehicle types, high emitting vehicles, and the effect of cold starts on vehicle emissions. The VT-Micro Version 2.0 has been incorporated into the INTEGRATION software and is available for public use.

The application of the model that is presented in this paper is intended to demonstrate a comprehensive framework for quantifying traffic-related energy and emission effects rather than to present specific results.

3.1 Raw Data Description

The data that were utilized to develop the fuel consumption and emission models were gathered on a dynamometer at the Oak Ridge National Laboratory (ORNL) (West *et al*., 1997). Given that the focus of this paper is on the development of evaluation tools that are sensitive to vehicle dynamics and not on the ORNL data per se, these data are not described in much detail; however, they are described elsewhere in the literature (West *et al*., 1997). The ORNL data were in the form of look-up tables that included the steady state fuel consumption and emission rates as a function of the vehicle's instantaneous speed and acceleration levels. The emission data included hydrocarbon (HC), carbon monoxide (CO), and nitrogen oxide (NO_x) emissions. A total of eight light-duty vehicles of various weights and engine sizes were utilized (West *et al*., 1997). The reference indicates that these eight vehicles are representative of internal combustion (IC) engine technology at the time the data were gathered.

The fuel consumption and emission rates were provided for a range of speeds from 0 to 120 km/h (75 mph) at increments of 1.1 km/h (0.69 mph) and for a range of accelerations from –1.5 m/s^2 (-5 ft/s^2) to 3.6 m/s^2 (12 ft/s^2) at increments of 0.3 m/s^2 (1 ft/s^2). These data included typical driving conditions that ranged from decelerating (acceleration less than zero), idling (acceleration and speed equal to zero), and acceleration (acceleration greater than zero). Some of the speed/acceleration combinations were unachievable by the vehicles (e.g. high accelerations at high speeds). In general, the number of data points ranged from 1300 to 1600 depending on the power of the vehicle (maximum number of potential points was 1980 points [110 speed bins $\times$ 18 acceleration bins]).

Utilizing the data for the eight vehicles, composite fuel consumption and emission surfaces were derived by averaging across all the vehicles (West *et al*., 1997). The composite vehicle fuel consumption data varied fairly linearly when the vehicle was cruising or decelerating; however, the relationship was significantly non-linear for higher levels of acceleration (acceleration greater than or equal to 1.2 m/s^2). In terms of emissions, the HC and CO surfaces appeared to be very similar except for the fact that CO emissions were much higher (up to 2500 mg/s in the case of CO versus 60 mg/s in the case of HC). The NO_x surface appeared to be more non-linear than the HC and CO surfaces when the vehicle was decelerating or cruising.

The authors are aware that the ORNL data utilized in developing these models are limited (only nine vehicles), and do not account for cold-start effects or high-emitting vehicles. Furthermore, these data were collected under hot stabilized conditions and, as a result, may not adequately represent transient catalytic conversion behavior; however, the ORNL data were the only energy and emission data that were available for third party usage at the time the models were developed. The authors are currently utilizing EPA data (101 vehicles) and will be using the University of California, Riverside data (Barth *et al*., 1997), which includes over 300 vehicles, to expand these statistical energy and emission models.

3.3 Model Structure

The Virginia Tech Microscopic energy and emission model (VT-Micro) was developed from experimentation with numerous polynomial combinations of speed and acceleration levels (Rakha *et al*., 2000; Ahn *et al*., 2002). Linear, quadratic, cubic, and quartic terms of speed and acceleration were tested using chassis dynamometer data collected at the ORNL. The final regression model included a combination of linear, quadratic, and cubic speed and acceleration terms because it provided the least number of terms with a relatively good fit to the original data (R^2 in excess of 0.92 for all MOEs). Due to the simplicity of the model structure, the model can be easily incorporated within any microscopic traffic simulation model. While a more detailed description of the model derivation and model validation is provided in the literature (Ahn *et al*., 2002), it is sufficient at this point to note that the final structure of the model, summarized in Equation 12, involved a logarithmic transformation of a dual-regime third order polynomial. Figure 29 further illustrates the effectiveness of the hybrid log-transformed models in predicting vehicle fuel consumption and emission rates as a function of a vehicle's instantaneous speed and acceleration levels showing good estimations against the ORNL data.

The use of polynomial speed and acceleration terms could result in multi-colinearity between the independent variables, as a result of the dependency of these variables. A measure of multi-colinearity, the Variance Inflation Factor (VIF) can be reduced by removing some of the regression terms; however, this also results in a reduction in the accuracy of the model predictions. The existence of multi-colinearity results in model estimations of the dependent variable that are unreliable for dependent variable values outside the bounds of the original data.

Consequently, the model was maintained with the caveat that it should not be utilized for data outside the bounds of the ORNL data. Figure 30 illustrates the feasible range of the ORNL data (shaded area) superimposed on the maximum vehicle acceleration envelope for an average composite vehicle. The figure demonstrates that the maximum acceleration bounds exceed the VT-Micro feasible range. Because of the existence of variable multi-colinearity, the dependent variable estimates (fuel consumption and emissions) outside the VT-Micro feasible range were estimated using MOE values at the boundary of the feasible regime for an identical vehicle speed. In addition, Figure 30 illustrates the vehicle speed/acceleration envelope for a vehicle that accelerates from a complete stop to a speed of 100 km/h at an acceleration rate of 60 percent the maximum acceleration rate as obtained from the INTEGRATION simulation model. This example is consistent with the VT-Micro feasible range. The default maximum acceleration level embedded in the INTEGRATION model is currently 100 percent; however, users can modify the acceleration level.

$$MOE_e = \begin{cases} e^{\sum_{i=0}^{3}\sum_{j=0}^{3}(L_{i,j}^{e} \times u^i \times a^j)} & \text{for } a \geq 0 \\ e^{\sum_{i=0}^{3}\sum_{j=0}^{3}(M_{i,j}^{e} \times u^i \times a^j)} & \text{for } a < 0 \end{cases} \qquad [12]$$

4. Model Application

The energy and emission models that were described earlier were incorporated within the INTEGRATION model as subroutines. Although the simulation model updates vehicle's speed and accelerations every 0.1 seconds, the fuel consumption and emission model estimates are made every second, for two reasons. First, a 0.1s level resolution in computing vehicle emissions would only increase the computational load with minimum enhancements to the emission estimate accuracy. However, the use of a 0.1 second resolution is required for accurate modeling of gap acceptance behavior. Consequently, the INTEGRATION model uses the average speed and acceleration of the entire second to compute the vehicle's fuel consumption and emission rate.

In addition to accumulating the MOEs across all the vehicles that travel between two O-D pairs, the model accumulates MOEs across all the vehicles that traverse a specific link. Simulation runs required only a few minutes to complete because they did not involve the simulation of a large traffic demand., and summary statistics are provided on a vehicle, link, and O-D basis. Details of how vehicles are generated and the specifics of the INTEGRATION model can be found elsewhere (M. Van Aerde & Assoc. Ltd., 2002a and b).

Incorporating the previously described energy and emission models within the INTEGRATION traffic assignment and simulation model provides a unique evaluation tool that can be utilized to evaluate alternative ITS and non-ITS applications. This section describes a sample application of the evaluation tool to a traffic-signalized network. A more comprehensive and realistic application in which simulated vehicle speed profiles and energy and emission estimates were compared to estimates that were computed using second-by-second GPS speed measurements along a signalized arterial are provided elsewhere (Rakha *et al*., 2000).

The objective of the comparison presented in this paper is to demonstrate the flexibility of the framework in analyzing the sensitivity of vehicle fuel consumption and emissions to operating conditions. This approach represents a great enhancement to the standard correction-factor based approaches using MOBILE or EMFAC. A detailed comparison of the proposed framework to the current state-of-practice approach using MOBILE and EMFAC is beyond the scope of this paper but will be presented in a future publication.

The paper demonstrates that the two main building blocks (traffic modeling and energy and emission modeling) together produce valid fuel consumption and emission estimates, using systematic simple scenarios. The scenarios are ordered to evaluate the tool's various levels of sophistication, ranging from simple constant-speed scenarios to more sophisticated types of adaptive traffic signal control scenarios. Specifically, the initial set of scenarios involves simulating a single vehicle driving at a constant speed in order to demonstrate the validity of the approach under steady state conditions. The objective of this scenario is two-fold. First, it validates the energy and emission models that are incorporated within the INTEGRATION software when the vehicle is cruising. Second, it validates the simulated vehicle speed profile when the vehicle does not interact with other vehicles.

In the second set of scenarios, various levels of complexity are introduced to the first scenario. These include variable speeds along a trip and engaging in a number of complete stops. The objective of this set of scenarios is to quantify the increase in fuel consumption and emissions as a result of vehicle accelerations. Different levels of vehicle accelerations are analyzed in order to identify changes in vehicle emissions as a function of vehicle acceleration levels.

The final scenario involves the interaction of vehicles with one another and with traffic control devices considering different levels of vehicle acceleration. The objective of this scenario is to demonstrate the validity of the combined modeling framework for the evaluation of typical traffic operation applications.

4.1 Constant Speed Scenario

The first step in the evaluation exercise was to validate how the combined traffic and energy/emission models operated for a number of simple constant speed scenarios. These constant speed scenarios represent artificial scenarios given that they do not involve any vehicle accelerations or decelerations.

The network that was utilized in the analysis was an eight-kilometer arterial section. The network was simulated within the INTEGRATION model as four two-kilometer links in order to allow the same network to be utilized for the remaining scenario runs.

Within the constant-speed scenario, a series of sub-scenarios were evaluated in which the maximum speed was varied from 25 km/h to 100 km/h at 25 km/h increments (Scenarios 1a through 1d). The objective of Scenarios 1a through 1d was two-fold. First, these scenarios validate the use of a combined traffic/energy and emission model under constant speeds (no deceleration/acceleration). Second, they develop relationships between the steady state speed and the various Measures of Effectiveness (MOEs) against which the reasonableness of the model's responses to other scenarios can be compared.

The simulation output indicated that the instantaneous speed remained constant throughout the entire trip. Because the vehicle traveled at a constant speed, the acceleration remained at 0 m/s^2 for the entire trip. The fuel consumption rate remained constant at approximately 0.78 liters/s for a cruising speed of 25 km/h (0.11 liters/km). This fuel consumption rate is consistent with the ORNL data for a constant speed of 25 km/h. The CO emission rates were approximately ten-fold higher than the HC and NO_x emission rates (8 versus 0.8 mg/s). These findings are consistent with the raw data that were obtained from the ORNL.

Figure 31 illustrates the impact of various constant speeds on the fuel consumption along the eight-kilometer trip. The fuel consumption varies from a maximum of 0.113 l/km (at a constant speed of 25 km/h) to a minimum of 0.078 l/km (at a constant speed of 75 km/h). The fuel consumption function, together with the fuel consumption rates, is consistent with the raw data that were obtained from ORNL. Figure 31 illustrates that CO emissions are considerably higher than HC and NO_x emissions. Furthermore, the relationship indicates that fuel consumption, HC, and CO emissions are optimum at a speed of approximately 75 km/h; however, NO_x emissions are highly sensitive to travel speeds as indicated by the four-fold increase from a speed of 25 to 100 km/h (increase from 0.5 grams/trip to 2.0 grams/trip).

4.2 Variable Speed Scenario

The next scenario to be evaluated was a variable speed scenario (Scenario 2). In the variable speed scenario, the free-speed was set at 25 km/h for links 1 and 3 (0-2km and 4-6km), and on links 2 and 4 was set at 75 km/h (2-4km and 6-8km). Again, a single vehicle was simulated to travel between origin 1 and destination 2.

Figure 32 illustrates the temporal variation in vehicle speed and acceleration as the vehicle traversed the test network. Figure 32 demonstrates that the vehicle required approximately 10 seconds to accelerate from a speed of 25 km/h to a speed of 75 km/h (average acceleration rate of 1.0 m/s^2). Furthermore, the figure illustrates that the vehicle acceleration decreased as the vehicle speed increased (decreased from 1.2 to 0.8 m/s^2, which corresponds to an acceleration rate equivalent to the maximum acceleration rate).

Figure 32 also illustrates a seven-fold increase in the fuel consumption rate when the vehicle accelerated at a rate of 1 m/s^2 at a speed of 60 km/h versus cruising at a speed of 25 km/h, and one can observe a two-fold increase in the instantaneous fuel consumption rate for a cruising speed of 75 km/h versus 25 km/h. Figure 32 demonstrates that the combination of vehicle acceleration and speed significantly impacts vehicle fuel consumption and emission estimates. The combined impact of vehicle acceleration and speed is more evident for the HC emission estimates where the emissions do not increase significantly until the vehicle has attained a speed of approximately 50 km/h although the acceleration level is higher at the lower speeds.

Figure 33 illustrates the percent change in vehicle fuel consumption and emissions for the variable speed scenario considering different vehicle acceleration levels. It illustrates the marginal increase in vehicle fuel consumption and emissions relative to a base acceleration rate of 20 percent the maximum rate. In general, apart from NO_x emissions, vehicle fuel consumption and emissions increase as the vehicle acceleration rate increases from 20 percent to 60 percent. The emissions tend to decrease at higher accelerations because the model utilizes the boundary emission rate for observations that are outside the feasible range. However, the higher acceleration rates reduce the time spent accelerating, resulting in a reduction in the overall emissions. Figure 33 also demonstrates that vehicle fuel consumption and NO_x emissions are comparatively insensitive to the vehicle acceleration level; however, HC and CO emissions are highly sensitive to the acceleration level.

4.3 Stop Sign Scenario

Three stop signs were simulated in the next scenario. These were located after 2, 4, and 6 kilometers, respectively. The stop signs required the approaching vehicle to make a complete stop before accelerating to its free-speed, as illustrated in Figure 34. Again, as was the case in Scenario 1, Scenario 3 involved four sub-scenarios in which the vehicle cruise speed varied from 25 to 100 km/h at 25 km/h increments. For each sub-scenario the vehicle acceleration rate was varied from 20 to 100 percent the maximum rate at increments of 20 percent. Figure 34 illustrates sample vehicle speed and acceleration profiles for travel at a cruise speed of 100 km/h and acceleration rates of 20, 60, and 100 percent the maximum acceleration rate. A forthcoming publication will characterize typical in-field driver acceleration rates under differing levels of congestion for usage within a microscopic simulation environment.

Figure 34 demonstrates that the vehicle did not decelerate in excess of 1 m/s^2 when it approached the stop sign. Furthermore, it illustrates a reduction in the level of acceleration as the vehicle speed increased. Figure 35 illustrates the temporal variation in fuel consumption associated with the stop sign scenario for three acceleration levels. The figure demonstrates that the fuel consumption increases as the level of acceleration increases, with a reduction in fuel consumption for accelerations above 60 percent the maximum rate. This again results from the fact that acceleration levels above 60 percent the maximum rate are beyond the feasible range of the VT-Micro model; thus, the fuel consumption rate is maintained at the upper bound boundary rate.

Figure 36, Figure 37, and Figure 38 demonstrate similar temporal variation in HC, CO, and NO_x emissions for the same stop sign scenario considering three levels of acceleration. In general, the vehicle emissions increase as the acceleration level increases. The figures demonstrate that HC and CO emissions are highly sensitive to acceleration levels (increase of thirty-fold for an acceleration rate of 0.6 versus 0.2). Alternatively, NO_x emissions are less sensitive to acceleration levels (increase of only 100 percent for an acceleration rate of 0.6 versus 0.2).

Figure 39 demonstrates an increase in vehicle fuel consumption and emissions as a result of introducing three vehicle stops to the constant speed scenario. Furthermore, the figure demonstrates that energy and environmental effects of vehicle stops are more significant at higher cruise speeds. As was the case for the variable speed scenario, Figure 40 illustrates that vehicle fuel consumption and NO_x emissions appear to be comparatively insensitive to the vehicle acceleration rate. Alternatively, HC and CO emissions are highly sensitive to vehicle acceleration rates.

4.4 Traffic Signal Coordination Scenario

The final evaluation exercise involved modeling three equally spaced traffic signals along the same arterial section (signals located after 0.35, 0.70, and 1.05 kilometers). Three types of traffic signal control were considered: sub-optimal, off-line signal coordination; good, off-line signal coordination; and a form of adaptive signal control.

Figure 41 illustrates that the benefits of optimizing traffic signal timings vary marginally as a function of the vehicle acceleration levels. Figure 41 demonstrates that the benefits of signal coordination increase as vehicle acceleration levels increase. Figure 42 demonstrates that the optimization of traffic signals results in a 40 percent reduction in fuel consumption regardless of the traffic fleet acceleration levels. Alternatively, NO_x emissions vary between 70 to 90 percent depending on the traffic fleet acceleration level. Figure 42 shows that the impact of traffic signal coordination on CO emissions is highly dependent on the acceleration level.

5. Conclusions of Study

This paper describes and applies the INTEGRATION framework for quantifying the energy and environmental impacts of ITS and non-ITS alternatives. The framework combines a microscopic traffic simulation model with a microscopic energy and emission model to provide a unique evaluation tool. As a test of feasibility, this tool was utilized to evaluate alternative types of traffic control.

The study demonstrated that for steady state conditions (no vehicle accelerations) the tool predicted that vehicle fuel consumption and emissions are consistent with field data that were obtained from ORNL, and that vehicle fuel consumption and emissions are sensitive to the combined level of vehicle acceleration and speed. Furthermore, this study has demonstrated that the energy impacts of traffic signal control are marginally dependent on the level of acceleration, yet the environmental impacts of traffic signal control are highly dependent on the level of vehicle accelerations. The benefits of traffic signal control are within the level of variability in vehicle emissions that is associated with different acceleration levels. The findings of this study demonstrate the need to characterize typical vehicle acceleration levels under varying levels of congestion in order to develop reliable evaluation tools. Finally, the study demonstrates that aggressive driving behavior can result in significant environmental disbenefits.

Acknowledgements

The authors would like to acknowledge the funding provided by the Intelligent Transportation System (ITS) Implementation Center. Furthermore, the authors are indebted to the late Michel Van Aerde, who initiated the work that is presented in this paper. Finally, the authors would like to thank the anonymous reviewers for their thorough review and valuable comments.

Appendix References

Ahn, K., Rakha, H., Trani, A., and Van Aerde, M. (2002). "Estimating vehicle fuel consumption and emissions based on instantaneous speed and acceleration levels." *Journal of Transportation Engineering,* ASCE, 128(2), 182-190.

Barth, M., Younglove, T., Wenzel, T., Scora, G., An, F., Ross, M., and Norbeck, J. (1997). "Analysis of model emissions from diverse in-use vehicle fleet." *Transportation Research Record,* 1587, 73-84.

Greenshields, B.D. (1935). "A study in highway capacity." *Highway Research Board Proceedings*, 14, 458.

M. Van Aerde and Associates, Ltd. (2002a). "INTEGRATION release 2.30 for Windows: User's guide – Volume I: Fundamental features."

M. Van Aerde and Associates, Ltd. (2002b). "INTEGRATION release 2.30 for Windows: User's guide – Volume II: Advanced features."

Pipes, L.A. (1953). "An operational analysis of traffic dynamics." *Journal of Applied Physics*, 24:3, 274-287.

Rakha, H. and Crowther, B. (2003). "Comparison and calibration of FRESIM and INTEGRATION steady state car-following behavior." *Transportation Research: Part A.* 37 (2003) 1-27

Rakha, H. and Lucic, I. (2002). "Variable power vehicle dynamics model for estimating maximum truck acceleration levels." ASCE *Journal of Transportation Engineering*, Vol. 128(5), pp. 412-419.

Rakha, H., Lucic, I., Demarchi, S., Setti, J., and Van Aerde, M. (2001). "Vehicle dynamics model for predicting maximum truck accelerations." *Journal of Transportation Engineering*, ASCE 127(5), 418-425.

Rakha, H., Medina, A., Sin, H. Dion, F., Van Aerde, M., and Jenq, J. (2000). "Field evaluation of efficiency, energy, environmental and safety impacts of traffic signal coordination across jurisdictional boundaries." *Transportation Research Record,* 1727, 42-51.

Rakha, H. and Van Aerde, M. (1996). "Comparison of simulation modules of TRANSYT and INTEGRATION models." *Transportation Research Record,* 1566, 1-7.

Rakha, H., Van Aerde, M., Bloomberg, L., and Huang, X. (1998). "Construction and calibration of a large-scale micro-simulation model of the Salt Lake area." *Transportation Research Record,* 1644, 93-102.

Society of Automotive Engineers. (1996). "Commercial truck and bus SAE recommended procedure for vehicle performance prediction and charting." *SAE Procedure J2188*, Warrendale, PA.

Van Aerde M. (1995), "Single regime speed-flow-density relationship for congested and uncongested highways." *Presented at the 74th TRB Annual Conference*, Washington DC, Paper No. 950802.

Van Aerde, M. and Rakha, H. (1995). “Multivariate Calibration of Single Regime Speed-Flow-Density Relationships.” *VNIS/Pacific Rim Conference Proceedings*, Seattle, WA, pp. 334-341, ISBN 0-7803-2587-7, IEEE 95CH35776.

Van Aerde M., Rakha H., and Paramahamsan H. (2003), “Estimation of O-D Matrices: The Relationship between Practical and Theoretical Considerations.” Accepted for presentation at the 82nd Transportation Research Board Annual Meeting, Washington DC.

Van Aerde, M. and Yagar, S. (1988a). “Dynamic integrated freeway/traffic signal networks: Problems and proposed solutions.” *Transportation Research*, 22A, 6, 435-443.

Van Aerde, M. and Yagar, S. (1988b). “Dynamic integrated freeway/traffic signal networks: A routing-based modeling approach.” *Transportation Research*, 22A, 6, 445-453.

West, B., McGill, R., Hodgson, J., Sluder, S., and Smith, D. (1997). "Development of Data-Based Light-Duty Modal Emissions and Fuel Consumption Models", *Society of Automotive Engineers*, Paper No. 972910., 1274-1280

Variable Notation

The following symbols are used in this paper:

a = Instantaneous vehicle acceleration (m/s^2)
c_1 = fixed distance headway constant (km)
c_2 = first variable distance headway constant (km^2/h)
c_3 = second variable distance headway constant (h)
F = residual force acting on the truck (N)
F = tractive force acting on the truck (N)
F_{max} = maximum tractive force (N)
F_t = tractive force (N)
h = headway (km)
k_j = jam density (veh/km)
$L^e_{i,j}$ = Model regression coefficient for MOE “e” at speed power “i” and acceleration power “j”
M = vehicle mass (kg)
M_{ta} = vehicle mass on tractive axle, $M \times perc_{ta}$ (kg)
$M^e_{i,j}$ = Model regression coefficient for MOE “e” at speed power “i” and acceleration power “j”
MOE_e = instantaneous fuel consumption or emission rate (l/s or mg/s)
m = is a constant used to solve for the three headway constants (h/km)
P = engine power (kW)
q_c = flow at capacity (veh/h)
R = total resistance force (N)
R_a = aerodynamic resistance (N)
R_r = rolling resistance (N)
R_g = grade resistance (N)
u = vehicle speed (km/h)
u_f = free-speed (km/h)
u_c = speed at capacity (km/h)
x = distance traveled (km)
η= power transmission efficiency (ranges from 0.89 to 0.94)
μ = coefficient of friction between tires and pavement

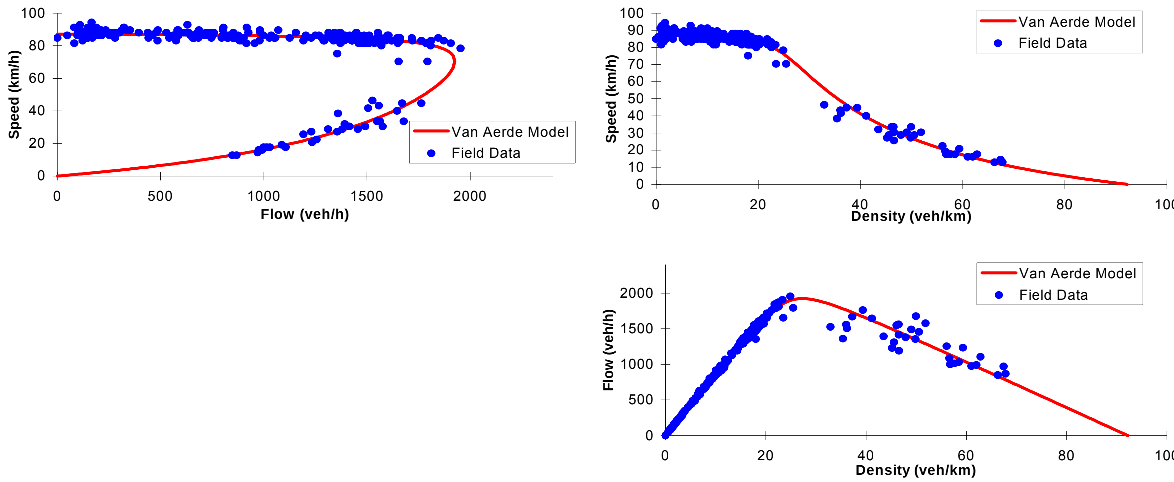

Figure 28: Sample Traffic Stream Models (I-4, Orlando)

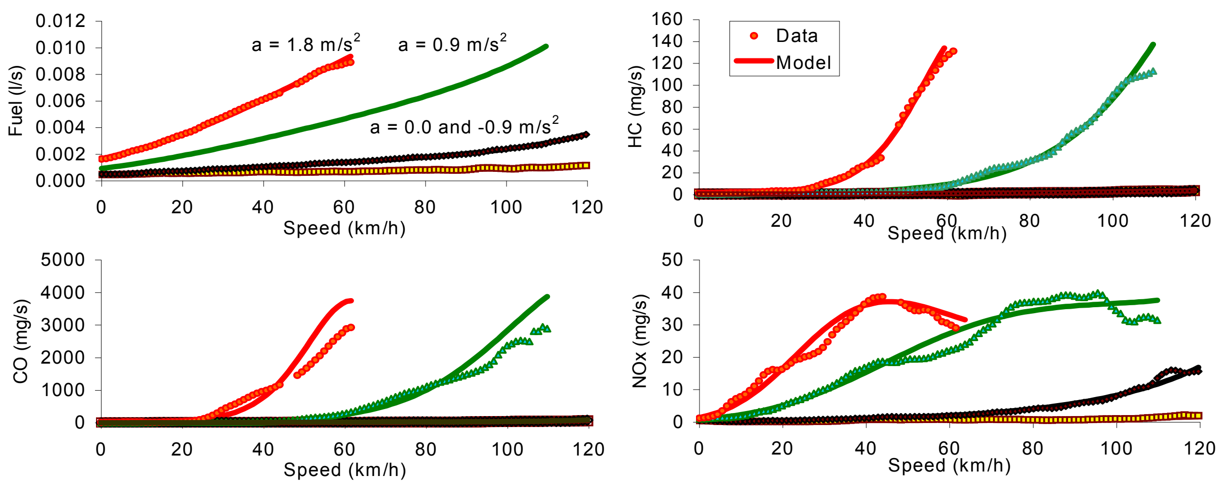

Figure 29: Regression Model Predictions (Composite Vehicle – Log-Transformed Hybrid Polynomial Model)

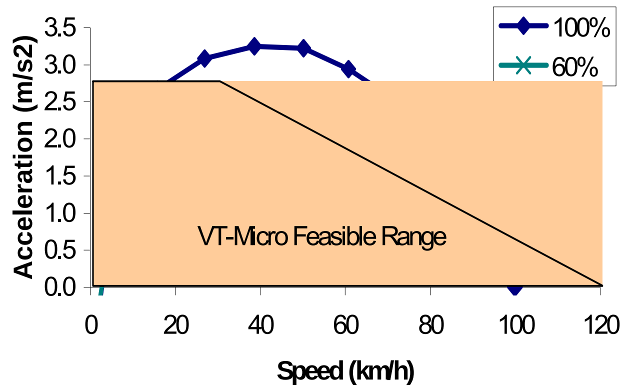

Figure 30: VT-Micro Feasible Range of Application

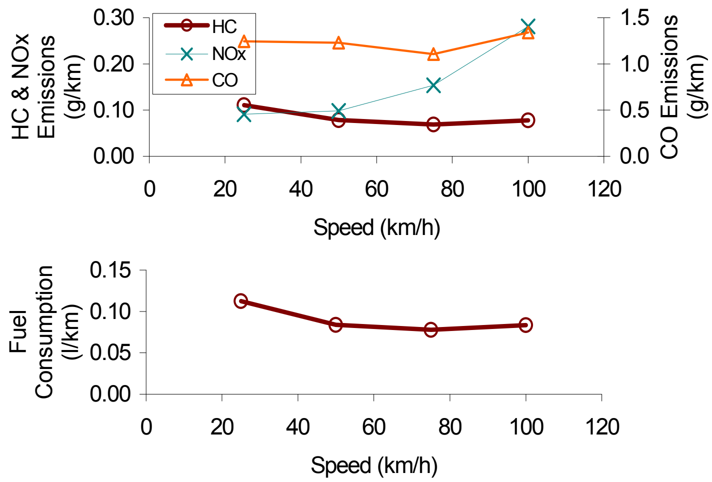

Figure 31: Impact of Constant Speed Level on Vehicle Fuel Consumption and Emissions

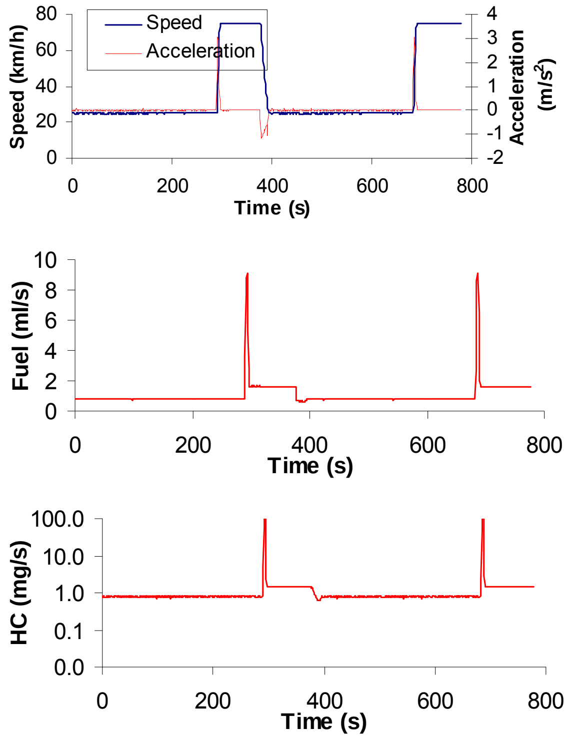

Figure 32: Variation in Instantaneous Fuel Consumption and HC Emissions for Variable Speed Scenario

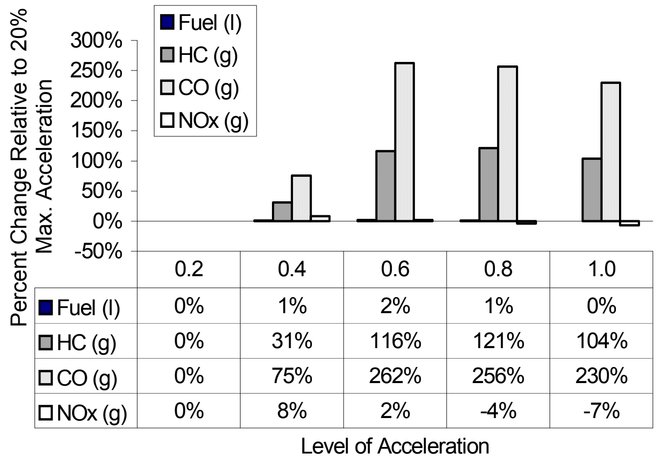

	0.2	0.4	0.6	0.8	1.0
Fuel (l)	0%	1%	2%	1%	0%
HC (g)	0%	31%	116%	121%	104%
CO (g)	0%	75%	262%	256%	230%
NOx (g)	0%	8%	2%	-4%	-7%

Figure 33: Effect of Variable Speed on Vehicle Emissions

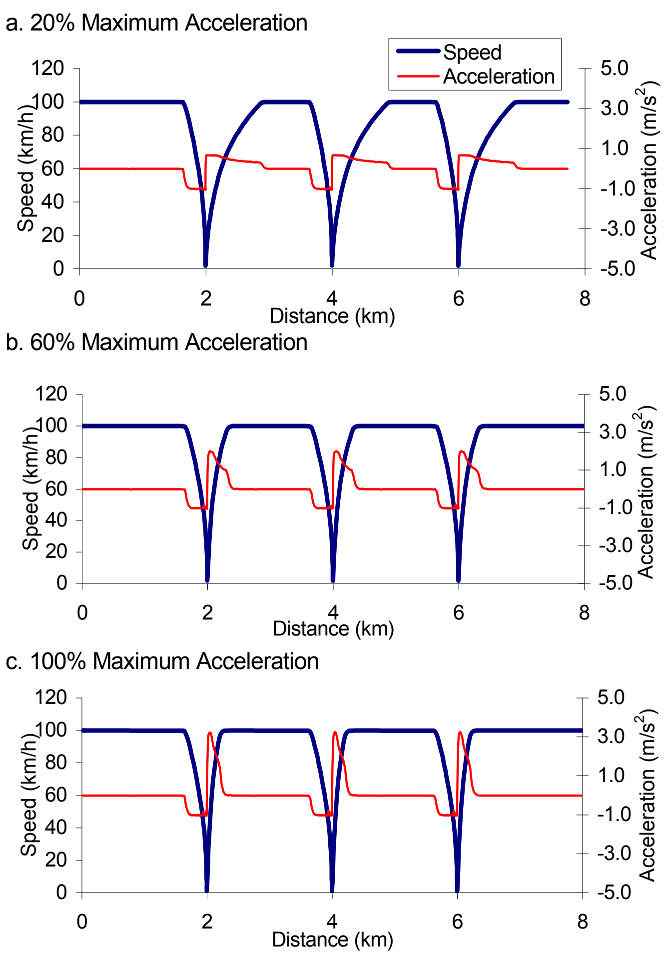

Figure 34: Speed and Acceleration Profiles for 3-stop Scenario (Cruise Speed of 100 km/h)

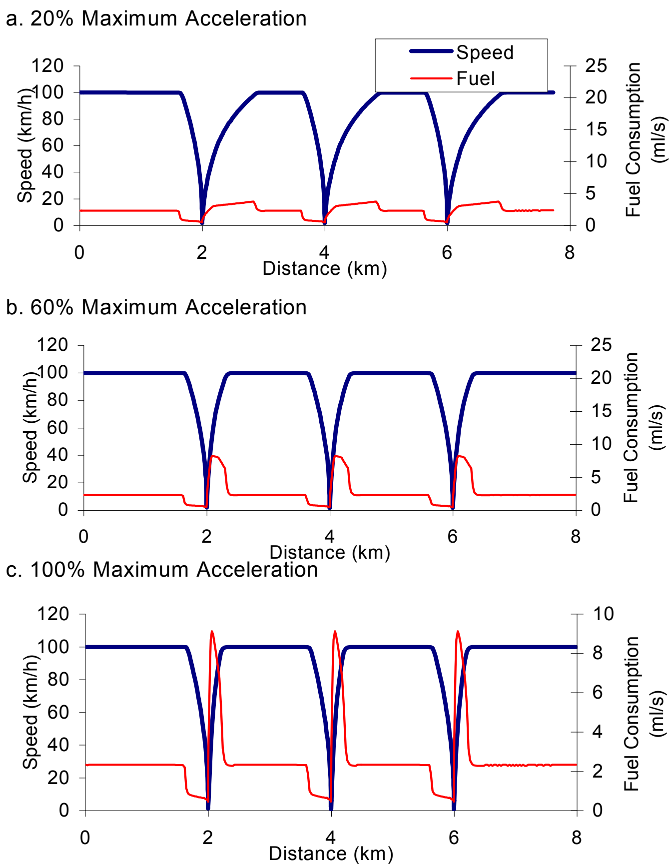

Figure 35: Variation in Instantaneous Fuel Consumption (3-stop at cruise speed of 100 km/h)

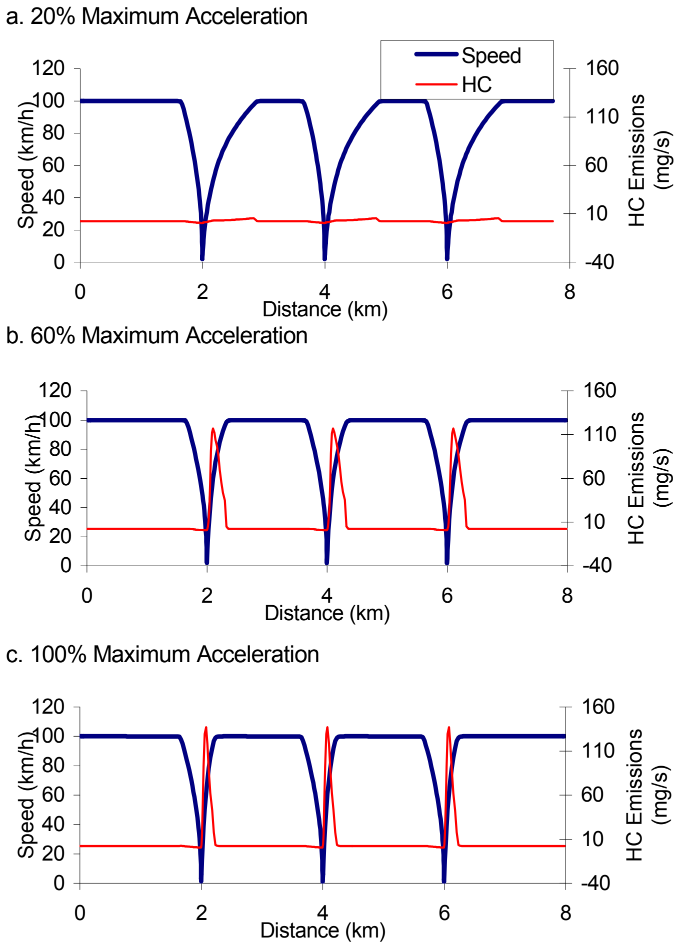

Figure 36: Variation in Instantaneous HC Emissions (3-stop at cruise speed of 100 km/h)

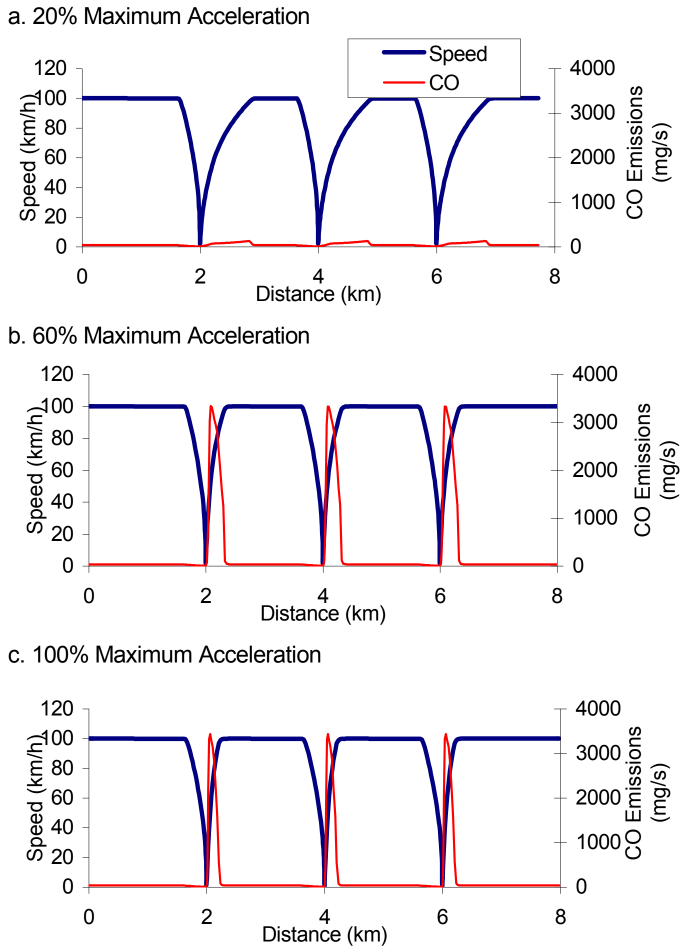

Figure 37: Variation in Instantaneous CO Emissions (3-stop at cruise speed of 100 km/h)

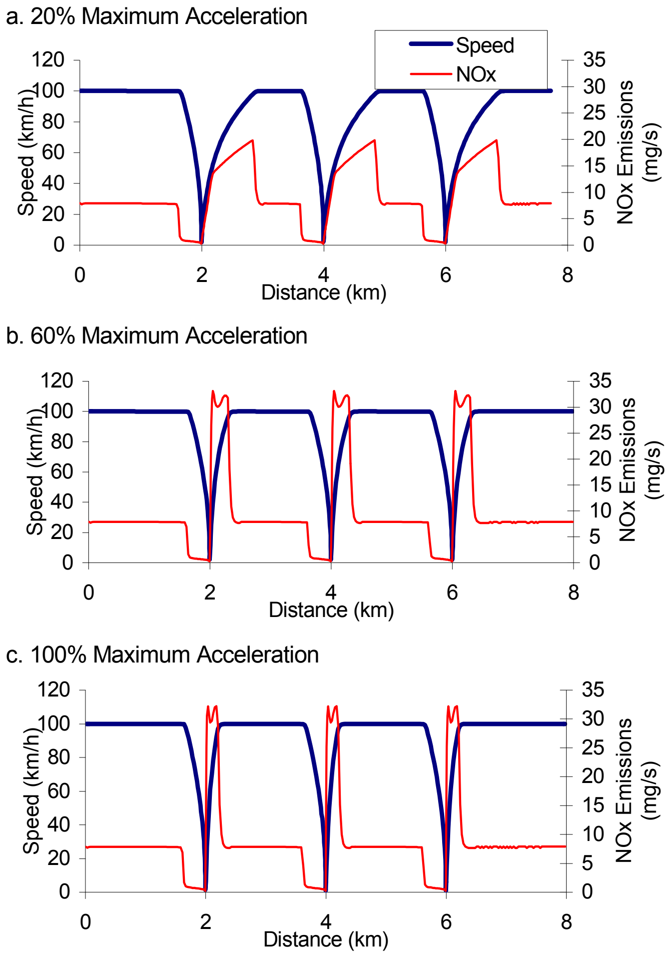

Figure 38: Variation in Instantaneous NO_x Emissions (3-stop at cruise speed of 100 km/h)

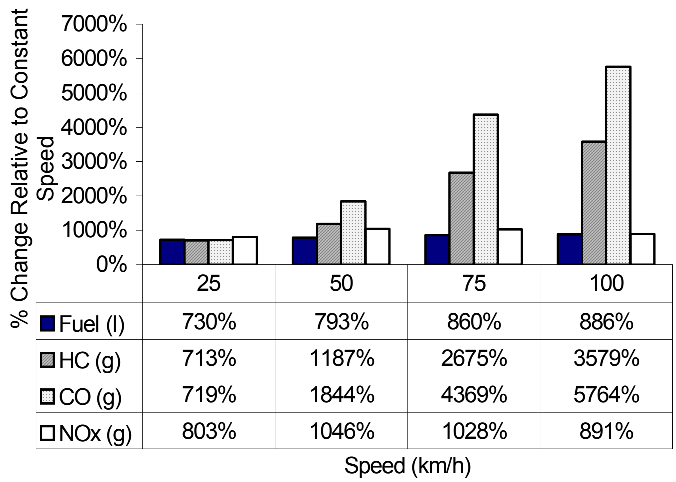

	25	50	75	100
Fuel (l)	730%	793%	860%	886%
HC (g)	713%	1187%	2675%	3579%
CO (g)	719%	1844%	4369%	5764%
NOx (g)	803%	1046%	1028%	891%

Figure 39: Effect of Stops on Vehicle Fuel Consumption and Emissions

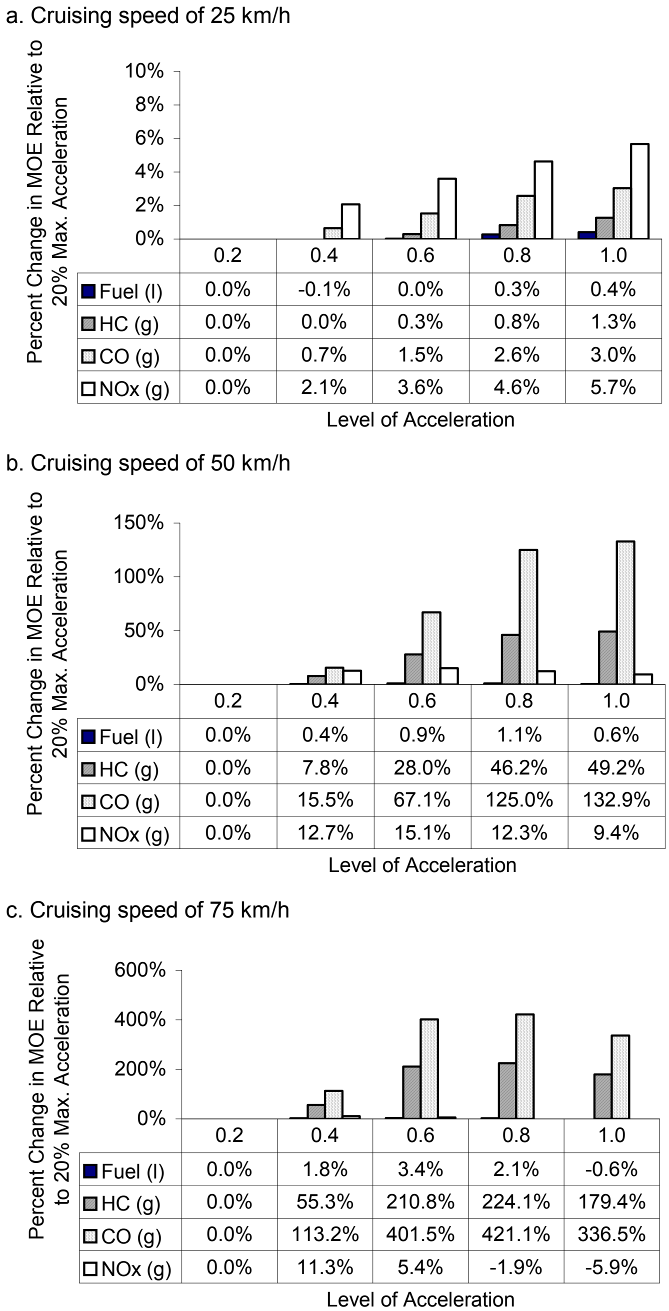

a. Cruising speed of 25 km/h

	0.2	0.4	0.6	0.8	1.0
Fuel (l)	0.0%	-0.1%	0.0%	0.3%	0.4%
HC (g)	0.0%	0.0%	0.3%	0.8%	1.3%
CO (g)	0.0%	0.7%	1.5%	2.6%	3.0%
NOx (g)	0.0%	2.1%	3.6%	4.6%	5.7%

b. Cruising speed of 50 km/h

	0.2	0.4	0.6	0.8	1.0
Fuel (l)	0.0%	0.4%	0.9%	1.1%	0.6%
HC (g)	0.0%	7.8%	28.0%	46.2%	49.2%
CO (g)	0.0%	15.5%	67.1%	125.0%	132.9%
NOx (g)	0.0%	12.7%	15.1%	12.3%	9.4%

c. Cruising speed of 75 km/h

	0.2	0.4	0.6	0.8	1.0
Fuel (l)	0.0%	1.8%	3.4%	2.1%	-0.6%
HC (g)	0.0%	55.3%	210.8%	224.1%	179.4%
CO (g)	0.0%	113.2%	401.5%	421.1%	336.5%
NOx (g)	0.0%	11.3%	5.4%	-1.9%	-5.9%

Figure 40: Impact of Cruising Speed and Acceleration Level on Vehicle Energy and Emissions (3-Stop Scenario)

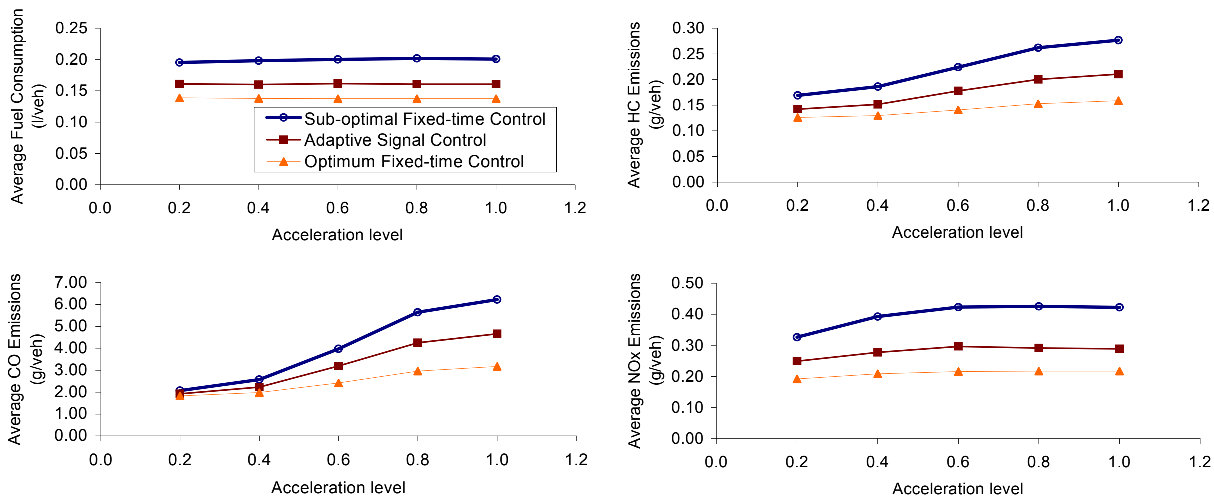

Figure 41: Variation in Fuel Consumption and Emissions as a Function of Type of Signal Control

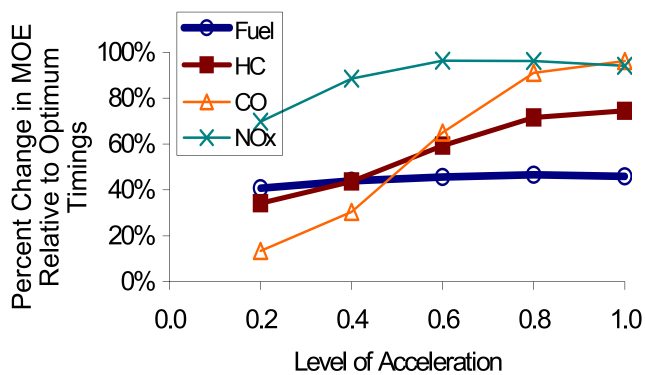

Figure 42: Increase in MOEs Relative to Optimum Scenario

APPENDIX D: FRAMEWORK FOR ESTIMATING NETWORK-WIDE SAFETY IMPACTS OF INTELLIGENT TRANSPORTATION SYSTEMS

A. Avgoustis, M. Van Aerde, and H. Rakha

Abstract

The paper presents a safety model that is based on US national crash statistics. The model computes the crash risk for 14 different crash types as a function of the facility speed limit and a time-dependent measure of exposure. The use of a time-dependent measure of exposure allows the model to capture differences in the crash risk that result from differences in the network efficiency. The model also computes the vehicle damage and level of injury to the passengers involved in the crash based on the vehicle's instantaneous speed. The use of the instantaneous speed means that the crash damage and injury level is responsive to the level of congestion. Consequently, the model can capture the safety impacts of operational-level alternatives including Intelligent Transportation Systems (ITS's).

A field and simulation application of the model indicates that it produces results that are consistent with the General Estimates System national database. Furthermore, the results indicate that the model can be applied to evaluate the safety impacts of alternative traffic-flow improvement projects, like for example re-timing traffic signals.

Introduction

During the period of 1988-96 over 58 million crashes were reported in the United States (U.S. DOT). In 1996 alone the total number of reported crashes was approximately 6.8 million, which was significantly higher than what was reported in the previous four years (1992-95). Furthermore, even though the total number of crashes remained almost the same from 1988 to 1994, the number of fatal crashes was not. Consequently, there is a need for a tool that can systematically evaluate the safety impacts of different traffic-flow improvement projects.

Transportation engineers have utilized existing accident/crash databases to evaluate the safety impacts of Intelligent Transportation Systems (ITS). However, there has not been a systematic approach to develop a safety model that is sensitive to ITS. This paper describes a safety model that was developed to address this unique problem. Specifically, the model that is described is sensitive to the facility's speed limit, the level of congestion on the facility, and the vehicle's instantaneous speed. The model computes the crash risk for 14 types of crashes, the level of damage incurred to the vehicles in the crash, and the maximum level of injuries to the people involved in the crash.

Objectives of Paper

The objectives of the paper are twofold. First, the paper describes a safety model that was developed for evaluating the safety impacts of ITS alternatives. The unique features of the model are its sensitivity to vehicle-to-vehicle and vehicle-to-control interaction. Second, the paper demonstrates the feasibility of the model within a simulation environment and its direct application to field data.

Paper Layout

The crash rate as a function of the facility speed limit is computed as the ratio of the number of crashes to the Vehicle Kilometers Traveled (VKT) (more commonly referred to as Vehicle Miles Traveled (VMT)), as illustrated in Figure 43. The VKT in turn, is the product of the traffic volume on the roadway network and the length of the roadway network.

Consequently, in terms of the paper layout, the first section provides a brief background of the available national crash databases and the typical highway statistics in the US. Section 3, describes how the crash data were extracted from the national crash database and how the VKT was computed. In addition, Section 3 describes how the number of crashes and the VKT were utilized to develop the safety model, while Section 4 provides a limited application of the safety model for the evaluation of the safety impacts of traffic signal coordination. Finally, Section 5 provides the conclusions of the paper together with suggestions for further research.

Background

A number of national crash databases are available for public usage, including the General Estimates System (GES), the Fatality Analysis Reporting System (FARS), the Highway Statistics Database, the Highway Safety Information System (HSIS), and the Crashworthiness Data System (CDS). The GES database is the largest and the most complete of these databases and thus was utilized for the model development. This section provides a brief overview of the GES database, typical US highway statistics and the current state-of-the-art in safety modeling.

The General Estimates System Database

The General Estimates System (GES) database was developed in 1988 by the National Center for Statistics and Analysis and is operated by the National Highway Traffic Safety Administration (NHTSA) (USDOT, 1996). GES data are obtained from a nationally representative probability sample selected from all police-reported crashes. The primary objectives for the development of this system were the identification of traffic safety problem areas and for usage as a basis for benefit/cost analyses of traffic safety initiatives.

The level of exposure makes GES, the largest crash database available in the United States. Due to its level of exposure, DOT agencies, lawyers, doctors, researchers and insurance companies use it extensively. By using the database one can estimate different crash frequencies (number of vehicle crashes).

For a crash to be eligible for the GES sample, it has to meet a number of criteria including: (a) a Police Accident Report (PAR) must be completed, (b) it must involve at least one motor vehicle traveling on a traffic way, and (c) the result must be property damage, injury or death. GES data collectors perform weekly visits to approximately 400 police jurisdictions in 60 sites across the United States. The GES 1996 file that was used for the purposes of developing the safety model included approximately 56,000 Police Accident Reports (PAR's).

The crashes in the database are classified in a variety of ways, for example by a typical speed limit, crash severity, time-of-day and vehicle type. A statistical model that the database utilizes enables the user to extract national statistics on crash frequencies.

There are three main files (Statistical Analysis Data Sets) in the GES database that include all the variables. The first of these files, the accident file, contains information describing environmental conditions and roadway characteristics at the time of the crash. It also includes information such as the time the crash occurred, the manner of collision and speed limit of the facility on which the crash occurred. The second file, the vehicle/driver file contains information describing the vehicles involved in the crash and their drivers. It also includes information about the model/make of the vehicle, the model year of the vehicle, the driver's maneuver to try and avoid the crash, and the reason for the driver distraction. The third file, the person file, contains general information describing all persons involved in the crash. These include the drivers, passengers, pedestrians, pedalcyclists and non-motorists who were involved in the crash. The file also includes information about the age, sex and injury severity of each of the persons involved in the crash.

Highway Statistics

The computation of the crash rate from the frequency of crashes requires a unit of vehicle exposure, which is typically the VKT. This section briefly describes some of the data available for computing VKT for different facility types.

The Federal Highway Administration (FHWA) and the Office of Highway Management publish the Highway Statistics publication once a year. The Highway Statistics provides information on highway mileage and VKT. Most of the data are divided into urban and rural tables according to the population and Federal-aid legislation definition and are presented primarily on a State-by-State basis.

The Highway Statistics indicates that the United States transportation network is the largest network in the world. Specifically, in 1996, the U.S. transportation system served 265 million people and supported 7.04 trillion passenger kilometers (BTS, 1997). Many factors influence the expansion and growth of this network such as population increase, economy expansion, higher consumer incomes and vehicle availability.

According to the Bureau of Transportation Statistics (BTS, 1997) the public roads in the US transportation network in 1996 included a total of 6,271,120 kilometers (3,919,450 miles) of roads, as summarized in Table 24. Five facility types categorize these highway kilometers. Almost 134 million vehicles (passenger cars and motorcycles) existed in the system during 1996, as opposed to less than 93 million in the 70's (BTS, 1997). In terms of vehicle kilometers, these increased from 1.76 trillion VKT in the 70's, to approximately 4.0 trillion VKT in 1996, as demonstrated in Table 24.

State-of-the-Art in Safety Modeling

Many researchers have attempted to find the independent variables most highly associated with crashes. For example, Bernardo and Ivan (1997) attempted to establish the relationship between the number of crashes versus the crash rate using Poisson regression. In their study, small data sets for several intersections were utilized while applying different representations of traffic exposure and intersection effects as independent variables. Bernardo and Ivan (1997) suggested that the Poisson distribution allows for the relationship between exposure and crashes to be more accurately modeled as opposed to the linear relationship assumed in crash rate prediction. However, this study was limited to a rather small sample of localized intersections.

Zegeer *et.. al*. (1997) developed motor vehicle crash rates by crash type and roadway class in eight states, including California, Illinois, Maine, Michigan, Minnesota, North Carolina, Utah and Washington. The crash data were extracted from the Highway Safety Information System (HSIS). The most important variables for calculating the crash rates were the urban or rural code, the functional roadway class, number of lanes and divided versus undivided roads. Eight different roadway classes were considered, including urban freeways, urban two-lane highways, urban multi-lane divided non-freeways, urban multi-lane undivided non-freeways, rural freeways, rural two-lane highways, rural multi-lane divided non-freeways, and rural multi-lane undivided non-freeways. The results of this study showed that the most common crash type in most states was the rear end/same direction sideswipe, with angle and turning crashes ranked second. In terms of crash rates produced, these were lower on freeways than any other roadway class. The study showed significant variation in the crash rates, even within common roadway classes. This was justified by the differences in reporting procedures, the nature of the highway system, driving populations and other factors that varied from state-to-state. Severity, light and surface conditions and collision types were also considered, yielding very similar results for all eight states. They concluded that the results from their study were considered reasonable and that the crash rates could be used as a baseline in order to better understand crash trends.

In another study, Mohamedshah and Kohls (1994) developed crash rates using the Highway Safety Information System database for the development of the so-called Interactive Highway Safety Design Model (IHSDM). A crash prediction model was developed to produce average crash rates for different highway crash types. The objective of the study was to determine if the HSIS data could be used to develop a crash prediction model. The results of the study showed that data from a database such as the HSIS could be used to develop a crash prediction model for different roadway types. However, Mohamedshah and Kohls (1994) suggested that the development of average crash rates required judicious manipulation of the data and sound engineering judgement.

Zhou and Sisiopiku (1997) developed crash rates and examined their relationship to volume-to-capacity ratios. Data from Interstate I-94 in Detroit, Michigan were used to examine this relationship. Particular emphasis was given on the development of models to explain the differences between crash rates during weekends and weekdays, rear-end crashes and fixed-object collisions and property damage only crashes versus crashes involving injury and fatality. Zhou and Sisiopiku (1997) concluded that the crash rates were highest at low levels of congestion (low volume-to-capacity ratio (v/c)) and decreased rapidly when the v/c ratio increased. This finding is consistent with the model that is described in this paper, as will be demonstrated later. The final outcome of this study was that the correlation between property damage crash rates and the volume-to-capacity values followed a general U-shaped pattern. Alternatively, the injury and fatality crash rates decreased as the v/c ratio decreased.

Vogt and Bared (1997) developed crash models for two-lane rural segments and intersections. Advanced statistical techniques were used in this study, as well as extensive crash and roadway data. The Highway Safety Information System (HSIS) was used in this study as the main source of data. Models were focused on segments and intersections. Negative binomial and Poisson models were considered for both cases. Vogt and Bared (1997) concluded that the data used for these models offered reasonable representations of the effects of highway variables on crashes. However, the Poisson, negative binomial and logistic models that were used to model crash severities did not produce significant results.

Persaud and Musci (1995) used hourly traffic volumes in regression models for estimating the crash potential on two-lane rural roads. They used data from Ontario, Canada and used different combinations of time periods and geometric characteristics. Single vehicle crashes were particularly studied and the models showed that the crash potential was higher during the night. On the other hand, for multi-vehicle crashes the crash potential was higher during the day. The study also emphasized the importance in differentiating between single and multi-vehicle crashes and day versus night conditions.

In its Special Report 254 ("Managing Speed"), the Transportation Research Board described the relationship between speed and safety. The link between speed and safety was characterized as complex and the researchers emphasized the fact that both speed and speed dispersion are associated with crash involvement. Also in the report, the difficulties of relating the road class with speed-safety are described and it is mentioned that there is a limitation of data to analyze the speed-safety relationships with road class. As will be described below, speed was one of the key variables that were used for the development of the safety model therefore caution must be used when speed and speed limits are associated with safety and crash involvement.

In summary, extensive effort has been devoted to the development of crash risk models, however, these models lack the level of resolution that is required to evaluate the safety impacts of operational-level projects. Namely, they are not sensitive to the level of congestion on the network and/or the smoothness of traffic flow. This paper describes a model that serves as a first step in addressing this unique problem.

Development of Safety Model

As illustrated in Figure 43 the crash rate is computed as the ratio of the crash frequency to the vehicle kilometers traveled. This section describes how the crash frequencies were derived from the GES database as a function of the type of crash, the facility speed limit and the time-of-day of the crash. In addition, this section describes how the crash rates were computed using the GES crash frequencies and the national highway statistics in the US. Finally, the limitations of the model are discussed.

Estimation of Crash Frequencies

The GES database for 1996 was utilized for the development of the safety model because it constituted the latest and most comprehensive crash data that were available at the time of the study. The variables that were considered in the development of the model included the crash type, the time at which the crash occurred, and the facility speed limit on which the crash occurred. Other factors that were considered included the maximum injury to the people involved in the crash and the severity of vehicle damage.

The crash frequencies were extracted based on the speed limit of the facility on which the crash occurred for speed limits ranging from 5 mph to 75 mph, as illustrated in Figure 44. For each roadway speed limit the crash frequencies were further classified by type of crash (14 types in addition to the total number of crashes) and the time-of-day at which the crash occurred (24 hourly periods). The 14 crash types that were considered are summarized in Table 25. These crash types were extracted by considering 80 pre-crash states in the database and then grouping the pre-crash states into 14 categories. Others have typically used the manner of collision variable to compute crash frequencies by crash type, however, in order to capture more crash types the pre-crash state was utilized and merged with the other variables, namely the speed limit and time of crash.

In terms of specific trends, the GES database indicated that the number of fatalities in the US were highest during the PM peak. The data also indicated that the number of crashes were highest on facilities with speed limits in the range of 40 to 72 km/h (25 to 45 mph), as illustrated in Figure 45. The database also indicated a reduction in the total number of crashes for the even numbered speed limits versus the odd numbered speed limits (e.g. 30 versus 35 mph). This difference is a result of a smaller sample size of facilities with even numbered speed limits (i.e. more facilities with a speed limit of 35 mph versus 30 mph).

The database also demonstrated that the angle type of crashes represented the highest frequency (36 percent of all crashes) in terms of crash types followed by rear-end crashes (27 percent), as illustrated in Figure 46. Furthermore, the frequency of rear-end crashes was found to be highest during the AM and PM peaks, as illustrated in Figure 47.

For each crash type, the crash severity was estimated in terms of the vehicle damage and injury to the people involved in the crash. Specifically, five injury severity levels were considered in the database. These included no injuries, possible injuries, non-incapacitating injuries, incapacitating injuries, and fatal injuries. In addition, four vehicle damage levels were considered, including no damages, minor damages, moderate damages, and severe damages. The severity damage was computed as a probability a crash was of a specific level of severity.

Estimation of Crash Rates

As described in the previous section, the crash frequencies were derived from the GES database as a function of the type of crash, the facility speed limit and the time-of-day of the crash. Unfortunately, the vehicle kilometers traveled along the US highways were available at a more aggregate level of resolution, as indicated in Table 24.

Consequently, the first step in computing the crash rates was to disaggregate the vehicle kilometers traveled to a level of resolution that was consistent with the crash frequency data. Specifically, the vehicle kilometers traveled were disaggregated by roadway speed limit (ranging from 5 to 75 mph at 5 mph increments) and by time-of-day (24 periods), as illustrated in Figure 48.

The disaggregation of vehicle kilometers traveled by speed limit was done using a lookup table that summarized the range of roadway speed limits that were associated with each roadway type, as demonstrated in

Table 26. It was assumed that the vehicle kilometers traveled were equally distributed across the speed limits for a specific facility type. For example, local streets with a speed limit of 25 mph were assumed to contribute one fifth of the local-street vehicle kilometers traveled given the five speed limit levels associated with local streets. In disaggregating the vehicle kilometers traveled by speed limit it was ensured that the sum of the vehicle kilometers traveled for all the speed limits associated with a specific facility type was equal to the facility type vehicle kilometers traveled that were presented in Table 24.

The next disaggregation exercise involved disaggregating the vehicle kilometers traveled by time-of-day. The disaggregation by time-of-day was made consistent with the proportion of daily volume associated with each of the 24 hours of the day. In some cases typical daily volume distributions were generated from field data, as illustrated in Figure 49, while in other cases these distributions were estimated from the literature (TRB, 1994).

Once the vehicle kilometers traveled were disaggregated by time-of-day and by the facility speed limit, the crash rates were computed. For example, Figure 50 illustrates the trend in variation of rear-end crash rates for a 45 mph facility as a function of the time-of-day. Figure 50 was generated by dividing the crash frequencies that are illustrated in Figure 47 by the vehicle kilometers for each time period based on Figure 49. It is interesting to note that the U-shape variation in the crash rate is consistent with other studies (Zhou and Sisiopiku, 1997).

The safety model also indicates that the crash rate decreases as the speed limit increases, as illustrated in Figure 51. Exponential functions were fit to the data with a coefficient of determination ranging from 30 to 80 percent depending on the crash type. The form of the relationship for each of the 15 crash types (including the total number of crashes) is presented in Equation 1. The relationship indicates that the crash frequency in dependent on the speed limit (S_f). The regression coefficients for Equation 1 are summarized in Table 25. The exponential reduction in crash rates as a function of the facility speed limit is consistent with other studies in the literature that have shown that the crash rate on arterial streets is higher than that on freeways for a distance-based unit of exposure.

Finally, by multiplying the distance-based crash rate by the facility free-speed it was possible to estimate a time-based crash rate. The advantage of a time-based crash rate is that the rate level of exposure increases with higher levels of congestion even though vehicles might not necessarily travel longer distances.

$$CrashRate_i = e^{a_1^i \times S_f + a_2^i} \quad \forall\ i = 1,15 \qquad [1]$$

It must be emphasized at this point, that the distance-based crash rate was modeled as a function of posted speed but it did not take into account time-of-day or actual speeds. Because of the fact that the distance-based crash rate depends on observed speeds or level of congestion by multiplying it by the observed speeds it may misrepresent the time-based crash rate.

Estimation of Crash Severity

In addition, the proposed safety model probabilistically computes the level of damage to the vehicles involved in the crash together with the highest level of injury incurred to the passengers involved in the crash. Specifically, Figure 52 illustrates the level of damage relationships that were derived from the GES database. The thin lines indicate the GES estimated probability of each of the four damage levels, while the thick lines represent the third degree polynomial regressed relationships that were derived from the data. The damage level is dependent on the instantaneous speed (S), as demonstrated in Equation 2. The values of the regression coefficients are presented in Table 27. The coefficient of determination for these relationships ranged from 55 percent to 69 percent.

In general the relationships indicate a reduction in the no damage crashes with an increase in the other crash damages in the 25 to 45 mph range. The figure does indicate the no damage crashes are the least probable of the different damage levels (less than 10 percent probability).

$$Damage_i = b_1^i + b_2^i \times S + b_3^i \times S^2 + b_4^i \times S^4 \quad \forall\ i = 1,4 \quad [2]$$

Figure 53 indicates that the injury severity level is fairly constant as a function of the facility speed limit and that the no injury crashes are dominant when compared to the other levels of severity (on average 40 percent probability). The coefficient of determination for these third degree polynomial relationships ranged from 16 percent to 88 percent, as illustrated in Figure 53. As was the case for the damage level, the injury level is dependent on the instantaneous speed (*S*) as demonstrated in Equation 3. The values of the regression coefficients are presented in Table 28.

$$Injury_i = c_1^i + c_2^i \times S + c_3^i \times S^2 + c_4^i \times S^4 \quad \forall\ i = 1,5 \quad [3]$$

Caveats of the Safety Model

The crash frequencies utilized within the safety model were derived from a national crash database. Clearly, the accuracy of the safety model is governed by the accuracy of the crash database. There are several problems with national databases including, the fact that not all crashes are reported to the police, there are errors in police reporting, and there are sampling errors. In addition, the merging of different files within the GES database results in errors, as was the case in extracting the 14 crash types from the 80 pre-crash states.

Furthermore, the estimation of the crash rates involved certain errors and assumptions. Clearly, there is a level of error associated with the vehicle kilometers traveled that are reported in the literature. Furthermore, in disaggregating the vehicle kilometers traveled, a number of simplifying assumptions were made. First, it was assumed that the vehicle kilometers traveled could be equally distributed to all the speed limits within a facility type. Second, there was a level of error associated with the typical volume profiles that were assumed for each of the facility types. Also, the fact that the GES database did not provide roadway classification for the crashes (it only identifies crashes on interstate highways and National Highway System (NHS) roadways) imposed some limitations to the model. As explained in the literature review the relationship of speed (or speed limit) and crash involvement is complex. Clearly, the GES database did not yield a substantial amount of data for crashes associated with low speed limits, for example 5-25 mph. Consequently, the crash rates that are estimated by the model should be viewed within the context of the caveats that were described.

Safety Model Application

The safety model that was described earlier was tested in two ways. First, it was applied to second-by-second floating car field data. Second, the model was incorporated within a microscopic simulation environment and tested on different traffic networks.

This section describes how the model can be applied directly to field data, how it can be utilized within a simulation environment and reasonableness of the estimated crash rates.

Field Application

In order to demonstrate the applicability of the safety model for operational level evaluations, the model was utilized to evaluate the safety impacts of coordinating traffic signals across an inter-jurisdictional boundary. In conducting the analysis, second-by-second speed measurements from floating cars along the study section (9.6-kilometer section of Scottsdale/Rural Road in Phoenix) were gathered prior and after the signal timings were changed.

Three Global Positioning System (GPS)-equipped vehicles were driven along the study corridor for three days (Tuesday through Thursday) prior and after changing the signal timings. The GPS runs were conducted during the AM peak (7:00 to 9:00 AM), the off-peak (11:00 to 1:00 PM), and the PM peak (4:00 to 6:00 PM). The GPS unit measured the vehicle's latitude and longitude, its heading, and its speed every second or in some cases every two seconds. The speed was measured based on the shift in the GPS signal (Doppler technology). The vendor stated speed accuracy was 0.1 m/s. It should be noted that the GPS unit did not include any differential correction resulting in a vehicle location accuracy to within 100 meters. However, the relatively low accuracy in locating the vehicle had no bearing on the accuracy of the speed estimates given that they were not computed from the vehicle location.

A total of 141 runs were conducted for the before conditions and a total of 160 runs were conducted for the after conditions, as demonstrated in Table 29. The larger number of runs for the after case versus the before case demonstrates a 12 percent increase in throughput as a result of the improvements in signal timings. Most of the benefits occur during the PM peak (39 percent increase in throughput).

Applying the proposed model to the second-by-second speed measurements resulted in an overall reduction in the crash rate by approximately 8 percent as demonstrated in Table 30. The crash risk was in the range of 25×10^{-6} which translates to a crash rate of approximately 2.5×10^{-6} crashes per million vehicle kilometers (dividing by the trip length of 9.6 kilometers). By conducting an Analysis of Variance (ANOVA) test on the data it was concluded that these results were statistically significant at a 5 percent level of significance. Noteworthy is the fact that the differences in the crash rates are a result of differences in the trip travel times because the facility speed limit was the same for the before and after case. The crash damage and injury level, on the other hand, was directly impacted by the instantaneous speed measurements given that the two independent inputs to the model were the instantaneous speed and the travel time.

A separate study by Science Applications International Corporation (SAIC) investigated the safety impacts of traffic signal coordination by analyzing crash statistics using the ALLIS database at a number of coordinated and uncoordinated traffic signals in the Phoenix area (Carter and St-Onge, 1999). The analysis included a total of 158 traffic signals of which 121 were coordinated and 37 were uncoordinated. Five years of crash data (1993 to 1997) were analyzed which included a total of 345,000 crashes. Annual Average Daily Traffic (AADT) counts that were available for the same time period were utilized to compute the crash rate. The study concluded that the crash rates for coordinated traffic signals were less than those for uncoordinated traffic signals in the range of 14 to 43 percent. Based on these two independent studies it was concluded that the proposed safety model produced results that were reasonable in trend. Furthermore, the absolute value of the crash rates was also found to be reasonable.

Simulation Application

The safety model was also incorporated within the INTEGRATION simulation model (Van Aerde, 1999a and b) and tested on a simple 5-link network. The speed limit along the network was varied from 40 km/h to 120 km/h at increments of 20 km/h. The simulation results indicated that the crash rate decreased from 3.0×10^{-6} crashes per million VKT at a speed limit of 40 km/h to 0.4×10^{-6} crashes per million VKT for a speed limit of 120 km/h. Both the absolute magnitude of the crash rate together the variation in the crash rate as a function of the facility speed limit were found to be consistent with the GES database.

The simulation model was then applied to the same corridor in Phoenix (Scottsdale/Rural Road). Using turning movement and tube counts the O-D demand was calibrated to the field data, which included a total of approximately 130,000 vehicles. The simulated crash rate was approximately 2.6 crashes per million vehicle kilometers traveled. Again, as was the case using the field floating car data, the simulation indicated that by improving traffic signal coordination, the crash risk was reduced by approximately 5 percent.

Conclusions and Recommendations for Further Research

This paper presented a safety model that is based on US national crash statistics. The model computes the crash risk for 14 different crash types as a function of the facility speed limit and a time-dependent exposure measure. The use of a time-dependent exposure measure allows the model to capture differences in the crash risk as a result of differences in travel times. The model also computes the vehicle damage and level of injury to the passengers involved in the crash based on the vehicle's instantaneous speed. The use of the instantaneous speed means that the crash damage and injury level is responsive to the level of congestion. Consequently, the model can capture the safety impacts of operational-level alternatives including Intelligent Transportation Systems (ITS's).

A field and simulation application of the model indicates that it produces results that are consistent with the GES national database. Furthermore, the results indicate that the model can be applied to evaluate the safety impacts of alternative traffic-flow improvement projects, like for example re-timing traffic signals.

The safety model that was presented in this paper does not consider vehicle-to-vehicle or vehicle-to-control interaction explicitly. Consequently, further research is required to develop safety models that compute the crash risk based on micro-level vehicle interaction parameters. These parameters could include the distance headway and relative speed between following vehicles, the number of lane change maneuvers, and/or the number of path intersecting maneuvers (e.g. the number of left turners that must find a gap in an opposing through movement). While the development of such a micro-level approach is currently underway (Van Aerde and Rakha (1999)), the safety model that is presented in this paper can not only be utilized to evaluate the safety impacts of traffic-improvement alternatives but can also serve as a benchmark for validating such microscopic safety model approaches. Additionally, in a future study, a smaller data set within a corridor can be used for developing a safety model. By doing this instead of assumed data, real data can be used. Such a model can be used to evaluate changes in speed, congestion and other operational characteristics to evaluate the sensitivity of such a model with respect to these changes. In a similar fashion, other databases, such as the Fatality Analysis Reporting System (FARS) can be used for the retrieval of specific data associated with speed limits, time-of-day and crash types.

References

Bernardo N. and Ivan J. (1997), "Predicting Number of Crashes Vs Crash Rate Using Poisson Regression", Presented at Transportation Research Board 76th Annual Meeting, January.

Bureau of Transportation Statistics (1996), *National Transportation Statistics 1996*, U.S.DOT/BTS: DOT-BTS-VNTSC-95-4

Carter M. and St-Onge C. (1999), "Analysis of the Safety Impacts of Signal Coordination in Phoenix, MMDI Safety Workshop Slides", Presentation made at the MMDI Safety Workshop, January.

Transportation Research Board (1994) "Highway Capacity Manual Special Report 209", Third Edition.

Mohamedshah Y. Khols A. (1994), "Accident Rates Using HSIS", Turner-Fairbanks Highway Research Center:

Persaud B. and Musci, (1997), "Microscopic Accident Potential Models for Two Lane Rural Roads", Presented at Transportation Research Board 76th Annual Meeting, January.

Transportation Research Board (1998) “Managing Speed: Special Report 254, Review of current practice for setting and enforcing speed limits”

U.S Department of Transportation, NHTSA (1996) “National Automotive Sampling System, General Estimates System (GES) User’s Manual”, 1996 File

Van Aerde M. (1999a), INTEGRATION © RELEASE 2.20 FOR WINDOWS: User's Guide-Volume I: Fundamental Model Features.

Van Aerde M. (1999b), INTEGRATION © RELEASE 2.20 FOR WINDOWS: User's Guide-Volume II: Advanced Model Features.

Van Aerde M. and Rakha H. (1999), A Framework for the Evaluation of System Safety Benefits of Intelligent Cruise Control Systems, ITS Journal, Vol. 00, pp. 1-27.

Vogt A. and Bared J. (1997), "Accident Models for Two-Lane Rural Segments and Intersections", Presented at Transportation Research Board 76th Annual Meeting.

Zegeer C., Huang H., Stewart J., Williams C. and Mohamedshah Y. (1997), *"*Comparison of Crash Rates and Characteristics in Eight States by Roadway Class*",* Turner-Fairbank Highway Research Center:

Zhou M. and Sisiopiku V. (1997) *Relationship Between Volume-to-Capacity Ratios and Accident Rates*, Transportation Research Record Vol. 1581, pp. 47-52.

Table 24. US Highway Statistics for 1996

Facility Type	Length (km)	Vehicle Kilometers Traveled (VKT)
Interstates	73,658	935,014,000,000
Principal Arterials and Expressways	256,202	1,210,381,000,000
Minor Arterials	362,210	729,515,000,000
Collectors	1,269,166	591,261,000,000
Locals	4,309,885	505,352,000,000
Total	**6,271,120**	**3,971,523,000,000**

Table 25. GES Crash Type Configurations and Safety Model Regression Coefficients

Crash Type	Description	Regression Coeff. (a_1^l)	Regression Coeff. (a_2^l)
1	Single Driver - Right Roadside Departure	-0.021501436	-4.903643188
2	Single Driver - Left Roadside Departure	-0.023559071	-5.013290246
3	Single Driver - Forward Impact	-0.01709544	-4.483434319
4	Same Traffic Way and Same Direction - Rear-end	-0.019589495	-4.283242043
5	Same Traffic Way and Same Direction - Forward Impact	-0.041110596	-6.600147706
6	Same Traffic Way and Same Direction - Sideswipe/Angle	-0.023089944	-5.340775704
7	Same Traffic Way and Opposite Direction - Head-on	-0.026041357	-6.694593649
8	Same Traffic Way and Opposite Direction - Forward Impact	-0.032079684	-5.641286798
9	Same Traffic Way and Opposite Direction - Sideswipe/Angle	-0.020100423	-5.154935427
10	Change Traffic Way and Vehicle Turning – Turn Across Path	-0.020957402	-4.715896567
11	Change Traffic Way and Vehicle Turning – Turn Input Path	-0.019926275	-4.589321771
12	Intersecting Paths – Perpendicular Crash	-0.019976246	-5.073630589
13	Backing Vehicle	-0.014536839	-7.133251805
14	Other or Unknown	-0.017781349	-4.848826862
15	Total Crash Rate	-0.020170247	-2.419018353

Table 26. Facility Types and Assumed Corresponding Speed Limits

Facility Type	Speed Limit (mph)
Locals	5-25
Collectors	30-35
Minor Arterials	40-45
Principal Arterials & Interstates	50-75

Table 27. Vehicle Damage Level Regression Coefficients

Damage Level (i)	b_1^i	b_2^i	b_3^i	b_4^i
1	-0.239700394	0.020748326	-0.000456083	3.07144E-06
2	1.880157356	-0.115168621	0.002713999	-1.98096E-05
3	-0.408725633	0.053370557	-0.001282669	9.55118E-06
4	-0.361429514	0.044930641	-0.001113984	8.48361E-06

Table 28. Maximum Injury Level Regression Coefficients

Injury Level (i)	c_1^i	c_2^i	c_3^i	c_4^i
1	0.684906791	-0.018349016	0.000404226	-2.93146E-06
2	0.061498825	0.001148376	8.36568E-05	-1.31214E-06
3	0.381316662	-0.011131083	0.000156714	-7.44377E-07
4	-0.330753659	0.030304057	-0.00069379	5.08542E-06
5	-0.033918500	0.002760289	-6.63681E-05	5.31696E-07

Table 29. Classification of GPS Before and After Runs and Safety Results

	Northbound			Southbound			
	AM Peak	**Midday**	**PM Peak**	**AM Peak**	**Midday**	**PM Peak**	**Total**
Before	26	26	17	27	27	18	141
After	29	27	26	27	26	25	160
Total	55	53	43	54	53	43	301

Table 30. GPS Floating Car Safety Results (Crashes $\times 10^{-6}$) – (Model Predictions)

	Northbound				Southbound			
	AM Peak	**Midday**	**PM Peak**	**Average**	**AM Peak**	**Midday**	**PM Peak**	**Average**
Before	24.780	25.650	28.960	26.463	23.670	24.040	37.350	28.353
After	23.540	24.450	27.350	25.113	23.300	24.800	29.910	26.003
Difference	**5.00%**	**4.68%**	**5.56%**	**5.10%**	**1.56%**	**-3.16%**	**19.92%**	**8.29%**

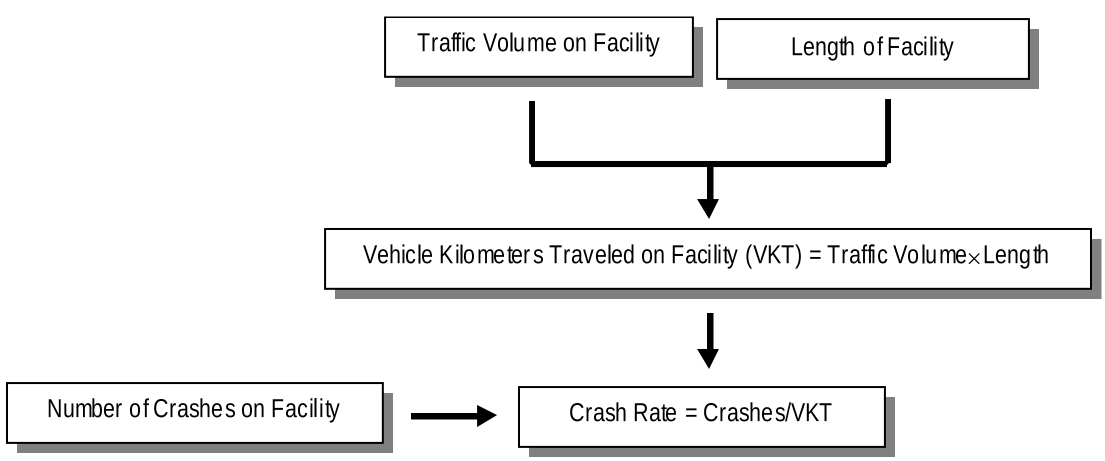

Figure 43. Schematic of Crash Risk Computation

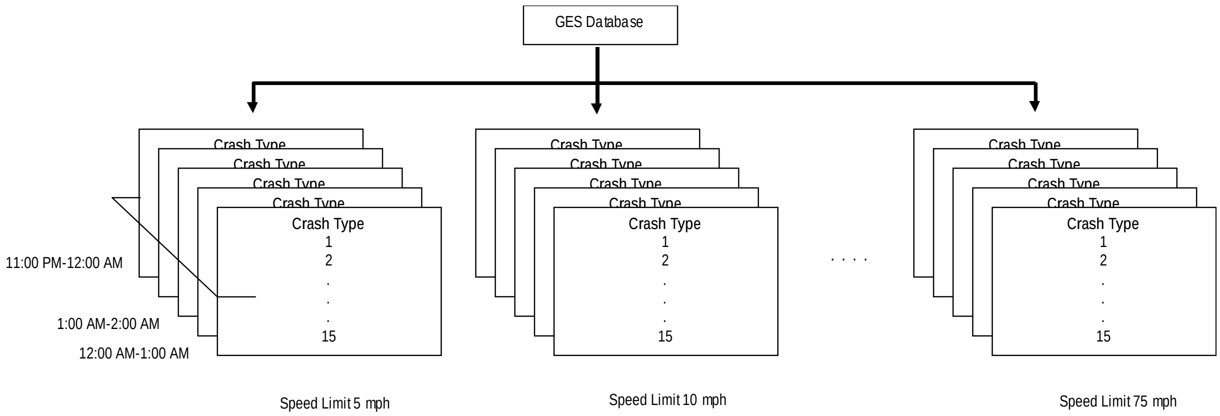

Figure 44. Crash Frequency Grouping

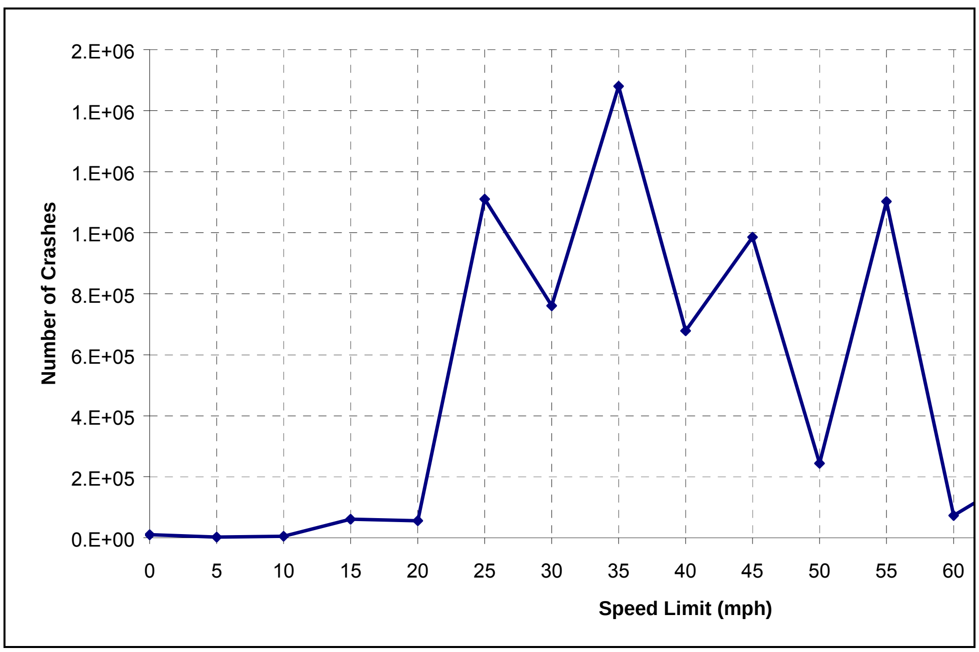

Figure 45. Number of crashes as a Function of Speed Limit (Based on GES 1996 Data)

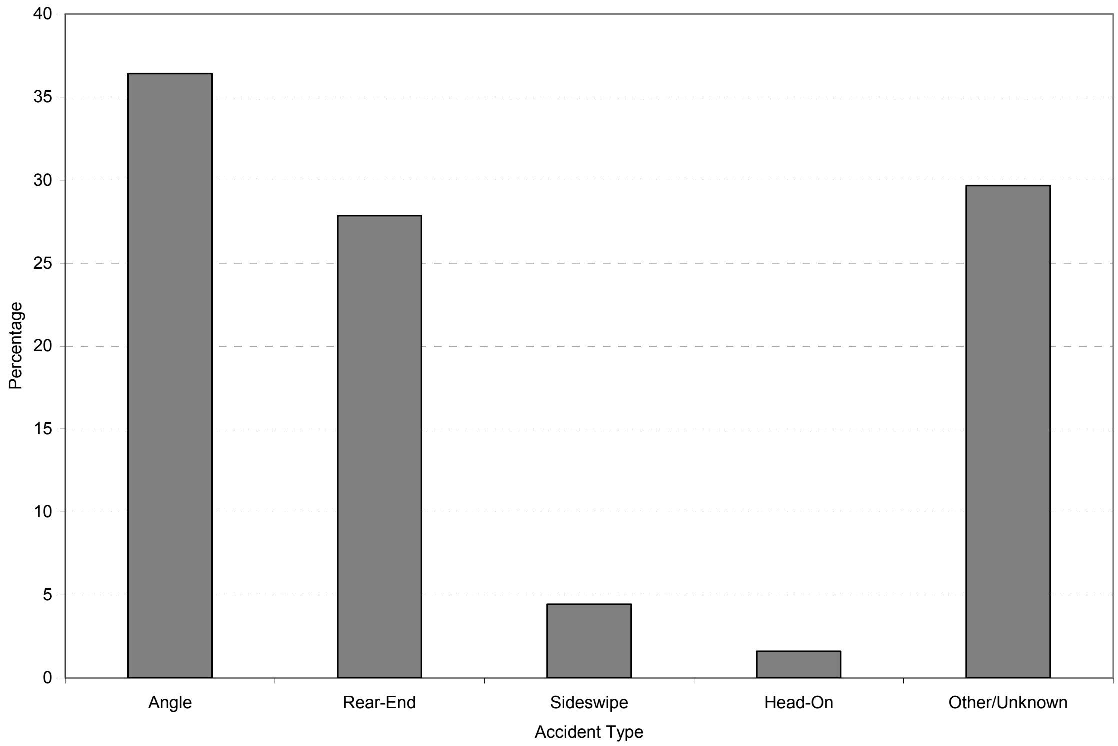

Figure 46. Crash Type Distribution

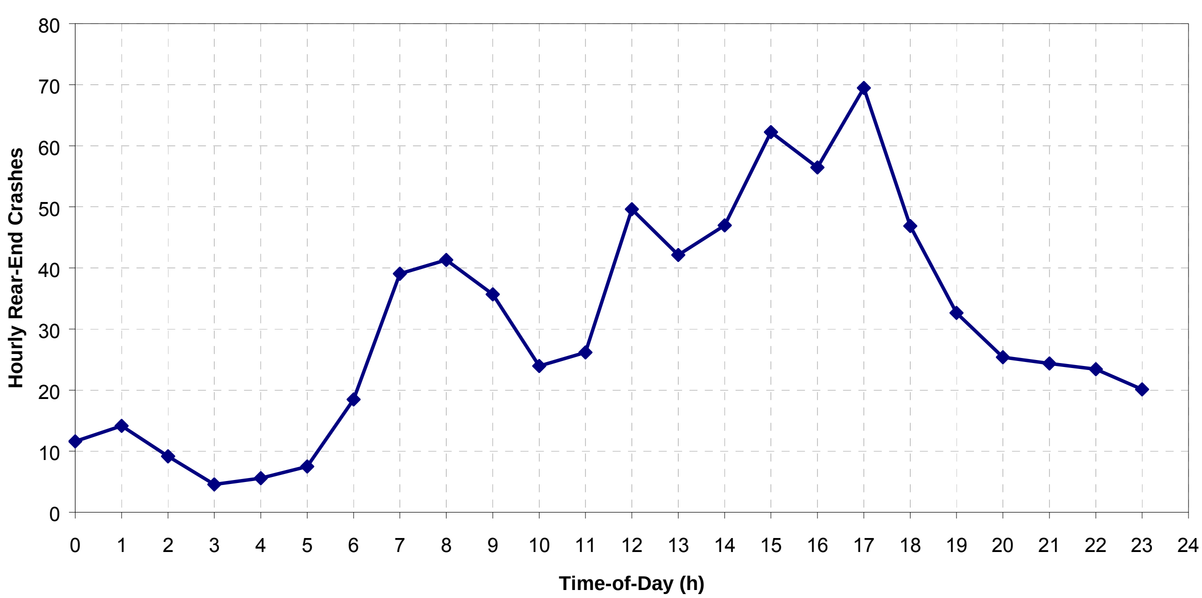

Figure 47. Variation in Rear-End Crashes as a Function of Time-of-day (45 mph Speed Limit)

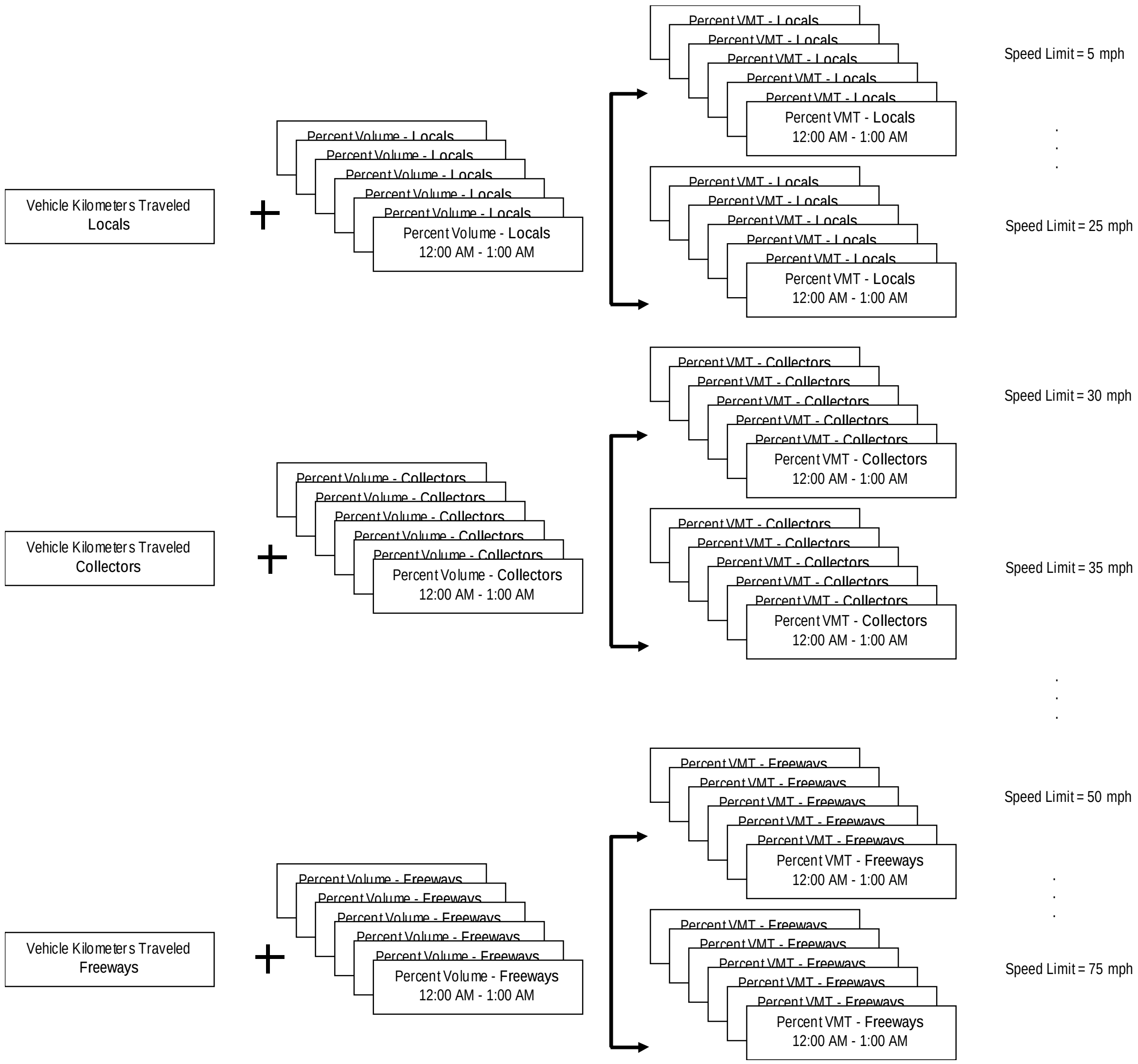

Figure 48. Vehicle Kilometers Traveled Grouping

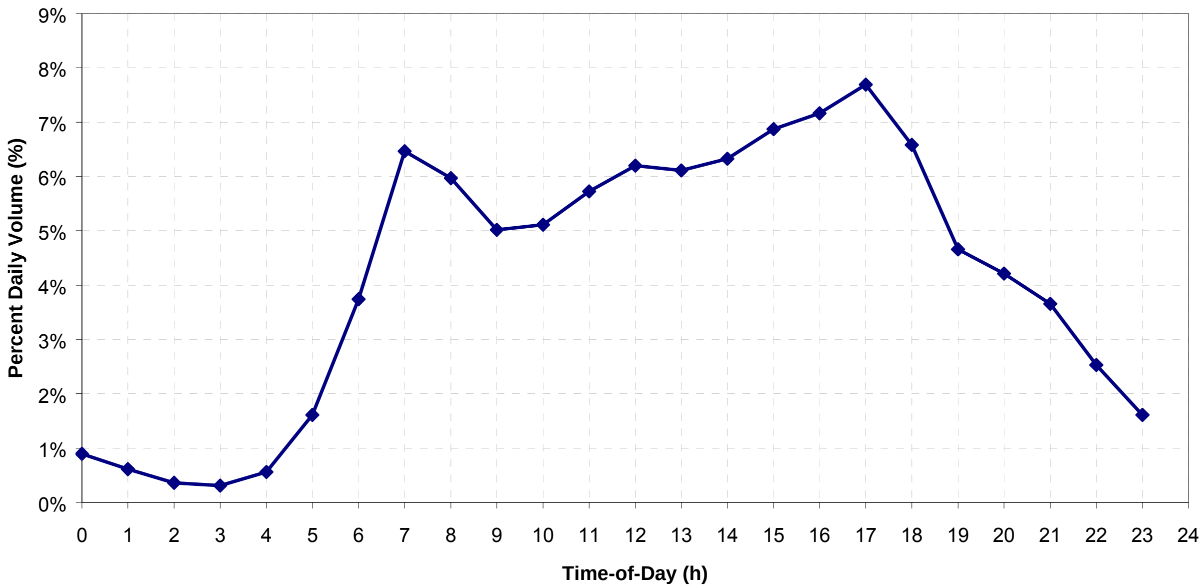

Figure 49. Scottsdale/Rural Road Tube Counts as a Function of Time-of-Day (45-mph Speed Limit)

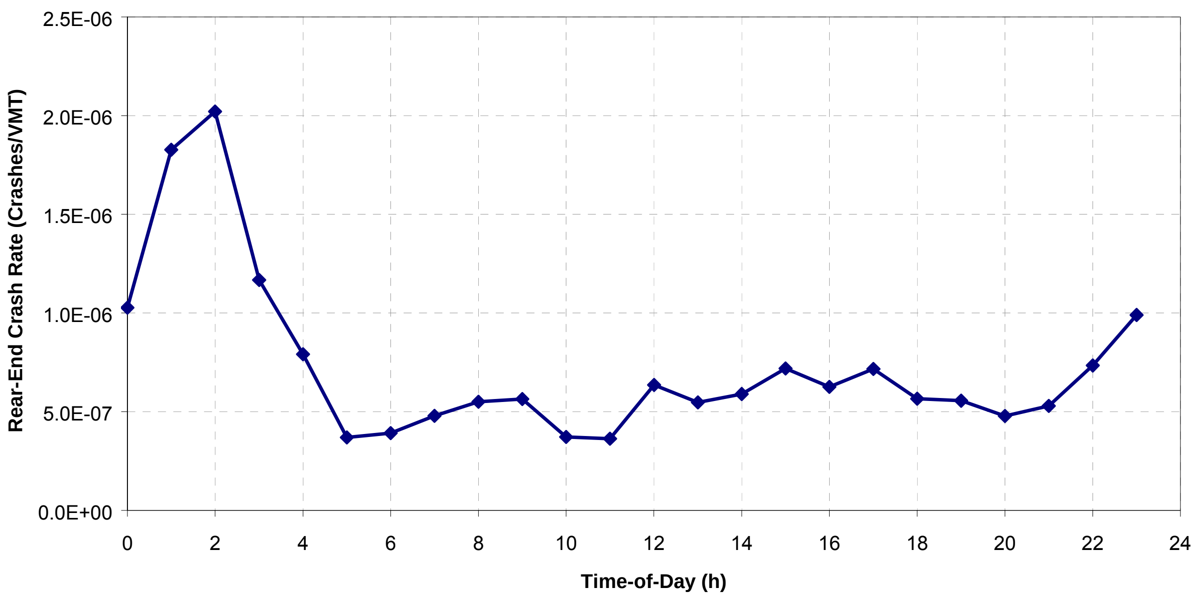

Figure 50. Rear-End Crash Rate as a Function of Time-of-Day (45 mph Speed Limit)

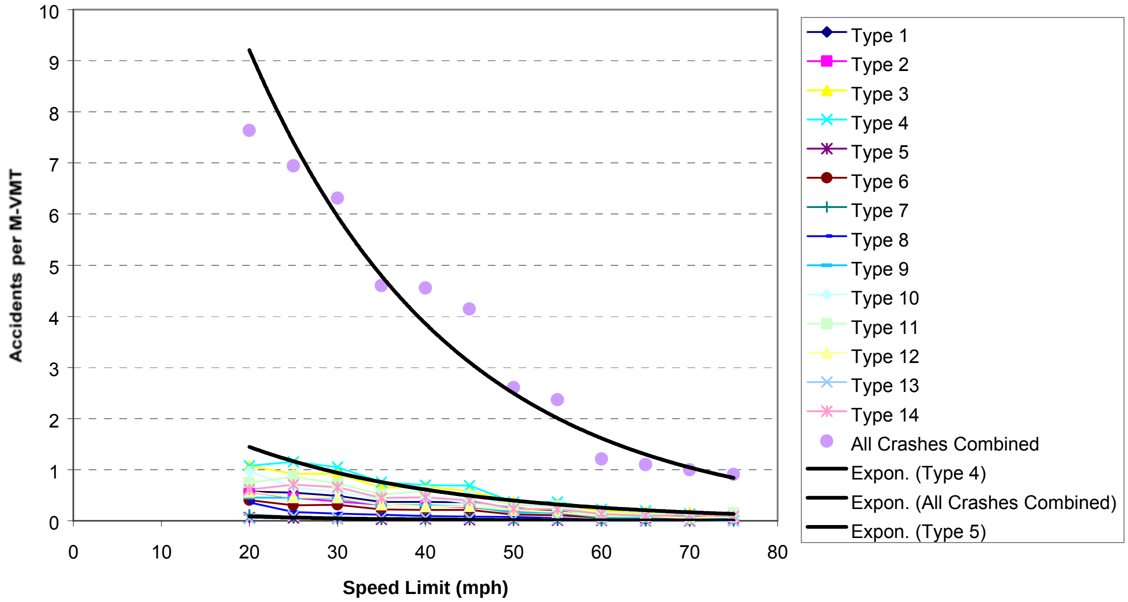

Figure 51. Crash Rate Variation as a Function of Facility Speed Limit

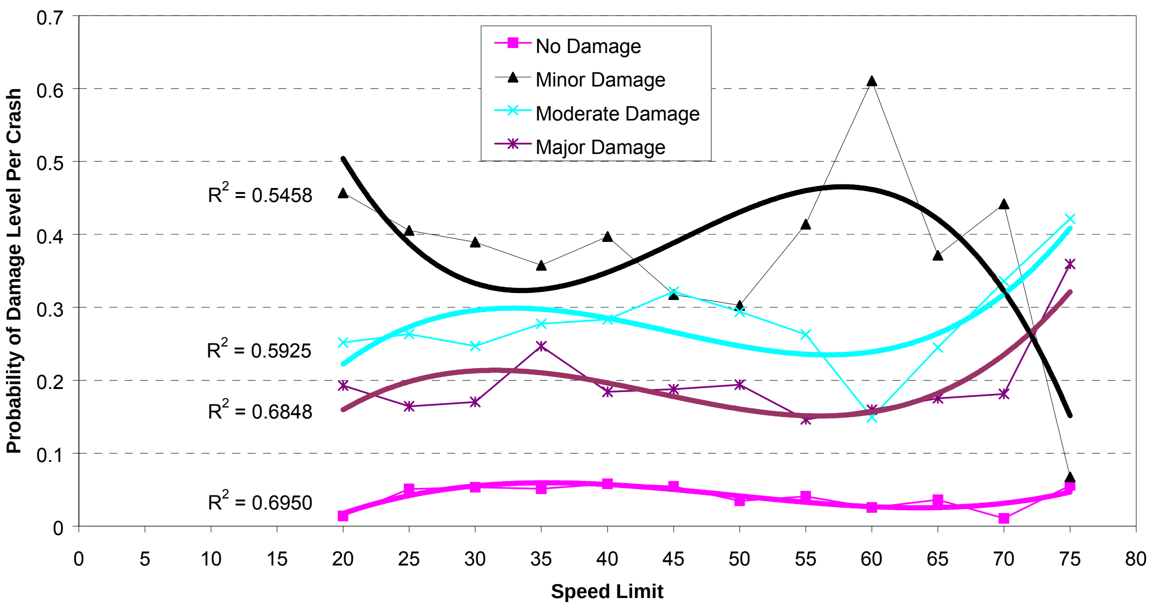

Figure 52. Variability in Damage Level as a Function of Facility Free-speed

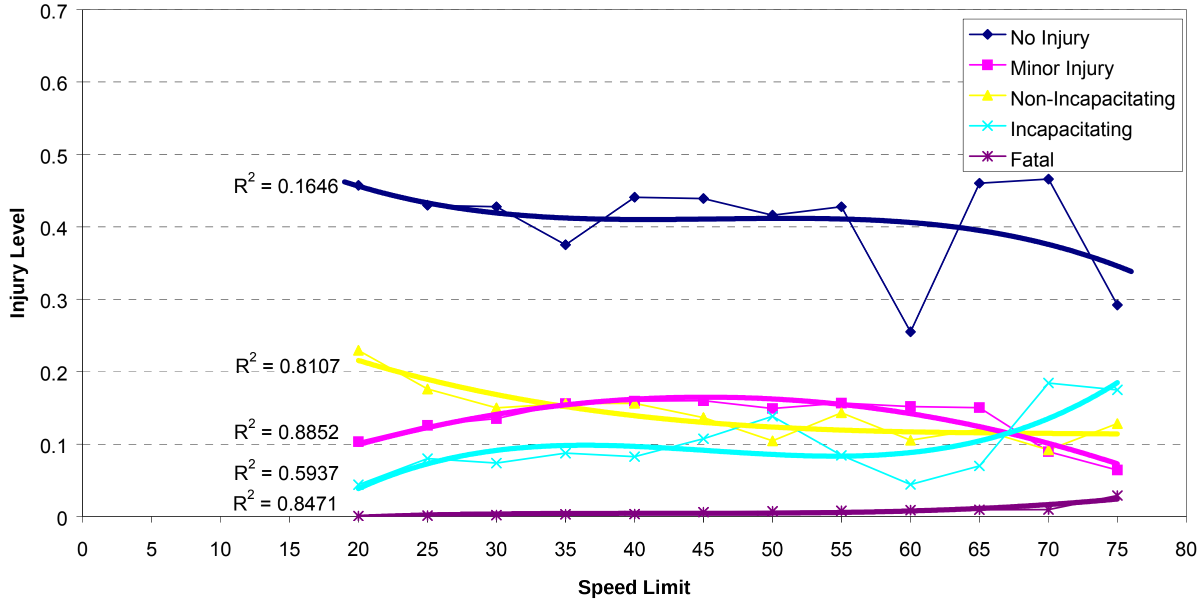

Figure 53. Variability in Injury Level as a Function of Facility Free-speed